SYNTHESIS AND CHARACTERIZATION OF NANOFLUIDS FOR COOLING APPLICATIONS

SUBELIA SENARA BOTHA

A thesis submitted in partial fulfillment of the requirements for the degree of Doctor of Philosophiae in the

SOUTH AFRICAN INSTITUTE FOR ADVANCED MATERIALS
CHEMISTRY
FACULTY OF NATURAL SCIENCES
UNIVERSITY OF THE WESTERN CAPE

Supervisor: Prof. V.M. Linkov
Co-Supervisor: Dr. B.J. Bladergroen

October 2007

KEYWORDS

Synthesis and Characterization of Nanofluids for Cooling Applications

Subelia Senara Botha

Nanofluid

Thermal conductivity

Silver nanoparticles

Effect of surfactant

Nanoparticle dispersion

Ethylene glycol based nanofluids

Transformer oil

Nanofluid viscosity

Dielectric strength

ABSTRACT

Synthesis and Characterization of Nanofluids for Cooling Applications

S.S. Botha

PhD Thesis, Department of Chemistry, University of the Western Cape

Low thermal conductivity is a primary limitation in the development of energy-efficient heat transfer fluids that are required in numerous industrial sectors. Recently submicron and high aspect ratio particles (nanoparticles and nanotubes) were introduced into the heat transfer fluids to enhance the thermal conductivity of the resulting nanofluids. The aim of this project was to investigate the physico-chemical properties of nanofluids synthesized using submicron and high aspect ratio particles suspended in heat transfer fluids.

Ethylene glycol and oil-based nanofluids were prepared containing either silver nanoparticles (0.01 - 1.0 vol.%), carbon nanotubes (0.4 – 4.0 vol.%), silica (0.3 – 4.4 vol.%), silver nanoparticles (0.01 – 0.07 vol.%) supported on carbon nanotubes (1.0 – 4.0 vol.%) supported on silica (0.07 – 1.4 vol.%) via a one-step method. The reducing ability of ethylene glycol was used to prepare silver nanoparticles at room temperature with mechanical agitation. Oil-based nanofluids were prepared using higher temperatures (130 °C) and mechanical agitation. The rheological, thermal and where applicable, dielectric properties of the nanofluids were investigated.

Ethylene glycol and oil-based nanofluids containing surfactant-stabilized silver nanoparticles showed Newtonian behaviour. The average particle sizes were mostly between 3-16 nm. Surfactant-stabilized silver-based nanofluids did not show any increase in thermal conductivity.

The surfactant, although essential for the stabilization of single digit-sized nanoparticles, has been identified as a critical component in the heat transfer

process of nanofluids. The surfactant suppresses the heat transfer process to the extent where no increase of thermal conductivity was measured. The effect of the surfactants on the thermal conductive properties of nanofluids has not been reported in the open literature and can be regarded as a breakthrough in nanofluid development.

Oil-based nanofluids containing carbon nanotubes showed shear-thinning behaviour and 13 % enhancement in thermal conductivity (at 4 % loading). Silver nanoparticles with sizes <5 nm were supported on carbon nanotubes and showed a further 6 % enhancement in thermal conductivity.

The dielectric strength of the nanofluids containing silver nanoparticles and carbon nanotubes were drastically reduced from 56 kV to 2 kV, while the dielectric strength of oil-based nanofluids containing silver nanoparticles (size < 5nm) was only reduced from 56 kV to 51 kV and can still be considered for application in electrical transformers.

Oil-based nanofluids containing silica showed Newtonian behaviour (at lower concentrations), the thermal conductivity was found to increase to a maximum of 5.2 % and the dielectric strength decreased from 56 kV to 34 kV. When silver nanoparticles (~5 nm) supported on silica were used to make oil-based nanofluids *without* a surfactant, a 15 % increase in the thermal conductivity was obtained and the dielectric strength reduced to 22 kV.

Introducing a suitable support for surfactant-free silver nanoparticles during particle formation, agglomeration of particles is drastically reduced, allowing the heat transfer process to proceed effectively. A significant thermal conductivity increase was measured at very low particle loading, exceeding the predictions of various published models on nanofluids.

October 2007

DECLARATION

I declare that *Synthesis and Characterization of Nanofluids for Cooling Applications* is my own work, that it has not been submitted for any degree or examination in any other university and that all the resources I have used or quoted have been indicated and acknowledged by complete references.

SUBELIA SENARA BOTHA OCTOBER 2007

SIGNED ……..

ACKNOWLEDGEMENTS

I would like to thank GOD the Almighty for giving me the strength to remain on the path to success.

I am forever grateful to my PARENTS, Maggie and Peter Botha, and SISTERS, Angelic and Bernita, for their unconditional love and support. I could not have come thus far without your support and love.

To all my FRIENDS and COLLEAGUES (especially Dr. Patrick Ndungu, Mario Williams, Nicolette Hendricks and Rushanah Mohammed), who have helped me, supported me and encouraged me during stressful times, thank you so much.

J. Willemse and M. Malatsi are acknowledged for their help with some of the thermal conductivity measurements.
Dr. Basil Julies from UWC is acknowledged for all his help and training with the TEM.
Mohamed Jaffer from UCT is acknowledged for his help with some of the TEM micrographs.
Nazeem George from CPUT is acknowledged for his help with the viscosity measurements.

My supervisors, Prof. Vladimir Linkov and Dr. Ben Bladergroen, for all their help and support.
Dr. A. Nechaev for all his help and support during the finalization of my thesis.

Prof. Helmut Bönnemann, for all his kindness and support, especially during my stay/research visit in Germany (Max-Planck-Institute, 2004).

A special thanks to all the lecturers and students in the CHEMISTRY DEPARTMENT, UWC, for all their support.

The National Research Foundation (NRF) is acknowledged for financial assistance.

List of Publications

1. H. Bönnemann, S.S. Botha, B. Bladergroen, V.M. Linkov, Monodisperse copper- and silver-nanocolloids suitable for heat-conductive fluids, Appl. Organomet. Chem., 19, 768-773, 2005

2. S.S. Botha, W. Brijoux, R. Brinkmann, M. Feyer, H.W. Hofstadt, G. Kelashvili, S. Kinge, N. Matoussevitch, K.S. Nagabhushana, F. Wen, A review - How nanoparticles emerged from organometallic chemistry, Appl. Organomet. Chem., 18, 566-572, 2004

3. S.S. Botha, P. Ndungu, B.J. Bladergroen , The effect of surfactant on the thermal conductivity of silver nanofluids, Manuscript in preparation

4. S.S. Botha, B.J. Bladergroen, P. Ndungu, Nanofluids based on CNT and Ag supported on CNT, Manuscript in preparation

5. S.S. Botha, B.J. Bladergroen, P. Ndungu, V.M. Linkov, Physico-chemical properties of transformer-based nanofluids containing silver nanoparticles and silica, Manuscript in preparation.

Table of Contents

List of Tables

List of Figures

1 CHAPTER ONE: INTRODUCTION

Cooling is one of the most important challenges facing numerous industrial sectors. Despite the considerable amount of research and development focusing on industrial heat transfer requirements, major improvements in cooling capabilities have been lacking because conventional heat transfer fluids have poor heat transfer properties [1]. One of the usual methods used to overcome this problem is to increase the surface area available for heat exchange, which usually leads to impractical or unacceptable increases in the size of the heat management system [2]. Thus there is a current need to improve the heat transfer capabilities of conventional heat transfer fluids.

Crystalline solids have thermal conductivities that are typically larger than those of fluids by 1-3 orders of magnitude. Therefore, fluids containing suspended solid particles can be expected to display significantly enhanced thermal conductivities relative to those of pure fluids [3]. When crystalline solids with nanometer dimensions are suspended in a suitable base fluid to form stable homogeneous suspensions, and there is an increase in the thermal conductivity relative to the base fluid, the resulting suspensions are called nanofluids [2,4], as opposed to nanofluidics, which is concerned with flow in nanoscale channels [5]. The crystalline solid can be either spherical nanoparticles, or micrometer long nanotubes [4]. Nanofluids can be prepared by a one-step or a two-step method. In the two-step method, the preparation of the nanofluid is isolated from the synthesis of the nanoparticles. However, this approach may result in the formation of larger nanoparticles due to agglomeration which can occur during drying, storage, transportation and re-dispersion of nanoparticles. As a result, the thermal conductivity may be affected negatively. Hence the current interest is to develop one-step methods where nanoparticles are synthesized directly in the heat transfer fluid. Different methods have been used for the preparation of nanofluids, namely, thermal decomposition pathways [6,7], microwave [8] and laser [9] irradiation, chemical reduction [10] and ‘direct-evaporation’ techniques [2]. Nanofluids containing metals

such as Cu, Ag and Au have shown an increase in the effective thermal conductivities of the heat transfer fluid compared with the base fluid [2]. The large intrinsic thermal conductivity of carbon-based nanostructures, combined with their low densities compared with metals, make them attractive candidates for use in nanofluids [2, 4,11,12,13].

Until recently, there have been a limited number of studies on the characteristics of dispersion and rheological properties of nanofluids. Since nanofluids are expected to be used under flow conditions, the study of the rheological properties of the nanofluid is essential. Also, to understand the mechanism of heat transfer enhancement, it is crucial to have knowledge on the fluid-particle and particle-particle interactions within the fluid [14].

Stability of the suspensions is a crucial issue for both scientific research and practical applications. Particle aggregation and the formation of extended structures of linked nanoparticles will affect stability, and may be responsible for much of the disagreement between experimental results and the predictions of effective medium theory [2]. Simultaneous studies of thermal conductivity and viscosity may give additional insight [2].

An overview of the literature is given in Chapter 2 as well as a more detailed thesis layout in Section 2.4. All the experimental details of this work are outlined in Chapter 3. All the results obtained are presented and discussed in Chapter 4 and 5. Chapter 6 contains a summary of the work presented in this thesis as well as some recommendations.

2 CHAPTER TWO: LITERATURE OVERVIEW

2.1 Introduction to novel cooling fluids- Nanofluids

Modern nanoclusters differ from classical colloids in several important ways. Classic colloids typically (i) are larger in size (>10 nm), (ii) have broader size distributions (standard deviation >>15% of average particle size), (iii) have a poorly defined molecular composition, (iv) are not isolable and redissolvable, (v) are not reproducibly prepared, (vi) have irreproducible catalytic activities (up to 500%), (vii) contain surface-bound, rate-inhibiting species such as X^-, O^{2-}, OH^-, and H_2O and (viii) historically have been H_2O, but not organic solvent, soluble [15]. The region inbetween colloid and cluster chemistry is where this research lies.

The Argonne National Laboratory (Illinois, U.S.A.) has pioneered the concept of nanofluids by applying nanotechnology to thermal engineering. Nanofluids are a new class of solid-liquid composite materials consisting of solid nanoparticles (in the range of 1-100 nm) or carbon nanotubes, dispersed in a heat transfer fluid such as ethylene glycol, water or oil [2,3].

Heating or cooling fluids are of great importance to many industrial fields, including electronics, Heating, Ventilating and Air Conditioning (HVAC), and transportation. The thermal conductivity of these fluids plays a vital role in the development of energy-efficient heat transfer equipment. Conventional heat transfer fluids have a relatively poor thermal conductivity compared to most solids [2,12]. The latter have 1-3 orders of magnitude greater thermal conductivity than the former. From Table 2-1, the thermal conductivity of copper, for example, is 700 times that of water and 3000 times that of engine oil [7]. The orders-of-magnitude larger thermal conductivity of most solids compared with conventional cooling fluids such as water, ethylene glycol, and engine oil provided the original motivation to investigate the thermal transport properties of nanofluids [12].

Table 2-1: Thermal conductivity values for some solids and liquids at RT [12].

Material		Thermal conductivity (W/m-K)
Metallic solids	Silver	429
	Copper	401
	Aluminum	237
Non-metallic solids	Diamond	3300
	Carbon nanotubes	3000
	Silicon	148
	Alumina (Al_2O_3)	40
Metallic liquids	Sodium at 644 K	72.3
Non-metallic liquids	Water	0.613
	Ethylene glycol	0.253
	Engine oil	0.145

The unique properties of nanomaterials can be used to develop fluids with high thermal conductivity. However, nanofluid production faces some major challenges such as agglomeration of particles in solution and the rapid settling of particles in fluids. The most common techniques used to prepare nanofluids are discussed in Section 2.1.1, followed by the structural and physico-chemical properties in Sections 2.1.2 and 2.1.3 respectively.

2.1.1 Techniques used in the synthesis of nanofluids

Several studies, including the earliest investigations of nanofluids, used a two-step method in which nanoparticles or nanotubes are first produced as a dry powder and then dispersed into a fluid in a second processing step. In contrast, the one-step method entails the synthesis of nanoparticles directly in the heat transfer fluid. The two-step and one-step methods are discussed in more detail in Sections 2.1.1.1 and 2.1.1.2 respectively.

2.1.1.1 Synthesis of nanofluids containing metallic nanoparticles, metal oxide particles and carbon nanotubes via. two-step method

The preparation of nanofluids begins by direct mixing of the base fluid with the nanomaterials. In the first step, nanomaterials are synthesized and obtained as powders, which are then introduced to the base fluid in a second step.

Nanoparticles can be produced from several processes [16,17] which can be categorized into one of five general synthetic methods. These five methods are: (i) transition metal salt reduction [18,19], (ii) thermal decomposition and photochemical methods [6,20 ,21], (iii) ligand reduction and displacement from organometallics, (iv) metal vapor synthesis, and (v) electrochemical synthesis [22,23]. Transition-metal nanoclusters are only kinetically stable because the formation of the bulk metal is its thermodynamic minimum. Therefore, nanoclusters that are freely dissolved in solution must be stabilized in a way that prevents the nanoclusters from coalescing, because such agglomeration would eventually lead to the formation of the thermodynamically favoured bulk metal [24].

Bönnemann et al. developed a method for the production of very small (< 2 nm) and stable nanoparticles via chemical reduction pathways, which might be suitable for application in nanofluid synthesis [25]. Organoaluminum compounds have been used for the “reductive stabilization” of mono- and bi-metallic nanoparticles [26]. Triorganoaluminum compounds were employed as both the reducing agent and colloid stabilizer, which lead to the formation of an organo-metallic colloidal protecting shell around the particles [27,28]. This “modification” of the Al-organic protecting shell leaves the particle size untouched and allows tailoring of the dispersion characteristics of the original organosols at will. A vast spectrum of these solubilities of the colloidal methods in hydrophobic and hydrophilic media including water has been achieved this way [29]. Colloidal copper nanoparticles can be prepared by using the triorganoaluminium pathway, however, a large ratio of surfactant to metal is necessary in order to obtain stable suspensions. In the event of a lower surfactant concentration, precipitation occurs. However, it is possible to suspend the precipitated particles again by peptization [7].

Silver nanoparticles are one of the most widely studied nanomaterials because they exhibit unusual optical, electronic and chemical properties, which depend on their size and shape [30,31,32,33]. Silver is also one of the most thermally conductive metals (Table 1) and its use in cooling applications would be interesting.

Besides silver nanoparticles, Xuan et al. [34] have used commercially obtained Cu nanoparticles to prepare nanofluids in both water and transformer oil by sonication in the presence of stabilizers. Similarly, Kim et al. [14] prepared nanofluids consisting of commercially obtained CuO nanoparticles in ethylene glycol by sonication without stabilizers. The optimum duration of sonication was found to be 9 hours and the average nanoparticle size was 60 nm.

The two-step process is commonly used for the synthesis of carbon nanotube-based nanofluids. Single-wall carbon nanotubes (SWCNTs) and multi-walled carbon nanotubes (MWCNTs) are cylindrical allotropes of carbon. SWCNTs consist of a single cylinder of graphene, while MWCNTs contain multiple graphene cylinders nesting within each other [35]. The carbon nanotubes are usually produced by a pyrolysis method and then suspended in a base fluid *with* or *without* the use of a surfactant [2,11,12].

Some believe that the two-step process works well only for nanofluids containing oxide nanoparticles dispersed in de-ionized water as opposed to those containing heavier metallic nanoparticles [3]. Since nanopowders can be obtained commercially in large quantities, some economic advantage exists in using two-step synthesis methods that rely on the use of such powders.

2.1.1.2 Synthesis of nanofluids containing metallic nanoparticles, metal oxide particles and carbon nanotubes via one-step method

Few methods exist for the preparation of nanofluids through a one step process. These methods include the thermal decomposition of an organometallic precursor in the presence of a stabilizer [36], chemical reduction [8], and polyol synthesis [37,38,39].

The polyol method is one of the most well-known pathways to noble metal nanoparticles [30,37,38,39,40,41,42,43]. In the polyol process, a metal precursor is dissolved in a liquid polyol (usually ethylene glycol), after which the experimental conditions are adjusted to achieve the reduction of the metallic precursor by the polyol, followed by atomic metal nucleation and metal particle growth [41].

The 'direct-evaporation' technique was developed by Choi et al [1]. It consists of a cylinder containing a fluid which is rotated. In the middle of the cylinder, a source material is vaporized. The vapour condenses once it comes into contact with the cooled liquid (Figure 2-1) [1]. The drawbacks of this technique however, are that the use of low vapour pressure liquids are essential and only limited quantities can be produced.

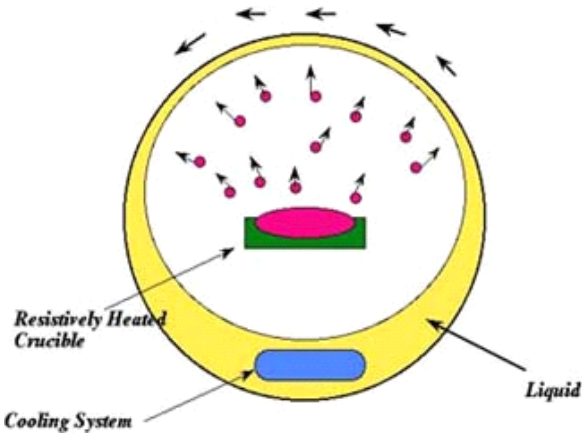

Figure 2-1: Diagram of the one-step nanofluid production system, which simultaneously makes and disperses nanoparticles into low vapour-pressure liquids [1].

Various single-step chemical synthesis techniques can also be employed to produce nanofluids. For example, Brust and co-workers [44] developed a technique for producing metallic nanoparticles in various solvents by the reduction of metal salts to produce colloidal suspensions for a wide range of applications, including studies of thermal transport. Excellent control of size and very narrow size distributions can be obtained by using such methods [2].

A submerged arc nanoparticle synthesis system (SANSS) was developed to prepare CuO nanoparticles dispersed uniformly in a dielectric liquid (deionized water). The method successfully produced a stable nanofluid [45]. In principle, a pure copper rod is submerged in a dielectric liquid in a vacuum chamber. A suitable electric power source is used to produce an arc between 6000 - 12000 ˚C which melts and vaporizes the metal rod in the region where the arc is generated. At the same time, the deionized water is also vaporized by the arc. The vaporized metal undergoes nucleation, growth and condensation resulting in nanoparticles dispersed in deionized water. Nanofluids containing CuO particles of size 49.1 ± 38.9 nm were obtained [45].

Carbon nanotubes have also been synthesized by carbon plasma discharging directly in water [46]. The resulting nanotubes, which were also filled with cobalt, are believed to have important applications as nanoprobes in the magnetic force microscope.

2.1.1.3 Study of the modes of stabilization in nanofluids

The attractive forces between particles can be balanced, and hence particle aggregation prevented, by two mechanisms namely, electrostatic stabilization and steric stabilization.

- **Electrostatic stabilization**

The existence of an electric charge on the surfaces of particles is a major source of kinetic stability. Electrostatic stabilization occurs by the adsorption of ions to the

electrophilic metal surface (Figure 2-2 A) [47]. The adsorption creates an electrical double/multi-layer which results in a Coulombic repulsion force between the nanoclusters [48,49,50]. The electrostatic stabilization is a pH sensitive method and of limited use.

- **Steric stabilization**

Steric stabilization is achieved by surrounding the metal center by layers of material that are sterically bulky, such as polymers [51,52] or surfactants [53,54,55]. These large adsorbates provide a steric barrier which prevents the metal particles from coming together (Figure 2-2 B) [56]. Carbon nanotube suspensions for nanofluid applications are usually stabilized using the steric mode of stabilization [2].

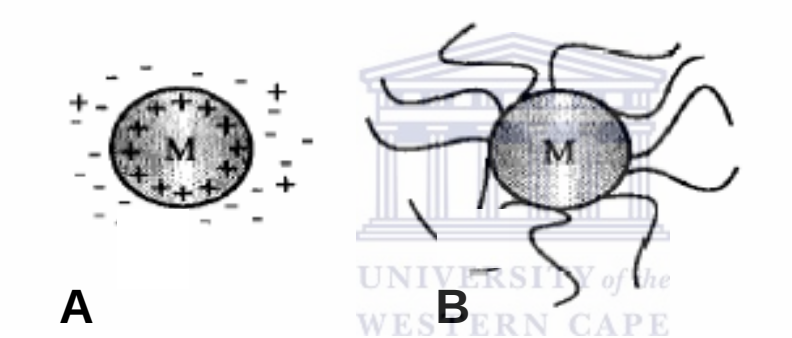

Figure 2-2: Schematic illustration for (A) electrostatically stabilized metal (M) particle and (B) a sterically stabilized metal particle [56]

Recently, a mechanism for colloidal stabilization through nanoparticle 'haloing' has also been presented [57,58]. It involves the addition of charged nanoparticles to microspheres, which tend to agglomerate due to their Van der Waals attractions. Stabilization of the suspensions is therefore achieved by the addition of small nanoparticle concentrations, which induce an effective repulsion, counteracting the Van der Waals attractions between the particles.

2.1.2 Structural studies of nanoparticle suspensions

Ultraviolet-Visible (UV-VIS) spectroscopy and Transmission Electron Microscopy (TEM) are the main characterization tools used to study the formation of silver nanoparticles.

2.1.2.1 UV-VIS

The oxidation state of silver can be studied with optical methods, such as UV-VIS spectroscopy. UV-VIS spectroscopy involves the absorption of electromagnetic radiation by the substances in the visible and ultraviolet regions of the spectrum. According to Mie theory, the optical absorption and light scattering of metal nanoparticles is due to the interaction of small metal particles with an external electromagnetic field, induced by light, resulting in a coherent oscillation of the conduction (free) electrons on the surface, called the surface plasmon resonance [30].

The presence of zerovalent silver in solution is related to a broad and strong absorbance peak whose maximum occurs at approximately 420 nm. In nanoparticles, the gap between excitation bands is widened and this implies absorption of a photon of a higher energy level (visible spectrum). The chemisorption of a nucleophilic molecule on the silver surface is also accompanied by a charge donation to the metal. The cumulative affect of the adsorption of many molecules produces a shift of the Fermi level energy. The shape and intensity of the absorption band depends on the complex dielectric constant of the metal, the cluster size of the metal nanoparticles, and the environment [33,34]. UV-VIS spectroscopy therefore, provides information on the kinetics as well as an indirect measure of the size and size distribution of the silver nanoparticles. A very uniform particle size implies that all particles will absorb at the same wavelength and a symmetrical peak is expected, whereas a broader peak would be indicative of particle aggregation or the presence of large particles.

It is universally accepted within the community that the surface plasmon resonance band for spherical silver particles < 20 nm is ~ 410 nm depending, of course, on the host matrix [59]. This band generally red shifts as the silver nanoparticles increase in size. Conversely, as silver particles decrease in size, this band will often blue shift to

shorter wavelengths. Absorption signals in the 250 – 350 nm range present in Ag containing systems have been attributed to the presence of Ag clusters of various sizes and charges. Determination of which cluster specie gives rise to which absorption signal is still widely debated in literature today. Researchers have varying degrees of certainty with respect to peak assignments due to the short lifetime of Ag clusters and the fact that the UV-VIS absorption signal positions are system dependant [60; and references therein].

Since the surface plasmon absorption band (SPAB) is extremely sensitive to the nanoparticle shape, size, polydispersity, surrounding medium, adsorbed substances on their surfaces, aggregation, a change in the particle electron density and geometric arrangements of nanoparticles [30], changes in the UV-VIS spectra of silver nanoparticles are very informative and have been used to study a vast spectrum of parameters such as electromagnetic interactions, changes in particle electron density and propositions for formation and growth mechanisms.

2.1.2.2 TEM

Transmission Electron Microscopy (TEM) is used to determine the size, distribution and the morphology of the synthesized nanoparticles. A transmission electron microscope works in much the same way as an optical microscope. A beam of electrons, generated by the high voltage electron emitter situated at the top of the lens column, interacts with the sample as it passes through the entire thickness of the sample and a series of magnifying magnetic lenses, to where they are ultimately focused at the viewing screen at the bottom of the column. The image is essentially a projection of the entire object, including the surface and the internal structures.

2.1.3 Physico-chemical properties of suspensions containing nanosized particles

The idea of dispersing solid particles into liquids initially came from James Clerk Maxwell [61, and references therein]. In previous years, the lack of industrial interest

for enhanced thermal properties by those suspensions containing millimeter– or micron-sized particles was mainly due to their poor stability and rheological problems. Particle sedimentation from the suspensions resulted in clogged channels. It has recently been demonstrated that solid nanoparticles with dimensions of ~10-40 nm are extremely stable and exhibit no significant settling under static conditions, even after weeks or months [61]. Conventional heat transfer fluids such as water, ethylene glycol or oil, containing ultra-fine metallic particles have been of special interest amongst many researchers in recent years [62,63,64,65]. This is because the prepared nanofluids gave rise to a heat transfer enhancement compared to the conventional heat transfer fluids.

The heat transfer rate of a nanofluid involves three main parameters. These are viscosity, thermal conductivity and heat capacity, where one or more of these parameters may be quite different from the base fluid [66].

2.1.3.1 Rheological properties of nanofluids

Rheological properties play a very important role in fluid flow. During application of nanofluids they are likely to flow either by forced or natural convection and hence, the flow properties such as viscosity are therefore essential in the study of suspensions containing nanosized particles.

All materials that show flow behaviour are referred to as fluids. In all fluids, there are frictional forces between the molecules and, therefore, they display a certain flow resistance which can be measured as viscosity [67]. Viscosity is a transport property which refers to the resistance of a material to flow. When dealing with nanofluids, one is often tempted to consider the dispersed medium under question as a homogeneous fluid characterized by properties such as density and viscosity which in turn will only require a single set of mass and momentum conservation equations. However, such a simple picture will not provide useful explanations for cases where the fluid is unsteady and non-uniform [34].

i. Newtonian flow behaviour

Isaac Newton found that the shear force acting on a liquid is proportional to the resulting flow velocity [67]. Hence, a fluid is said to be Newtonian if the viscosity remains constant with an increase in shear rate. Newtonian flow behaviour is observed in low molecular liquids such as water, mineral oils (without polymer additives) and solvents. However, more complex flow behaviour is expected for fluids containing suspended particles.

ii. Non-Newtonian flow behaviour

Fluids, whose viscosity changes with an increase in shear rate, are referred to as Non-Newtonian. These fluids could be further classified according to their flow behaviour. Shear-thinning and shear-thickening flow behaviour is discussed in the following sections.

a) Shear-thinning flow behaviour

For samples that display shear-thinning behaviour, the shear viscosity is dependent on the degree of shear load. Thus, the viscosity decreases with an increase in shear stress. In dispersions, shearing can cause the particles to orient in the flow direction and in the direction of the flow gradient. This can lead to disintegration of agglomerates or change in particle form. The interaction forces between particles may decrease during the process and cause a lowering in the flow resistance. Examples of shear-thinning materials include shampoos, paints and polymer solutions [67].

b) Shear-thickening flow behaviour

Similar to shear thinning fluids, the shear viscosity of samples displaying shear-thickening behaviour is also dependent on the degree of shear load. However, the viscosity increases with an increase in shear stress. With highly concentrated suspensions, the probability of particle interaction is much higher and may result in

particles becoming wedged together and thus increase the flow resistance. Particle shape plays an important role since during the shear process, particles rotate as they move. Cube-shape particles take up more volume when rotating than spherical particles and hence less free volume is available for the liquid between the particles. Compared to shear thinning materials, shear thickening materials are much less common in industrial practice. Examples of shear-thickening materials include dispersions with a high concentration of solids or polymers such as ceramic suspensions [67].

c) The yield point

The yield point or yield stress refers to the external force required before a material will start to flow. A typical example is toothpaste; a certain amount of force must be applied before the toothpaste starts to flow. Materials with yield points tend to flow inhomogeneously.

iii. Model functions used to describe flow behaviour

This section describes the following model functions; Newtonian, and Non-Newtonian such as the Ostwald and Bingham flow models. These functions described the various nanofluids discussed in this thesis very well. More complex model functions such as Steiger/Ory and Eyring/Prandtl/Ree [67] were not required.

Newtonian behaviour:

Idealviscous (or Newtonian) flow behaviour is described formally using Newton's law:

$$\tau = \eta \cdot \gamma$$

where τ is the shear stress, η is the viscosity and γ the shear rate. Flow behaviour is represented graphically using flow curves and viscosity curves.

Non-Newtonian behaviour:

For shear-thinning and shear-thickening flow behaviour, three model functions are available for flow curves without a yield point.

The Ostwald/de Waele (or Power Law) refers to the flow curve model function:

$\tau = c \cdot \gamma^{p}$,

where c is the flow coefficient (or power-law-index) [Pas] and the exponent p.

The following applies:

$\rho < 1$ for shear-thinning

$\rho > 1$ for shear-thickening

$\rho = 1$ for idealviscous flow behaviour

This model holds the disadvantage that it cannot be fitted well to curves at very low and very high shear rates for most polymer solutions [67].

iv. Flow curves with yield point

The Bingham model can be described as follows:

$\tau = \tau_B + \eta_B \cdot \gamma$,

where τ_B is the Bingham yield point (intersection of linear graph on τ axis) and η_B is the Bingham flow coefficient, as shown below (Figure 2-3).

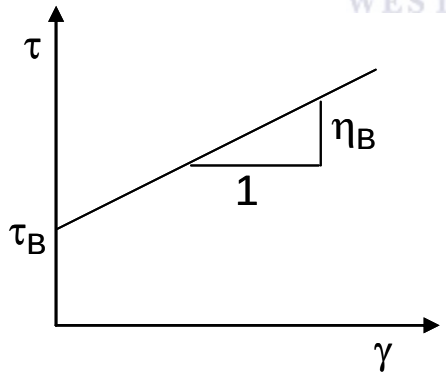

Figure 2-3: Flow curve according to Bingham [67].

The viscosity of a nanofluid can also be estimated with well-known formulas. However, a more reliable and direct way to the apparent viscosity is through experimental investigation [66].

2.1.3.2 Heat conduction in solids and heat capacity of nanofluids

When heat is transferred via conduction it implies that heat is transferred internally, by vibrations of atoms and molecules. The vibrations of the atoms which are coupled together can be envisaged as giving rise to the vibrations of the whole crystal, that is, to lattice vibrations. The energy of the whole vibrating system is quantized and the quantum of thermal energy absorbed or emitted by an atom is called a phonon. Therefore, a phonon is essentially a quantized mode of vibration occurring in rigid crystal lattice and plays a major role in a material's thermal conduction. A greater phonon density exists in a hot region of a crystal than in cooler regions. Therefore, heat conduction is essentially due to the diffusion of phonons down the temperature gradient from the hot to the cold regions. Electrons can also carry heat and since metals have many free electrons which move around randomly, heat can be transferred from one part of the metal to another quite effectively. That is why metals are generally very good conductors of heat.

Heat capacity is a material property and expresses the fact that the internal energy of a substance changes with temperature. It is measured by monitoring the resulting temperature increase when heating a sample of known mass. The heat capacity is then calculated as the ratio of the heat supplied to the temperature rise. Hence, a large heat capacity implies that only small increases in temperature will be observed. The specific heat capacity is also useful and is essentially the heat capacity per unit mass, usually per gram of material [68].

2.1.3.3 Thermal conductivity of nanofluids

The apparent thermal conductivity is the most important parameter to demonstrate the enhancement potential of heat transfer in nanofluids. It has been shown that the thermal conductivity of the nanofluid is influenced by the heat transfer properties of the base fluid and nanoparticle material, the volume fraction, the size, and the shape of the nanoparticles suspended in the liquid, as well as the distribution of the dispersed particles [66]. So far, the development of a sophisticated theory to predict

the thermal conductivity of nanofluids has been an unsolved problem, although some guidelines exist to calculate the apparent conductivity of two-phase mixtures [34].

Theoretical Study of Nanofluid Thermal Conductivity

A theory for the thermal conductivity of nanofluids is non-existent. Therefore, scientists have used an existing model for estimating the thermal conductivity of nanofluids. The Maxwell model was developed in earlier years to explain the heat transfer characteristics of larger particles. Due to the developments in nanofluid research in recent years, the Maxwell model has served as a foundation for the development of models to explain the much higher conductivity increase observed in nanofluids [69]. The effective thermal conductivity, k_{eff}, according to Maxwell, is

$$k_{eff,Maxwell} = \frac{k_p + 2k_l + 2(k_p - k_l)\phi}{k_p + 2k_l - (k_p - k_l)\phi} k_l$$

Where k_p is the thermal conductivity of the particle, k_l is the thermal conductivity of the liquid and ϕ is the particle volume fraction of the suspension. Hence, the Maxwell model shows that the effective thermal conductivity of fluids containing ultra-fine particles depends on the thermal conductivity of spherical particles, the base liquid and the volume fraction of the solid particles [70].

Hamilton and Crosser (1962) developed a model for the effective thermal conductivity of suspensions in which the ratio of conductivity of the two phases is larger than 100, taking into account the thermal conductivities of the pure materials, the composition of the mixture and the shape of the dispersed particles i.e.

$$\frac{k_{eff}}{k_f} = \frac{k_p + (n-1)k_f - (n-1)\alpha(k_f - k_p)}{k_p + (n-1)k_f + \alpha(k_f - k_p)}$$

where k_p is the thermal conductivity of the discontinuous particle phase, k_f is the thermal conductivity of the fluid, α is the volume fraction of particles, and n is the empirical shape factor given by:

$$n = \frac{3}{\psi}$$

where ψ is the sphericity defined as the ratio of the surface area of a sphere, with a volume equal to that of the particle, to the surface area of the particle [71]. For spherical particles, the Hamilton-Crosser model is identical to the Maxwell model. For particles of other shapes, *n* can be allowed to vary from 0.5 to 6.0 [34]. Thus the model is a function of the conductivity of both the particle and base fluid as well as the shape of the particles. Their predictions agreed well with experimental results for spherical particles with volume fractions up to 30% [34]. However, in application, nanofluids are more likely to show much lower volume fractions (typically below 1 %), and therefore another model should be considered. Eastman et al. [3] showed that the thermal conductivities predicted by the Hamilton-Crosser model are much lower than the measured data for oxide nanofluids and even less for metallic nanofluids.

Wasp [34 and references therein] introduced an alternative means for calculating the effective thermal conductivity of solid-liquid mixtures:

$$\frac{k_{eff}}{k_f} = \frac{k_p + 2k_f - 2\alpha(k_f - k_p)}{k_p + 2k_f + \alpha(k_f - k_p)}$$

The model is also identical to the Maxwell model. The volume fraction α of the particles is defined as:

$$\alpha = \frac{V_p}{V_f + V_p} = m\frac{\pi}{6}\bar{d}^3_p$$

where m is the number of particles per unit volume and đp is the average diameter of the particles [34].

Keblinski et al. [61] listed four possible explanations to understand the heat transfer enhancement in nanofluids: Brownian motion of the nanoparticle, molecular-level layering of the liquid at the liquid/particle interface, the nature of heat transport in the

nanoparticles, and the effects of nanoparticle clustering. Brownian motion, by which particles move through the liquid and possibly collide, thereby enabling direct solid-solid transport of heat from one particle to another, can be expected to increase thermal conductivity. However, it has been found that the movement of nanoparticles due to Brownian motion is too slow to transport significant amounts of heat through a nanofluid. The interface effect refers to the layers of liquid in direct contact with the solid (liquid nanolayer) where the atomic structure of the liquid layer is more ordered than that of the bulk liquid. Crystalline solids, which display much better thermal transport than liquids, are more ordered and therefore such liquid layering at the interface would be expected to lead to a higher thermal conductivity. Although the presence of the interfacial layer may play a role in heat transport, it is unlikely to be the only parameter responsible for the thermal conductivity increase. The nature of heat transport in nanoparticles was found to be ballistic, rather than diffusive since phonons, which are essentially the heat carriers in crystalline solids, cannot diffuse through the 10 nm particles, but move ballistically across the particle [61]. The enhancement in thermal conductivity could also be explained in terms of the packing fraction, which is the ratio of the volume of the solid particles in the cluster to the total volume of the cluster.

Xuan and Koo [34,72] summarized previous experimental observations and concluded that the effective thermal conductivity was a function of both the thermal conductivities of the base fluid and the nanoparticles, particle volume fraction, nanoparticle distribution in the fluid, surface area of the nanoparticles, and the shape of the nanoparticles.

Wang et al. [73] proposed a fractal model for predicting the thermal conductivity of liquids containing nanoparticles based on the effective medium and fractal theory. However, the proposed fractal model only agreed well with experimental data for 50 nm CuO particles suspended in deionized water when the particle concentration was less than 0.5%.

Similarly to Keblinski et al. [61], Yu and Choi [74] suggested that there are ordered nanolayers around the nanoparticles (Figure 2-4), and proposed that the solid-like nanolayer acts as a thermal bridge between a solid nanoparticle and the bulk liquid and hence is the key to enhancing thermal conductivity. The prediction proved to be effective when dealing with nanoparticles with diameters less than 10 nm [74].

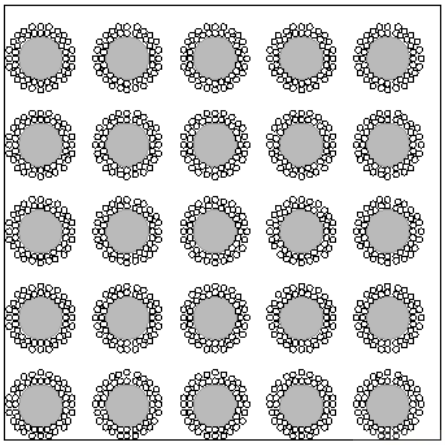

Figure 2-4: Schematic cross-section of nanofluid structure consisting of nanoparticles, bulk liquid, and nanolayers at the solid/liquid interface [74].

Kleinstreuer et al. [72] developed a thermal conductivity model that takes into account the effects of particle size, the particle volume fraction, temperature dependence of the thermal conductivity, the properties of the base fluid and the particle phase. They viewed the surrounding liquid traveling with randomly moving particles. In contrast to Keblinski et al [61], where Brownian motion was ruled out, they believe that Brownian motion is a very important mechanism for augmented heat transfer.

Other mechanisms, using more complex models, have also been suggested. Xuan and Roetzel [66] suggested a mechanism that assumes that the nanofluid in a tube behaves similar to that of a single phase fluid. Xue et al. [69] derived an expression for the effective thermal conductivity of nanofluids by taking the effect of particle size and interfacial properties, in addition to the relative volume fraction, into account. Their theoretical results for the CuO/water and CuO/EG nanofluids agreed well with experimental results. However, no clear explanation was given for the use of the

assumed values for thickness and thermal conductivity of the interfacial shell [69]. The fact that the theoretical results on the effective thermal conductivity of nanotube/oil nanofluid and Al_2O_3 /water nanofluid were in good agreement with the experimental data for an assumed interfacial shell thickness and thermal conductivity, does not make this an accurate model.

Das et al. [75] developed a comprehensive theoretical model explaining the enhancement in thermal conductivity of a nanofluid in terms of particle volume fraction, variation in particle size, and temperature. The large surface area of the nanoparticles has been shown to be responsible for the enhancement in the effective thermal conductivity. In addition, a strong dependence of thermal conductivity with temperature is observed, since at higher temperatures, the fluid becomes less viscous and in turn the particle velocity also increases. However, this particular model is not suitable for large concentrations of particles where inter-particle interactions become important.

Leong et al. [76] compared their experimental results and the theoretical predictions and concluded that all the traditional models, including Maxwell, Hamilton-Crosser, Wasp, and Bruggemann, under-predicted the effective thermal conductivity of the nanofluids, their reason being that the models do not account for particle size, particle Brownian motion, nanolayering, and the effect of nanoparticle clustering, similar to the proposition by Keblinski et al. [2].

It is evident from all the different models described above that no model exist yet that could explain the enhancement in thermal conductivity observed and that all the models developed thus far can only account for the results obtained within a specific research group.

2.1.4 Influence of submicron and high aspect ratio particles on physico-chemical properties of Newtonian liquids

In this section, the influence of various submicron and high aspect ratio particles such as metals, metal oxides and carbon nanotubes, on the rheological properties and thermal conductivity of Newtonian liquids are discussed.

2.1.4.1 Metals

- **Rheological properties**

Very few studies have been done on the rheological properties of nanofluids. Xuan and Li [34] compared their suspensions of Cu in transformer oil and Cu nanoparticles in water and suggested that viscosity may be an important factor affecting the dispersion of ultra-fine particles and the stability of suspensions.

Leong et al. [76] showed that the viscosity of nanofluids containing spherical particles increases more significantly with an increase in volume fraction, compared to those suspensions containing rod-like particles.

Putra et al. [77] reported that the fluids between 1% and 4% particle volume concentration, proved to be Newtonian. The viscosity of the fluids were found to be constant against shear rate, higher compared to the base fluid, showed an increase in viscosity with particle concentration, and remained Newtonian in nature.

It would thus appear that not much attention has been given to the rheological properties of nanofluids containing submicron and high aspect ratio particles.

- **Thermal conductivity**

Thermal conductivity plays a key role in the enhancement of heat transfer performance of a heat transfer fluid. Since the thermal conductivity of solid metals is much higher than that of fluids, the suspensions containing ultra-fine metal particles are expected to show improved heat transfer properties.

Hot-wire

The transient hot-wire method is most widely used for measuring thermal conductivity and well documented in literature [14,34,66]. One of the biggest advantages of the method is the almost complete elimination of natural convection due to the short measurement time, which may give rise to complex problems for measurements.

Many researchers have reported experimental studies on the thermal conductivity of nanofluids using the transient hot-wire method, and rarely the temperature oscillation and the steady-state parallel plate methods [78]. The hot-wire technique entails measuring the temperature/time response of a platinum wire to an abrupt electrical pulse. The wire is used as both heater and thermometer

Xuan and Li [34] presented a study on thermal conductivity of water- and transformer oil-based nanofluids containing Cu nanoparticles varying in size up to 100 nm. Results showed that the suspended nanoparticles increased the thermal conductivity of the base fluid. The thermal conductivity was found to increase with an increase in volume fraction of the particles. For the water-based nanofluid containing Cu nanoparticles, the ratio of thermal conductivity of the nanofluid to that of the base fluid increased from 1.24 to 1.78 when the volume fraction of the nanoparticles varied from 2.5 to 7.5%.

Eastman et al. [3] presented results from ethylene glycol-based nanofluids containing Cu nanoparticles with average diameter of less than 10 nm and loadings up to 0.5 vol.%, prepared via a one step method. A significant improvement in thermal conductivity enhancement was observed for nanofluids containing Cu nanoparticles (up to 40% observed for particle loadings below one volume percent) compared to base fluids or those containing oxide particles, which was prepared via a two step method. The largest increase in thermal conductivity was from the nanofluids containing thioglycolic acid as stabilizing agent. Freshly prepared nanofluids showed slightly higher conductivities than those that were stored for up to two months prior to measurement.

2.1.4.2 Metal oxides

- **Rheological properties**

Kim et al. [14] investigated the rheological properties of copper oxide nanoparticles, with an average diameter of 12 nm, dispersed in ethylene glycol. They found the viscosities of the nanofluid to be very shear thinning and the infinite shear viscosities became almost identical to the solvent viscosity. Based on this result it would appear that metal oxide-containing nanofluids are Non-Newtonian in contrast with what has been reported for metal-containing nanofluids.

- **Thermal conductivity**

Leong et al. [76] reported an experimental study on water-based nanofluids containing TiO_2 nanoparticles of different shapes. Spherically shaped particles with average diameters of 15 nm and rod-shaped particles with average diameters of 10 nm and average lengths of 40 nm were studied. Different volume fractions of 0.005 - 0.05 in deionized water were used. A maximum enhancement in thermal conductivity of 29.70% and 32.80% for a particle volume fraction of 5% was observed for spherically shaped and rod-shaped particles respectively. Hence, the thermal conductivity of nanofluids increases with increasing volume fraction of nanoparticles. Particle shape and size also influenced the thermal conductivity enhancement of the nanofluids. However, it is not clear if the surface area rather than particle shape is the determining factor since rods have a larger surface area than spheres.

2.1.4.3 Carbon nanotubes

- **Rheological properties**

Grulke et al. [79] studied the viscosity of nanotube suspensions and found a close relationship between viscosity and thermal conductivity where both increased with the size of the agglomerates. Most of their samples showed shear-thinning behaviour with a yield stress. A similar result was obtained by both Alstaedt et al. [80] and Song

[81]. In general, nanofluids containing carbon nanotubes are Non-Newtonian with a yield stress.

- **Thermal conductivity**

Carbon nanotubes suspended in various base fluids have been prepared and the thermal conductivities measured [2,11,12,82,83,84]. Choi et al. [4] reported an enhanced thermal conductivity of 160% for nanofluids consisting of oil and 1.0 vol.% of carbon nanotubes. In contrast, Liu et al. [12] reported an increase of 30% for nanofluids made up of 2.0 vol.% carbon nanotubes in synthetic poly olefin oil. When ethylene glycol was used as a base fluid to prepare suspensions of carbon nanotubes, the enhanced thermal conductivities were in agreement between different authors. Liu et al. [12] reported a 12.7% increase with a 1.0 vol.% suspension of carbon nanotubes in ethylene glycol, and Xie et al. [11] reported a 12.4% increase with a similar suspension. Water suspensions containing carbon nanotubes have been shown to have increased thermal conductivities. Xie et al. [11] reported a 7.0% increase with a 1.0 vol.% suspension of nanotubes, and Assael et al. [83] reported a 38.0 % increase with a 0.6 vol.% suspension of carbon nanotubes in water with various weight percentages of sodium dodecyl sulfate surfactant. When aqueous suspensions of carbon nanotubes with hexadecyltrimethyl ammonium bromide (1- and 3 wt.%) and Nanosperse AQ (0.7%) surfactants were prepared, the increase in thermal conductivity was 34.0% and 27.0% respectively [84].

All the results from all available experimental studies reported thus far indicate that the heat transfer properties of the nanofluids are superior to the corresponding base fluids. Al_2O_3 and CuO are the most widely utilized nanoparticles by many researchers in their experimental work. An enhancement in thermal conductivity was observed irrespective of the size of the particles and type of base fluid [4].

2.1.5 Applications of nanofluids in power generated systems

The miniaturization of mechanical and electrical components creates a need for improved heat transfer characteristics in current cooling fluids. Nanofluids have the

potential to be used as cooling fluids since the nanoparticles suspensions are not abrasive and will not clog mechanical components. These fluids have also shown to exhibit substantially higher thermal conductivities compared to the conventional heat transfer fluids. Some useful applications for nanofluids are as alternative coolants, greases, or lubricants in automotive applications, coolants for microelectronics etc. Possible applications for the nanofluids will be discussed here.

- **Ethylene glycol based nanofluids containing silver nanoparticles:**

Ethylene glycol based nanofluids could find use in industry where cooling is required for batch processing of pharmaceutical products in multi-purpose reactors [85]. Ethylene glycol is currently used by some industrial sectors as a cooling medium; however, the need for a better cooling fluid is in demand.

Another possibility for ethylene glycol based nanofluids is in the automotive industry. Car radiators are normally cooled using a mixture of ethylene glycol and water. In heavy-duty trucks or racing cars, this could lead to smaller cooling systems, which in turn, in the case of racing cars, could have a positive effect on the total weight and aerodynamics of these vehicles.

- **Transformer oil-based nanofluids containing silver nanoparticles**

Oil based nanofluids containing silver nanoparticles could find application in deep-hole drilling, where it could help improve drilling penetration rate, clean, lubricate, and cool the drilling bit. Thus, nanofluids could significantly improve drilling speed and hence make it possible to extract more oil [86].

- **Transformer oil-based nanofluids containing carbon nanotubes and silver nanoparticles supported on carbon nanotubes**

Although the nanotube dispersions do not form homogeneous suspensions, and sedimentation could occur upon standing over long periods, the great demand for these fluids lead some research groups into developing an Oscillating Heat Pipe

(OHP). The OHP produces oscillating motions that make the nanoparticles suspend in the base liquid. [87]

Other high-flux applications include superconducting magnets, novel supersonic jet aircraft, high-power microwave tubes and electronic devices such as field effect transistor structures.

- **Transformer oil-based nanofluids containing silica and silver nanoparticles supported on silica**

Nanofluids containing electrically insulating materials could find use in low voltage transformers.

Thus, the use of nanofluids, for example in heat exchangers, may result in energy and cost savings and should facilitate the trend of device miniaturization. More exotic applications of nanofluids can be envisioned in biomedical engineering and medicine in terms of optimal nano-drug targeting and implantable nano-therapeutics devices [72].

2.2 Conclusions

Literature review shows that suspensions containing nanometer-sized particles (nanofluids) show potential for use as cooling fluids due to enhanced heat transfer properties. The two-step method is the most widely used method to prepare nanofluids, however, agglomeration during drying, storage and redispersion of the nanoparticles in the base fluid are some of the drawbacks which makes the one-step method a more attractive route to nanofluids. A surfactant is generally used to prevent particle agglomeration during nanoparticle formation and also to ensure very small nanoparticles are formed. It is also known that structural differences and defects present in most nanostructures have a noticeable effect on their physico-chemical properties. The rheological properties of the nanofluids are rarely investigated.

Nanofluids containing metal nanoparticles were found to be Newtonian, whereas nanofluids containing metal oxides as well as carbon nanotubes showed non-Newtonian, shear thinning behaviour. Since the interaction forces between particles usually decrease during flow conditions, the flow resistance is also decreased. With no significant interaction forces between the particles, separation of the particles in the form of sedimentation may occur and therefore, rheological studies could possibly provide more information about the stability of the nanofluids and also the interactions between the particles and fluid molecules. The mechanism of heat transfer will also remain a challenge for the future without the necessary theoretical background that is lacking in nanotechnology. However, experimental data from various research directions could eventually lead to a common basis towards understanding the heat transfer process.

The technological barrier is that the preparation of nanofluids using current literature methods are expensive and therefore more research is necessary to produce cost-effective nanofluids which will be easy up scalable.

To solve this problem, additional scientific study needs to be done on the influence of submicron and high aspect ratio particles on the physico-chemical properties of heat transfer fluids such as ethylene glycol, mineral oil and transformer oil.

2.3 Objectives

The main research goals are to prepare silver nanofluids (consisting of ethylene glycol, mineral oil and transformer oil containing silver nanoparticles, carbon nanotubes and silica) that are stable and investigate the effect of the various suspended nanoparticles on the thermal conductivity, the viscosity and the dielectric strength of the produced nanofluids. Based on the results, a recommendation will be given towards the potential application of the nanofluids. The methods used to prepare the nanofluids should be economically attractive, simple and reproducible. Amongst the various nanofluids, one nanofluid should be prepared with significant electrical strength to allow it any chance for application in electrical transformers.

The intrinsic properties of noble metal nanoparticle are strongly depended on its morphology and structure. Silver nanoparticles with different shapes have attracted a lot of interest because silver exhibits the highest electrical and thermal conductivities amongst all metals. Carbon nanotubes, however, have ~ 7 times higher thermal conductivity compared to silver, a high electric conductivity and good mechanical properties, making them ideal for use in nanofluids. Silica, with a much lower thermal conductivity than silver and carbon nanotubes, has a high thermal stability and is also chemically inert and could provide a good support for silver nanoparticles. In order to achieve the main objectives, the following workplan was developed:

1. Synthesize nanofluids based on silver nanoparticles dispersed in Newtonian liquids and study:-

- The stability of silver nanofluids and kinetics of silver nanoparticle evolution
- Influence of the exposure of wide wavelength spectrum of light on the formation of silver nanoparticles
- The effect of silver concentration during nanoparticle formation
- The effect of Poly(vinyl)pyrrolidone concentration during silver nanoparticle formation
- Influence of surfactant (nonionic, ionic and zwitterionic) behaviour during particle formation
- Use of Fe(III) as a surfactant free method to silver nanofluids
- Viscosity of silver nanofluids in ethylene glycol: Influence of silver concentration, water and temperature on the viscosity of silver nanofluids
- Thermal conductivity of silver nanofluids in ethylene glycol: Influence of silver concentration, water and absence of stabilizing surfactant on thermal conductivity

2. Synthesize nanofluids based on silver nanoparticles dispersed in Newtonian liquid such as mineral oil and study:-

- Effect of Korantin concentration on particle size

- Influence of silver concentration on nanoparticle formation
- Stability of mineral oil based silver nanofluids

3. Synthesize nanofluids based on silver nanoparticles dispersed in Newtonian liquid such as transformer oil and study:-

- Silver nanoparticle formation and structure in transformer oil: Oil based Ag-nanofluid synthesized by using a high temperature method and hydrogen reduction method
- Study of viscosity and thermal conductivity of silver nanofluids
- Influence of the absence of surfactant on the thermal conductivity of silver nanofluids
- Study of the dielectric strength of transformer oil-based silver nanofluids

4. Synthesize nanofluids based on silver nanoparticles dispersed in Non-Newtonian liquids

A) Synthesis and Physico-Chemical properties of transformer oil doped with carbon nanotubes

- Influence of carbon nanotube doping on Physico-Chemical properties of transformer oil
- Structural studies of carbon nanotubes dispersed in transformer oil
- Investigations of thermal conductivity of carbon nanotubes dispersed in transformer oil

B) Physico-Chemical properties of nanofluids based on silver nanoparticles dispersed in transformer oil modified with carbon nanotubes

- Synthesis and structural properties of nanofluids
- Rheological properties, thermal conductivity and dielectric strength of nanofluids

C) Synthesis and Physico-Chemical properties of silver nanoparticles dispersed in transformer oil doped with silica
   - Synthesis and structural studies of nanofluids dispersed in transformer oil modified with silica
   - Rheological properties and thermal conductivity of nanofluids containing silver nanoparticles and silica
   - Influence of silica concentration without silver nanoparticles on thermal conductivity
   - Influence of silver concentration on thermal conductivity in nanofluids containing silver nanoparticles supported on silica
   - Dielectric Strength of nanofluids containing silver nanoparticles and silica

By investigating all the parameters described above, it could help solve the main objectives of this work.

2.4 Thesis layout

Chapter 1 gives an introduction to the thesis and hence provides the motivation for the study. In Chapter 2, an overview of the relevant literature on the synthesis and the heat transport properties of nanofluids are provided. In section 2.2, some conclusions are drawn from the literature overview. The objectives of the work are stated in section 2.3.

Chapter 3 deals with the methods and materials that were used to prepare and characterize the nanofluid systems. Chapter 4 discusses the results obtained for investigations into the structural and physico-chemical properties of nanofluids based on silver nanoparticles in Newtonian liquids. Chapter 5 discusses the results obtained for investigations into the structural and physico-chemical properties of nanofluids based on silver nanoparticles in Non-Newtonian liquids. A summary of all the results obtained and some recommendations are given in Chapter 6.

3 CHAPTER THREE: EXPERIMENTAL

3.1 General

All glassware was cleaned with concentrated nitric acid (32 %) prior to use.

Ultra-Pure water and de-ionized water were obtained using a Modulab Water System.

All mineral oil based nanofluids (reactions and characterization) was performed at the Max-Planck-Institute (MPI), Germany and the results have been published [7]. Other sections from the published article are given in the Appendix (8.1).

All ethylene glycol-based and transformer oil-based nanofluids were prepared at the University of the Western Cape, South Africa.

The concentration of silver in all experiments is reported as vol.%, which was calculated based on the density of the bulk metal (10.49 kg/l) and the mass of the salt used.

3.2 Chemicals: Source and Purity

Table 3-1: Gases and chemicals used to perform the reactions

GAS	Supplier	Purity
Air	Afrox, South Africa	IG
10 % H_2 in Ar	Afrox, South Africa	Alpha Standard
LPG	Afrox, South Africa	IG
N_2	Afrox, South Africa	IG
ACID		
Nitric acid AR	Kimix	55%
Sulfuric acid AR	Kimix	98%
BASE LIQUIDS		
Ethylene glycol	Saarchem	AR; d = 1.113-1.116 kg/l
Mineral oil	Wunsch	TW 12
Transformer oil	Eskom Brackenfell,	d = 0.86 kg/l
SOLVENTS		
Toluene	Saarchem	99%
STABILIZERS		
Korantin SH	BASF	AG
Oleic acid	Alfa Aesar	99%
Oleylamine	Aldrich	70%
Poly(dipropylene glycol) phenyl phosphite	Aldrich	-
PVA	Fluka	MW = 15 000 g/mol
PVP K15	Fluka	MW = 10 000 g/mol
Sulfobetaine	Fluka	97%
NANOFLUID PRECURSORS		
Ferric nitrate	Saarchem	Unilab
Fumed silica, SA 380 m^2/g	Aldrich	99.8%
$LaNi_5$	Guangzhou Research Institute of Non-Ferrous Metals (China)	-
MWCNTs	Cheap Tubes Inc. (USA)	>95 wt%
Silver nitrate	Kimix	AR
Silver lactate	Alfa Aesar, Germany	AR

3.3 Methods used for structural characterization

3.3.1 Ultraviolet-Visible Spectroscopy (UV-VIS)

UV-VIS spectroscopy analyses were performed on a Varian Cary 500 UV spectrophotometer. To measure absorbancies during the reaction, known small volumes of samples were taken at different times and diluted with base liquid to give a final concentration of 0.5 mM. However, colour changes were observed in some cases after dilution and therefore it was decided, for further studies, to collect the samples straight from the reaction flask without dilution. Most samples were taken during and after the reaction and analyzed using 1-cm path length quartz cells.

3.3.2 Transmission Electron Microscopy (TEM)

Transmission Electron Microscopy (TEM) is used to determine the size, distribution and the morphology of the synthesized nanoparticles. A drop of the sample was placed on a Formvar coated Cu grid and dried at room temperature (RT). Selected Area Electron Diffraction (SAD) is used to confirm crystallinity of the samples.

TEM measurements were performed using a Hitachi H 800 instrument operated at an accelerating voltage of 200 kV (Electron Microscopy Unit, University of the Western Cape). The TEM samples were prepared by placing a drop of the colloidal dispersion onto a copper grid coated with a carbon film. The oil samples were mixed with toluene prior to dispersion on the copper grid. For the mineral oil-based nanofluids a Hitachi HF 2000 TEM operating at 200 kV was used. In order to determine the particle size, 2-3 of the particle images were taken randomly. The average particle size (d) and standard deviation (σ) were obtained from n_i number of particles ($n_i \geq$ 100 particles, unless otherwise specified) and calculated with equations:

$$d = \frac{\sum n_i d_i}{\sum n_i} \text{ and } \sigma = \left[\frac{\sum n_i (d_i - d)^2}{\sum n_i} \right]^{1/2}$$

Some of the TEM micrographs were taken at the Electron Microscopy Department, University of Cape Town, using a Leo 912 in-column EFTEM with OMEGA spectrometer.

3.3.3 Fourier Transform Infrared Spectroscopy (FT-IR)

Infrared spectra were recorded on a Perkin Elmer FT-IR Paragon 1000 spectrophotometer. Solid samples were recorded on potassium bromide pellets.

3.3.4 Inductively Coupled Plasma Spectroscopy (ICP)

Microanalysis for mineral oil-based nanofluids was performed by Kolbe Microanalysis Laboratory, Muelheim an der Ruhr, Germany.

The supernatant solutions, obtained from etching $LaNi_5$ by stirring in HNO_3:H_2SO_4 (1:1) for ½ hr prior the carbon nanotubes synthesis, were analyzed using Inductively Coupled Plasma (ICP) Spectroscopy. Analysis was performed at Stellenbosch University (Geology Department), South Africa.

3.3.5 Scanning Electron Microscopy/Energy Dispersive Spectroscopy (SEM/EDS)

A Hitachi X650 Scanning Electron Microscope (SEM) was used together with Energy Dispersive Spectroscopy (EDS) to determine the morphology as well as the elemental composition of the prepared nanoparticles. Samples are prepared by dropping/glueing some of the prepared nanofluids/solids onto aluminum stubs and allowing them to dry at room temperature. Some of the samples were analyzed at the Electron Microscopy Department, University of Cape Town.

EDS measurements of $LaNi_5$ were carried out using Hitachi S-4800 instrument located at the Institute for Energy Technology (IFE), Kjeller, Norway.

3.3.6 X-Ray Diffraction (XRD)

XRD spectra were recorded at iThemba Labs, Cape Town using a Bruker AXS D8 Advance diffractometer. XRD data were taken with CuKα radiation (λ = 1.5418 Å), on the powder diffractometer operated in the θ/2θ mode primarily in the 30-90° (2θ) range and step-scan of Δ2θ = 0.05°. Liquid samples were prepared using

nanofiltration membranes, where samples were filtered through the membranes and analysis was done on the membranes containing the nanoparticles.

3.3.7 Thermogravimetric Analysis

Oil-based nanofluids containing CNTs were washed with toluene and filtered through membrane filters (47 mm Nitrocellulose (Millipore) with pore size of 0.025 μm). Thermogravimetric analysis (TGA) of the dried CNT and Ag/CNT powders was carried out in air on a Rheometric Scientific Simultaneous Thermal Analyzer (STA) in the temperature range RT-900˚C at a scan rate of 5˚C/min.

3.4 Methods used for characterization of physico-chemical properties

3.4.1 Rheological properties: Viscosity

Viscosity measurements were performed using a Paar-Physica MCR 300 Rheometer (Cape Peninsula University of Technology (CPUT), Cape Town) at 30 °C.

3.4.2 Thermal conductivity

3.4.2.1 The hot-wire apparatus and procedure

The transient hot-wire method is one of the fastest and most accurate means to thermal conductivity measurements of fluids. The apparatus consists of a thin (101 micrometers coated, 51 micrometers bare) Teflon coated platinum wire (A-M Systems, Inc., 5.8 cm) in a 30.0 mL container. The platinum wire was soldered at each end to tinned copper wire. The soldered points were covered with a layer of epoxy which is an electrically insulating polymer. Since the resistance of the Pt wire is much higher than the resistance of the relatively thick current leads and tin solder points, only the resistance from the Pt wire was taken into account. A schematic of the apparatus is shown in Figure 3-1.

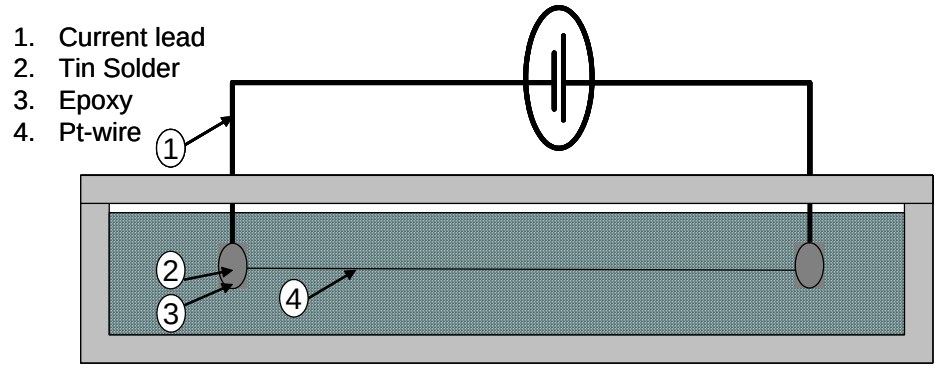

Figure 3-1: Schematic diagram of Hot-wire apparatus used for thermal conductivity measurements.

In order to derive the thermal conductivity, the temperature/time response of the platinum wire was recorded while a known current was passed through the wire. The wire is used as both a heater and a thermometer.

The slope of the resistance versus Log(time) is directly proportional to the thermal conductivity. In order to find the thermal conductivity, the "instrument factor" (Figure 3-2) was determined using ethanol (thermal conductivity: 0.14 W/Km)). The instrument factor was determined by the quotient of the temperature and the time. In order to check the validity of the instrument two other liquids ((methanol, thermal conductivity: 0.21 W/Km) and acetone (thermal conductivity: 0.16 W/Km)) were subjected to the hot wire experiment. The thermal conductivy was calculated using the instrument factor and compared with the theoretical value. The instrument was found to be very accurate showing not more than 1% deviation (theoretical/ experimental values of the thermal conductivy).

A typical "temperature versus time reponse" is shown in (Figure 3-2). The thermal conductivity of the nanofluid is inversely proportional to the slope of the temperature versus time response of the platinum wire.

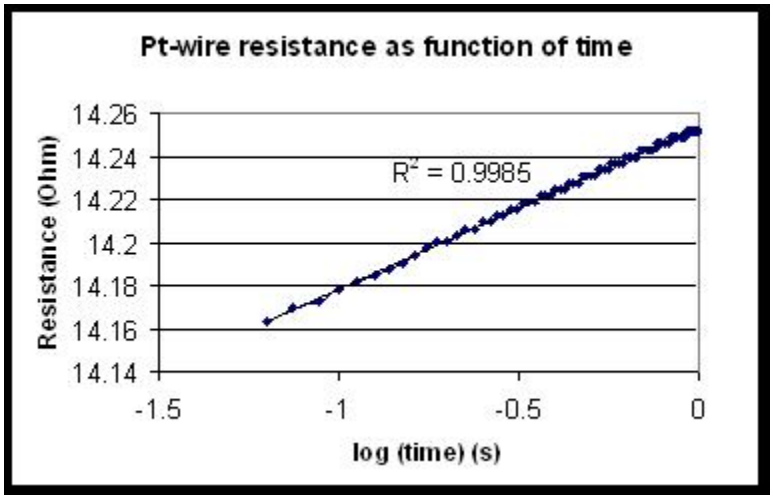

Figure 3-2: Validation and principle of Hot-wire method used for thermal conductivity measurements.

In a typical procedure, ~30ml of sample is poured into the reservoir of the hot-wire apparatus and allowed to stand for a few minutes before each measurement to minimize the effect of convection. A current of 0.1 A was applied. The duration of the measurement was 4s with a step of 0.05s.

3.4.3 Karl-Fischer

Water content of the samples was determined by Karl-Fischer Titration. The sample (0.5ml) was pipetted into a titration vessel containing methanol and titrated against Iodine. Results are given as % water present. The Karl Fischer Titrator (CPUT, Bellville) was used to determine the percentage water present in some samples.
Some of the oil samples were analyzed at ESKOM Enterprises, Brackenfell, using a 684 Metrohm KF Coulometer.

3.4.4 Electrical Properties: Dielectric Strength

All dielectric strength measurements were performed at ESKOM Enterprises, Brackenfell, using a BAUR Dielectric tester DTA. 1-Liter samples were needed for the analysis.

3.4.5 Acidity

Acid analysis was performed at ESKOM Enterprises, Brackenfell, using acid-base titrations. The acid solution consisted of 40% ethanol and 60% toluene and the base was KOH.

3.5 Synthesis of nanofluids based on silver nanoparticles in Newtonian liquids

Various nanofluids have been prepared containing silver nanoparticles suspended in ethylene glycol, mineral oil and transformer oil. Ethylene glycol based nanofluids were used as the model system since the preparation of silver nanoparticles in ethylene glycol is well documented in literature and therefore, the effect of various parameters, such as the effect of a wide spectrum of light, different surfactants, and the addition of Fe(III) on particle formation and structure have been investigated. All experimental details pertaining to ethylene glycol-based nanofluids are given in Section 3.5.1. Experimental methods for all mineral oil-based nanofluids are presented in Section 3.5.2, followed by the experimental details of transformer oil-based nanofluids in Section 3.5.3.

3.5.1 Synthesis of ethylene glycol based nanofluids containing silver nanoparticles

Chemical reduction pathways have been employed to synthesize ethylene glycol-based nanofluids, using the base fluid as the reducing agent as well as the solvent. PVP was used as the surfactant in most reactions. It has been shown that lower molecular weight PVP (MW < 15 000) could arrange itself to provide better coverage on the surface of silver colloids than those of higher molecular weight PVP (MW > 29 000) [97]. Based on this finding, PVP (MW ~10 000) was used in this research.
Silver and iron oxide containing nanofluids have been synthesized by direct mixing of the metal salt, stabilizer and base fluid at room temperature or slightly elevated temperatures by means of magnetic stirring. Since all the reactions were performed in

glassware, the effect of a wide spectrum of light on silver nanoparticle formation was investigated by performing the reactions in a reaction flask covered with aluminium foil.

A typical synthesis for the PVP-stabilized silver nanofluid is as follows:

PVP-stabilized Ag nanofluid

For 0.5 vol.% (0.5 M) Ag nanofluid: $AgNO_3$ (8.2600 g, 48.63 mmol) was dissolved in ~90ml ethylene glycol and PVP (0.5 g, 0.05 mmol) was dissolved in ~10ml ethylene glycol at RT. The PVP solution was then added dropwise over 10 minutes to the solution containing silver nitrate. A yellow solution resulted immediately upon reaction, showing the onset of silver nanoparticle formation. It was then allowed to stir at RT for a few days. The reaction conditions of some PVP-stabilized silver nanofluids are given in Table 3-2.

Table 3-2: Reaction conditions for EG-based nanofluids containing silver nanoparticles

Sample No.	$AgNO_3$ (M)	Surfactant	Surfactant (mM)	$C_2H_6O_2$ (ml)	Rxn temp (°C)	Rxn time (days)
3.5.1.1	0.01	PVP	0. 5	100	RT	8
3.5.1.2	0.01	PVP	0. 5	100	RT	3
3.5.1.3	0.04	PVP	0. 5	100	RT	5
3.5.1.4	0.07	PVP	0. 5	100	RT	5
3.5.1.5	0.1	PVP	0. 5	100	RT	5
3.5.1.6	0.3	PVP	0. 5	100	RT	5
3.5.1.7	0.3	PVP	0.1	100	RT	5
3.5.1.8	0.5	PVP	0. 5	100	RT	5
3.5.1.9	0.5	-	-	100	RT	5
3.5.1.10	0.002	-	-	100	RT	5
3.5.1.11	0.7	PVP	0. 5	100	RT	5
3.5.1.12	1.0	PVP	0. 5	100	RT	5
3.5.1.13	0.01 (Foil)	PVP	0.5	100	RT	5
3.5.1.14	0.01 (No foil)	PVP	0.5	100	RT	5

Influence of surfactant (nonionic, ionic and zwitterionic) behaviour during silver nanoparticle formation

Besides PVP, other surfactants such as PVA, Poly(dipropylene glycol) phenyl phosphite and SB12 were used in order to investigate the effect of different surfactants on particle size and morphology, and hence which surfactant offered the best capping abilities for silver nanoparticles.

Each surfactant, however, showed a unique contribution towards the formation of silver nanoparticles, where in the presence of some, no silver nanoparticles formed until the temperature was increased to above 100 °C. The surfactant to metal ratio for all the reactions described in this section is 1:1. Typical synthesis procedures are as follows:

- **EFFECT OF NONIONIC SURFACTANT: Polyvinylalcohol**

PVA (17.8623 g, 1.19 mmol) was dissolved in 80 ml ethylene glycol at 60 °C. A solution of $AgNO_3$ (0.2200 g, 1.30 mmol) in 20 ml ethylene glycol was added dropwise to the yellow suspension of PVA in ethylene glycol. It was allowed to stir at 60 °C for 3 hours and overnight at room temperature.
A summary of the reaction conditions are presented in Table 3-3.

- **EFFECT OF IONIC SURFACTANT: Poly(dipropylene glycol) phenyl phosphite**

$AgNO_3$ (0.2168 g; 1.28 mmol) and Poly(dipropylene glycol)Phenyl Phosphite (0.2 ml; 1.20 mmol) were each dissolved separately in 25 ml of EG. The $AgNO_3$ solution was then added dropwise to the surfactant solution and the mixture was allowed to stir at room temperature. Unlike the PVP-system which resulted in a yellow solution once the reactants were reacted together (showing the onset of silver nanoparticle synthesis), no colour change was observed for the Poly(dipropylene glycol)Phenyl Phosphite-system. The temperature was then increased to ~60 °C. Still no reaction

occurred. The temperature was then increased to 110 °C and allowed to stir at that temperature for 2-3 hours. Reaction conditions are summarized in Table 3-3.

- **EFFECT OF ZWITTERIONINC SURFACTANT: 3-(N,N-Dimethyldodecylammonio)propanesulfonate**

$AgNO_3$ (0.2112 g; 1.24 mmol) was dissolved in ~40 ml ethylene glycol. It was then added dropwise to a solution of 3-(N,N-Dimethyldodecylammonio)propanesulfonate (0.0404 g; 1.20 mmol) in ~60ml ethylene glycol, which was previously dissolved at 60˚C. No colour change was observed. It was allowed to stir for 30 minutes at 60˚C. A colourless solution was obtained. A sample was taken for UV-VIS measurements. The temperature was increased to ~157˚C and samples were taken for UV-VIS measurements at the following temperatures and time intervals: 120˚C = 1 ½ hrs after temperature was increased; 150˚C = 45 min later; 152˚C = 30 min later; 157˚C = 20 min later; RT = next day. Reaction conditions are summarized in Table 3-3.

Surfactant free method to silver nanofluids: Use of Fe(III)

Iron is believed to remove oxygen from the surface of the seeds during growth of silver particles and thereby prevent etching of the silver nanoparticles [88]. In addition, iron is normally found as a contaminant in ethylene glycol due to the steel vessels in which ethylene glycol are usually stored in. Therefore, the effect of iron on the formation of silver nanoparticles was investigated. Reaction conditions are also summarized in Table 3-3.

Effect of Fe(III) concentration on the stability of silver nanofluids at different temperatures: $AgNO_3$ (0.3181 g; 1.87 mmol) and $Fe_2NO_3{\cdot}9H_2O$ ((0.8175 g; 2.02 mmol) or (0.3074 g, 0.76 mmol)) was dissolved in 100 ml ethylene glycol at RT. The solution was allowed to stir overnight.

Effect of sequence in the preparation of silver nanofluids in the presence of Fe(III)

Dropwise addition:

$AgNO_3$ (0.5020 g; 3.00 mmol) was slowly dissolved in 90 ml EG. Ferric nitrate (0.0660 g; 0.16 mmol) was dissolved in 10ml EG. The ferric nitrate solution was then added dropwise over 15 minutes to the colourless solution containing silver nitrate. It was left to stir uncovered overnight and over a few days.

Mixing all reactants at once:
$AgNO_3$ (0.5166 g; 3.04 mmol) and ferric nitrate (0.0640 g; 0.16 mmol) was dissolved in 100 ml ethylene glycol at RT. The solution was allowed to stir overnight.

Table 3-3: Reaction conditions for EG-based nanofluids containing silver nanoparticles and varying surfactants and an iron salt. The surfactant concentrations are based on a 1:1 ratio between the silver and the surfactant.

Sample No.	$AgNO_3$ (M)	Fe_2NO_3 (M)	Surfactant	Surfactant (mM)	Rxn temp (˚C)	Rxn time (days)
4.1.2.15	0.01	-	PVA	0.01 M	65	3 hrs
4.1.2.16	0.01	-	PDPP	0.3 M	110	3 hrs
4.1.2.17	0.01	-	SB12	0.05 M	157	3 hrs
4.1.2.18	0.03	0.002	-	-	RT	7
4.1.2.19	0.03	0.002	-	-	100	3 hrs
4.1.2.20	0.03	0.008	-	-	RT	7
4.1.2.21	0.03	0.008	-	-	100	3 hrs
4.1.2.22	-	0.008	PVP	0.01	RT	7
4.1.2.23	0.03	0.008	PVP	0.01	RT	7

3.5.2 Synthesis of mineral oil based nanofluids containing silver nanoparticles stabilized by Korantin SH

Ag-colloid was prepared by thermal decompostion of Ag-lactate in the presence of Korantin SH. Unlike PVP, which was the surfactant of choice in the ethylene glycol-based nanofluids, Korantin SH is an apolar surfactant which dissolves easily in oil. The experiment was performed under Argon as well as in air. Different

concentrations of Ag namely 0.3 vol.%, 0.011 vol.% and 0.001 vol.% were prepared and the amount of surfactant was varied.

A typical procedure is as follows: For 0.011 vol.% Ag-colloid in mineral oil, Ag-lactate (0.32 g, 1.60 mmol), mineral oil (150 ml) and Korantin SH (1.08 g, 3.05 mmol) were stirred together at room temperature for ½ hour. The temperature of the oil bath was increased from RT to 90ºC. The mixture was heated for a total of 4 hours.

3.5.3 Synthesis of transformer oil based nanofluids containing silver nanoparticles

Transformer oil based samples were produced in two different ways. In the first method, the transformer oil itself was used as reducing agent. In the second method, hydrogen was used as the reducing agent. Both methods are described in section 3.5.3.1 and 3.5.3.2 resepectively. Hydrophobic stabilizers were used to prevent particle agglomeration. The complete overview of concentrations and other changing parameters is given Table 3-4 below.

A typical synthesis is as follows: $AgNO_3$ (0.2160 g, 1.27 mmol) was dissolved in 50 ml transformer oil at ~60 °C. Oleylamine (1.0 ml, 3.04 mmol) was dissolved in 50 ml transformer oil and the resulting yellow solution was added dropwise over ~15 minutes to the warm grayish yellow suspension of silver nitrate in transformer oil. The suspension was then subjected to each of the following two methods described above. A summary of the reaction conditions used for both methods is given in Table 3-4 and the detailed experimental procedures are presented below.

3.5.3.1 Oil-based Ag nanofluid synthesized by using a high temperature method:

During addition, the temperature was increased to 130 °C and once addition was complete, the heater was switched off and the suspension was allowed to stir overnight at room temperature.

3.5.3.2 Oil-based Ag nanofluid synthesized by using a hydrogen reduction method: Influence of reaction time.

The orange brown suspension was taken off the stirrer as soon as addition was complete. 10% H_2 in N_2 was then bubbled through the suspension (20 ml/min) using a borosilicate Pasteur pippette for 1 hour while sonicating in a 40 °C water-bath.

Table 3-4: Reaction conditions for oil-based nanofluids containing silver nanoparticles

Sample No.	$AgNO_3$ (M)	Surfactant	Surfactant (mM)	Rxn temp (˚C)	Red. agent	Rxn time (hrs)
3.5.3.1	0.01	Oleylamine	3.04	130	oil	2
3.5.3.2	0.01	Oleylamine	3.04	40	H_2	1
3.5.3.3	0.01	Oleylamine	3.04	130	oil	2
3.5.3.4	0.01	Oleylamine	3.04	40	H_2	6
3.5.3.5	0.001	-	-	130	oil	2
3.5.3.6	0.01	-	-	130	oil	2
3.5.3.7	0.5	-	-	130	oil	2

3.6 Synthesis of nanofluids based on silver nanoparticles in non-Newtonian liquids

The experimental methods used to study the effect of silver nanoparticles dispersed in transformer oil, which was doped with either carbon nanotubes or silica are presented in Sections 3.6.1 and 3.6.2 respectively.

3.6.1 Synthesis of transformer oil based nanofluids containing nanotubes and silver nanoparticles supported on carbon nanotubes

All the homemade nanotubes used were prepared by a hydrocarbon pyrolysis method. See Appendix (8.2) for further details.

Various carbon nanotube-based nanofluids have been synthesized and the thermal conductivity of the nanotubes has been measured. To prepare the nanotube-based nanofluids, carbon nanotubes were mixed with the base fluid and surfactant, followed by sonication in an ultrasound bath for 2–5 hours or heat treated at 130˚C for 2 hours. However, sonication caused the nanotubes to break. This was also observed by others [89] and hence resulted in lower aspect ratios, and in turn lower thermal conductivity values were observed. Stirring at increased temperature was used in an attempt to disperse the nanotubes in the oil. Oleylamine and oleic acid were used for stabilization purposes.

Some of the synthesized carbon nanotubes were subjected to pre-treatment. The pre-treatment step is an acid reflux treatment whereby various oxygen groups could be introduced onto the surface of the nanotubes. The acid reflux treatment consisted of a 4.0 hour reflux in a 50 ml mixture of concentrated sulphuric and nitric acids (1:1 by volume sulphuric: nitric acid), after the mixture had cooled down it was diluted with de-ionized water then filtered through a membrane filter (47 mm Nitrocellulose (Millipore) with pore size of 0.025 μm). The nanotubes were then washed with de-ionized water and centrifuged (Sigma 3-18, 10 000 rpm), until the pH of the filtrate was between 6 and 7, and then dried in an oven at 200˚C for ½ hr.

Nanofluid containing carbon nanotubes without surfactant

Homemade or commercial carbon nanotubes (0.3750 g, 1.0 wt%) was mixed with transformer oil (50 ml) and allowed to stir for ½ hr at room temperature. The temperature of the hotplate was then increased to 130 °C and the mixture was allowed to stir at that temperature for ~2hrs. A thick black mixture was obtained, which later settled at the bottom of the flask.

Nanofluid containing carbon nanotubes stabilized by oleylamine

Oleylamine (2.0042 g, 7.5 mmol, 4.3 wt%) and commercially obtained carbon nanotubes (1.6704 g, 3.5 wt%) were mixed together. Transformer oil (50 ml) was the added and the mixture was stirred for 10 minutes at room temperature. The temperature of the hotplate was then increased to 130 °C and the mixture was allowed to stir at that temperature for ~2hrs. A thick black mixture was obtained, which later settled at the bottom of the flask.

Nanofluid containing oleic acid- stabilized silver nanoparticles (0.07 vol.%) on 3.0 wt% homemade/commercial carbon nanotubes

Homemade, acid treated carbon nanotubes (1.4396 g, 3.1 wt%) and $AgNO_3$ (0.5786 g, 3.4 mmol, 1.2 wt%) were mixed with oleic acid (0.5609 g, 1.99 mmol, 1.2 wt%) in transformer oil (50ml) by mechanical aggitation. The mixture was heated at 130 °C for 2hrs. A black mixture was obtained, which later settled at the bottom of the flask.

A summary of the reaction conditions of oil-based nanofluids containing CNTs with and without silver nanoparticles is given in Table 3-5.

Table 3-5: Reaction conditions for CNT-based nanofluids with and without silver nanoparticles. All nanofluids were prepared using acid-treated CNTs, except for sample numbers 4.1.4.10, 4.1.4.11, 4.1.4.12, 4.1.4.13, and 4.1.4.15, where untreated CNTs were used.

Sample #	Ag (vol%)	CNT's (wt%)	Surfactant	Oil (ml)	Temp (°C)
4.1.4.1	0.07	4	Ol-amine (0.16M)	100	130, 2 hrs
4.1.4.2	-	4	Ol-amine (0.16M)	50	130, 2 hrs
4.1.4.3	-	3	Oleic acid (0.1M)	50	130, 2 hrs
4.1.4.4	0.07	3	Oleic acid (0.1M)	50	130, 2 hrs
4.1.4.5	0.07	3	Oleic acid (0.04M)	50	130, 2 hrs
4.1.4.6	0.07	3	Oleic acid (0.04M)	50	130, 2 hrs
4.1.4.7	0.07	1	Ol-amine (0.08 M)	1000	130, 2 hrs
4.1.4.8	0.07	1	Oleic acid (0.04M)	50	130, 2 hrs
4.1.4.9	0.07	1	Oleic acid (0.08M)	100	130, 2 hrs
4.1.4.10 (comm.)	-	1	Oleic acid (0.04M)	40	130, 2 hrs
4.1.4.11 (home)	-	1	Oleic acid (0.04M)	50	130, 2 hrs
4.1.4.12 (home)	-	1	-	50	130, 2 hrs
4.1.4.13 (home)	-	0.4	-	50	130, 2 hrs
4.1.4.14 (comm.)	-	1	Oleic acid (0.04M)	50	130, 2 hrs
4.1.4.15 (comm.)	-	0.4	-	50	130, 2 hrs

3.6.2 Synthesis of transformer oil based nanofluids containing silica and silver nanoparticles supported on silica

Nanofluids containing silica, with varying concentrations, were prepared by a one-step method where silica was mixed together with the base fluid by means of magnetic stirring and allowed to stir for 2 hours at 130˚C.

Silver nanoparticles supported on silica were prepared in a similar way by introducing the precursors to the base fluid and increasing the temperature to 130˚C for 2 hours. A typical procedure is as follows:

Nanofluid containing 0.03 vol.% silver on 0.07 wt% silica:

$AgNO_3$ (0.2183 g; 1.29 mmol) and SiO_2 (0.0294 g; 0.49 mmol) were added to 50 ml oil and stirred for ½ hr. The temperature was then increased to 130˚C and allowed to

stir at that temperature for 2 hrs. A summary of the reaction conditions of oil-based nanofluids containing silica with and without silver nanoparticles is given in Table 3-6.

Table 3-6: Reaction conditions for silica-based nanofluids with and without silver nanoparticles

Sample #	Ag (vol%)	SiO_2 (wt%)	Surfactant	Oil (ml)	Temp (°C)
4.1.5.1	-	4.4	-	50	130, 2 hrs
4.1.5.2	-	1.8	-	50	130, 2 hrs
4.1.5.3	0.06	1.4	-	50	130, 2 hrs
4.1.5.4	-	1.4	-	50	130, 2 hrs
4.1.5.5	-	0.5	-	50	130, 2 hrs
4.1.5.6	0.06	0.5	-	50	130, 2 hrs
4.1.5.7	0.03	0.5	-	50	130, 2 hrs
4.1.5.8	0.01	0.5	-	50	130, 2 hrs
4.1.5.9	-	0.3	-	50	130, 2 hrs
4.1.5.10	0.03	0.07	-	50	130, 2 hrs
4.1.5.11	0.06	0.07	-	50	130, 2 hrs
4.1.5.12	0.01	0.07	-	50	130, 2 hrs

4 CHAPTER FOUR: NANOFLUIDS BASED ON SILVER NANOPARTICLES DISPERSED IN NEWTONIAN LIQUIDS – RESULTS AND DISCUSSION

As mentioned in Chapter 2, nanofluids can be prepared by either a one-step or a two-step method and are usually obtained by combining conventional heat transfer fluids with metallic nanoparticles that has a much higher thermal conductivity than the former. Most fluids, including heat transfer fluids, show Newtonian flow behaviour, implying a constant viscosity with an increase in shear rate.

The preparation of monodisperse metal nano-colloids usually requires the addition of a protective agent (a surfactant or polymer), whose main role is to prevent particle agglomeration. Polymer coatings on particles are said to reduce susceptibility of particle aggregation, enhance compatibility with organic ingredients and protect particle surfaces from oxidation [90].

The synthesis of silver nanofluids via one-step methods for cooling applications is not well documented in literature. This method entails the synthesis of the nanoparticles directly in the heat transfer fluid such as ethylene glycol, mineral oil, or transformer oil. The favorable thermal properties of silver and carbon nanotubes placed them on top of the preferential list for enhancing the heat transfer properties of conventional cooling fluids. Herein the results obtained for hydrocarbon Newtonian fluids such as ethylene glycol, mineral oil and transformer oil, all containing silver nanoparticles, are reported and discussed in Sections 4.1, 4.2, and 4.3 respectively.

4.1 Nanofluids based on silver nanoparticles dispersed in Newtonian liquid -ethylene glycol as model system: Synthesis, structure and physico-chemical properties

Ethylene glycol is a dihydroxy alcohol derivative of aliphatic hydrocarbons. It is a Newtonian fluid since its viscosity remains constant with an increase in shear rate. Ethylene glycol is most often found in various antifreeze solutions and coolants and is commonly used as a coolant for car radiators. Due to its low freezing point, it is also used to deice windshields and aircraft. It has also found a use in brake fluid (due to its high boiling point), paints, glass cleaners and cosmetics.

The preparation of silver nanoparticles, in contrast to the synthesis of silver nanofluids, is well documented in literature [91, 92, 93, 94, 95, 96, 97,21], where different surfactants and different solvents have resulted in particles with sizes ranging from 20-50 nm, whereas sizes of 4-30 nm have been reported for PVP-stabilized silver nanoparticles in ethylene glycol. Although silver nanoparticles exhibit a number of novel properties, they are particularly characterized by a very high thermal conductivity [10]. This is a very important property for heat transfer applications.

Due to the reducing ability of ethylene glycol, silver nanoparticles were obtained by mechanical stirring at room temperature, in the presence of different stabilizing agents.

The structural (sections 4.1.1 and 4.1.2), rheological and thermal properties of various ethylene glycol-based nanofluid sytems were investigated. The effect of a wide wavelength spectrum of visible light (section 4.1.3), silver concentration (section 4.1.4), PVP concentration (section 4.1.5), different surfactants (section 4.1.6) and the use of iron as a surfactant-free method (section 4.1.7) were studied with respect to particle formation, size and morphology. The rheological property under investigation

was the viscosity (section 4.1.8) including the effects of temperature and water on it. The thermal properties entailed the thermal conductivity (section 4.1.9) and the effects of silver concentration, water and surfactant on it. All the experimental details pertaining to this work are presented in section 3.5.1.

4.1.1 Silver nanoparticle formation and its structure

The silver nanoparticles were stabilized by polyvinylpyrrolidone (PVP). PVP is a nonionic amphiphilic polymer having a hydrocarbon chain with strongly polar side groups [98], exhibiting a high protection function for the stabilization of metal nanoparticles [99]. Nonionic surfactants are known to stabilize metal particles through steric effects.

Figure 4-1 shows the UV-VIS spectrum obtained for the PVP-stabilized silver nanoparticles. Since PVP has no absorption in the ultraviolet spectrum (Figure 4-1), the resulting spectrum obtained indicates the presence of silver nanoparticles.

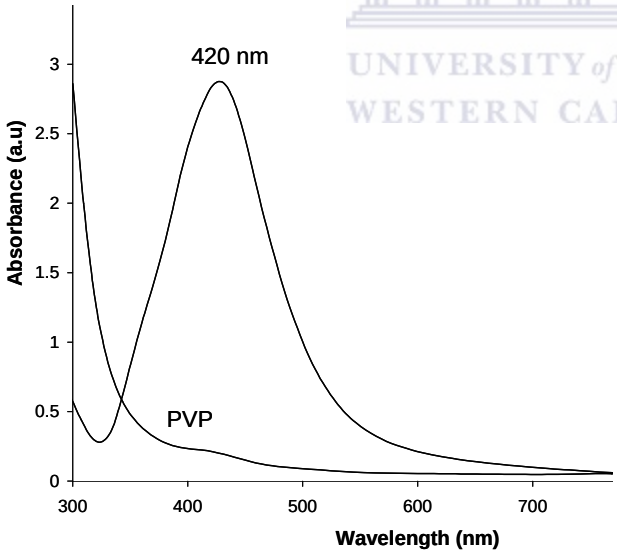

Figure 4-1 :UV-VIS spectrum obtained for 0.01 vol.% Ag nanofluid stabilized by 0.5 mM PVP, prepared at RT by mechanical aggitation. The spectrum obtained for PVP shows no absorption in the region where silver nanoparticles are known to absorb (~420 nm).

The nanofluid sample showed a symmetrical peak at 420 nm due to the surface plasmon resonance of silver nanoparticles. This peak typically represents the formation of small silver nanoparticles in solution. The UV-VIS spectrum suggests that the Ag salt has been reduced by ethylene glycol (Figure 4-1).
The broadband (97 nm) of Full Width at Half Maximum (FWHM) of the absorption spectrum suggests the presence of a broad distribution of particle size [100], implying standard deviation >>15% of average particle size [15].

TEM was used to study the size and morphology of the silver nanoparticles, which were prepared according to the procedure described in section 3.5.1. Figure 4-2 (A-B) shows the TEM micrograph with corresponding particle size distribution. The TEM micrograph revealed spherical silver nanoparticles with sizes less than 10 nm and agglomerates with sizes between 20-48 nm. A particle size distribution of 6.2 ± 5.8 nm was obtained, confirming the broad size range of the particles as evidenced by the broad UV-VIS spectrum in Figure 4-1. The particles remain well separated, despite the drying action during TEM preparation, and therefore is an indirect measure to indicate that the silver nanoparticles are well dispersed.

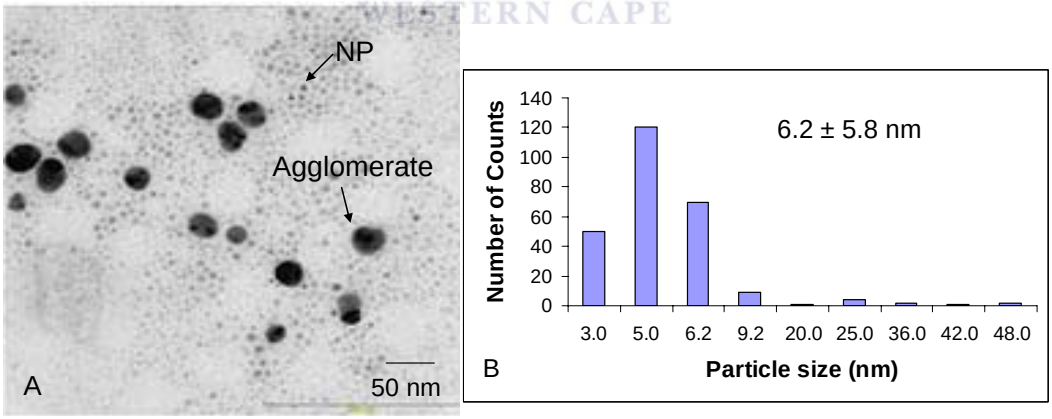

Figure 4-2: (A) TEM micrograph of (0.5 mM) PVP–stabilized silver nanofluid (0.01 vol.%), prepared at RT by mechanical stirring, with (B) corresponding particle size distribution.

It is well known that the surface free energy for nanoparticles is very high [101]. Therefore, aggregation, which is the means by which the system tries to attain the

thermodynamic equilibrium by reducing its total surface energy [101], readily occurs. For additional confirmation of the result and to exclude the possibility of artifacts instead of true silver nanoparticles in the TEM micrographs obtained, EDS analysis was performed. Figure 4-3 shows the EDS analysis obtained from TEM.

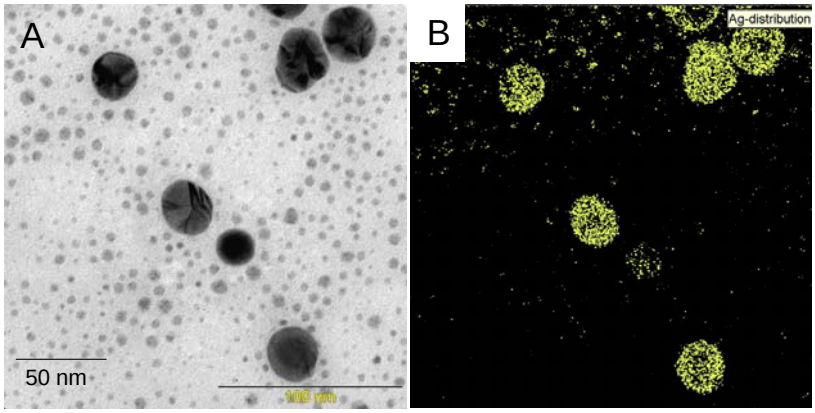

Figure 4-3: (A) TEM micrograph of (0.5 mM) PVP–stabilized silver nanofluid (0.01 vol.%), prepared at RT by mechanical stirring with (B) corresponding EDS analysis from TEM confirming the presence of silver nanoparticles.

All particles observed in the TEM micrograph are indeed silver nanoparticles and the larger particles are aggregates of many small ones (Figure 4-3). XRD analysis further confirmed the presence of silver nanoparticles.

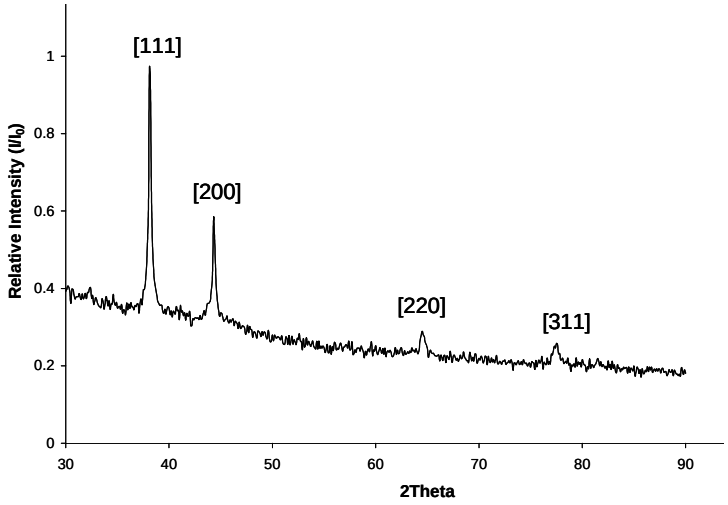

Figure 4-4: XRD pattern of silver nanoparticles protected by PVP

XRD results confirmed that the silver nanoparticles were crystalline (Figure 4-4). The diffraction peaks can be indexed to those of pure face-centered cubic (FCC), corresponding to the (111), (200), (220), and (311) planes respectively, in good agreement with literature [102].

The crystallite size was also determined by means of the Scherrer formula:

$$d = \frac{k\lambda}{\beta_{1/2}\cos\theta}$$

where β½ is the full-width at half maximum of the strongest peak at 2θ, k is a constant (k = 0.9), and λ = 1.5418Å is the CuKα1 wavelength. Considering the (111)* direction in the XRD spectrum, a value of d = 5.87 nm was found, compared to the 5.80 nm obtained from TEM analysis. Particle size calculated using the Scherrer formula agreed well with that observed by TEM.

4.1.2 Studies on the stability of silver nanofluids and kinetics of silver nanoparticle evolution

In order to investigate the kinetics of silver nanoparticle formation and study the reaction in more detail, a new nanofluid system was prepared under conditions identical to the previously prepared nanofluid system.

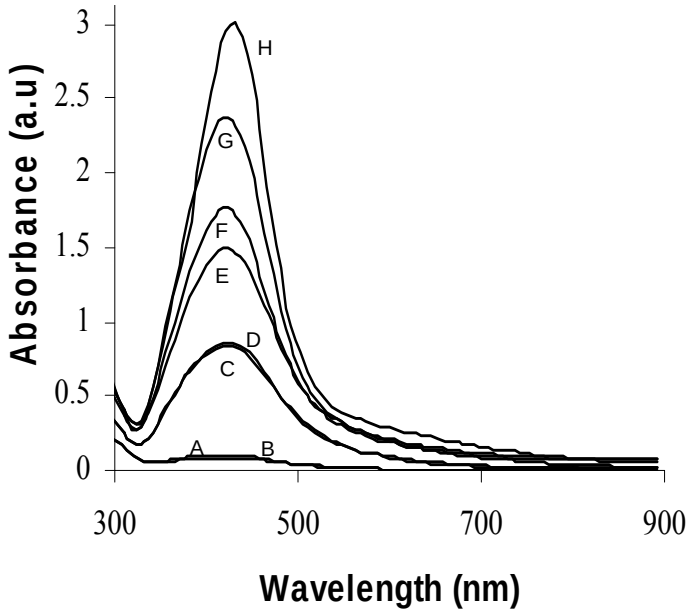

Figure 4-5: UV-VIS spectra of 0.01 vol.% Ag nanofluid stabilized by 0.5 mM PVP obtained at different times during the reaction. A = 1 hr later; B = 2 hrs later; C = 18 hrs later; D = 66 hrs later, E = 90 hrs later, F = 114 hrs later, G = 190 hrs later, H = 8 days later.

From the UV-VIS spectrum (Figure 4-5), very broad peaks were obtained at the initial stages (Times A and B) of the reaction. The absorption peak centered at about 420 nm (after 18 hours of reaction time) is the characteristic peak for silver nanoparticles and is attributed to the plasmon absorption band of silver nanoparticles. As the reaction progressed, the peak due to surface plasmon resonance (SPR) became more pronounced and highly symmetrical, showing the presence of monodisperse, spherical silver nanoparticles at 18 hours reaction time. At 90-114 hours reaction time, a slight peak shift to shorter wavelength (blue shift), accompanied by the higher absorption intensities is observed, indicating an increase in the amount of silver particles with very small sizes. This is due to the band gap increase of the smaller-sized particles [103]. The silver particles were generated gradually, as is clearly indicated by the increasing intensity of the surface plasmon band at ~420 nm in the UV-VIS spectra (Figure 4-5). At 190 hours reaction time, a broader peak, which was slightly red-shifted, was observed as the particle size started increasing, probably due to Ostwald ripening and coalescence [104]. Figure 4-5 also shows the absorption spectrum obtained for the Ag nanofluid after 8 days. From the spectrum, a much

higher concentration of silver nanoparticles was found and slightly bigger particles were expected as a result of the much wider FWHM at the end of the reaction. This could be due to the difference in the reaction time since a broadening of the absorption peak was observed as the reaction progressed. Time H corresponds to 8 days of reaction time, whereas Time G only represents 3 days of reaction time. Since only one absorption peak was obtained, the particles were mainly spherical [105], in agreement with previously discussed TEM results.

It thus follows that the processes involved in the formation of silver nanoparticles starts off with the reduction of the soluble silver nitrate by ethylene glycol, followed by nucleation of metallic silver and then growth of the individual nuclei in the presence of a stabilizer, PVP.

4.1.3 Influence of the exposure of wide wavelength spectrum of light on the formation of silver nanoparticles

Xu et al. successfully prepared silver colloids, stabilized by PVP, by photoreduction of silver nitrate using UV-light [106]. Since light seemed to play an important role in the synthesis of silver nanoparticles, the effect of a wide wavelength spectrum of light on the formation of silver nanoparticles was investigated. Ag nanofluids were prepared in the absence and presence of a wide spectrum of light, while keeping the reaction times constant. Experimental details are given in Table 3-2.

Initial UV-VIS results showed a very broad absorption peak at 420 nm, due to the surface plasmon resonance of silver particles with a broad size distribution, and another peak around 302 nm, due to the presence of Ag clusters of various sizes and charges (Figure 4-6).

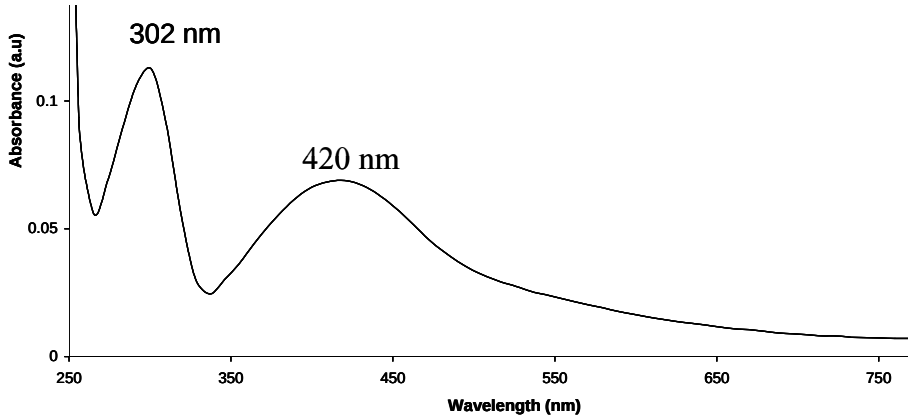

Figure 4-6: UV-VIS spectrum for silver nanofluid prepared in the absence of a wide spectrum of light

TEM further revealed the nature and size of the particles (Figure 4-7). Particle with sizes ranging from 10 nm to 450 nm were visible. Due to the slower reduction rate in the absence of light, much larger single platelets formed [107]. The larger flat platelets were in the form of irregular shaped hexagons and smaller sized spherical particles were also observed. El-Sayed et al. [108] studied the shape of Pt nanoparticles at different growth stages, and concluded that anisotropic particles form because the growth rates vary at different planes of a particle and that particle growth competes with the capping action of the stabilizer.

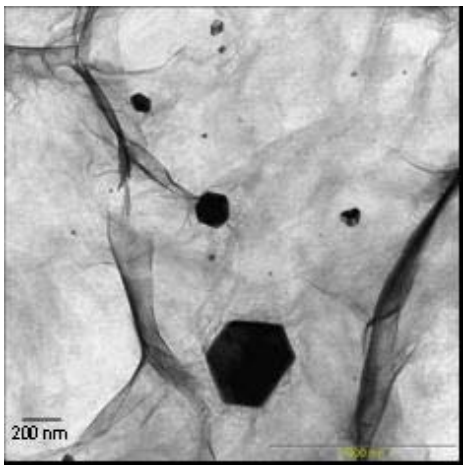

Figure 4-7: TEM micrograph of silver nanofluid prepared in the absence of a wide spectrum of light.

In addition, the reaction time of the light protected silver nanofluid was much slower compared to previously prepared nanofluids, which were prepared in a wide spectrum of light. The surface plasmon resonance peak was only visible ~7 days after the reaction was started, compared to the 1-hour reaction time observed for the reaction that was performed in a wide spectrum of light (Figure 4-5). Light therefore, plays an active role in the formation of silver nanoparticles by accelerating the reduction process. This phenomenon is also found in photography, where photons falling on a silver halide microcrystal in the emulsion cause a halide ion to lose an electron, which is then captured by a silver ion, converting it into a neutral atom and eventually gives rise to silver clusters [109].

4.1.4 Effect of silver concentration on nanoparticle formation

Various concentrations of silver nanoparticles have been prepared under identical reaction conditions and their morphologies studied. PVP was used to stabilize the silver nanoparticles. Experimental details for the prepared nanofluids are given in Table 3-2.

Figure 4-8 depicts the TEM micrographs with corresponding particle size distributions. Spherical particles with a broad size distribution were obtained in all cases. At low silver concentration, well-dispersed particles were visible with particle size distribution of 15.50 ± 6.98 nm. As the concentration was increased to 1.0 vol.% silver, agglomeration was observed since the collisions between particles becomes more frequent when a larger number of particles are in close proximity to each other. In addition, Ostwald ripening [110,111,112] could also be responsible for the increase in particle size observed at high concentrations. Particle size distributions of 16.25 ± 8.46 nm and 21.10 ± 3.65 nm were obtained for nanofluids containing 0.7 vol.% and 1.0 vol.% silver respectively.

Since the concentration of the stabilizer was kept constant, the higher concentration silver suspensions had insufficient stabilizer to capture all the particles formed during the reaction. Hence, sedimentation of silver nanoparticles and accumulation of it on

the sides of the reaction flask resulted in silver mirrors. The corresponding diffraction pattern showed that the material was polycrystalline (Figure 4-8 (insert)).

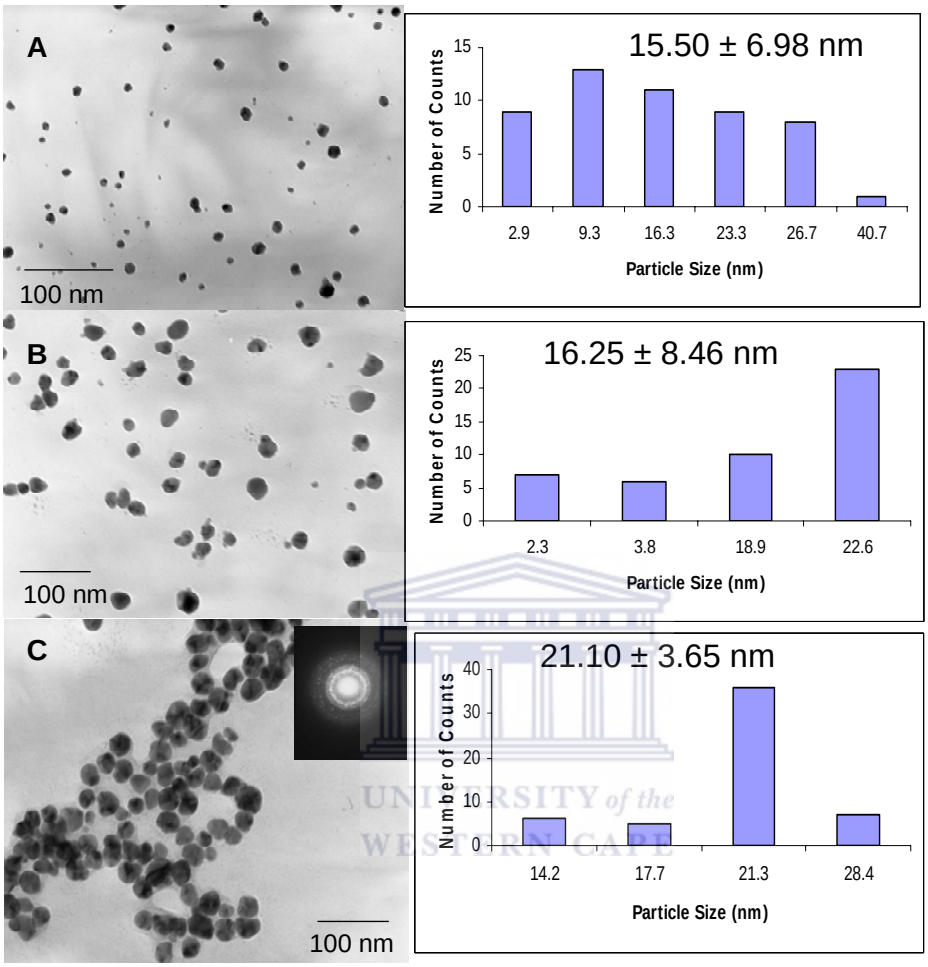

Figure 4-8: TEM micrographs and corresponding particle size distributions of PVP-stabilized silver nanoparticles at various Ag concentrations; A) 0.5 vol.% Ag, B) 0.7 vol.% Ag and C) 1.0 vol.% Ag. The inset shows the selected area electron diffraction (SAED) pattern of silver nanoparticles stabilized by 0.5 mM PVP in ethylene glycol.

It is evident from the TEM micrographs and in correspondence with literature that spherical particles are obtained when PVP is used as surfactant [113] and that the average particle size increases with an increase in silver concentration.

4.1.5 Effect of Poly(vinyl)pyrrolidone concentration on silver nanoparticle formation

The effect of PVP at a concentration of 0.1 mM compared to previously discussed 0.5 mM, on the formation of silver nanoparticle, was investigated. Experimental details are given in Table 3-2 (sample numbers 3.5.1.6 and 3.5.1.7). Higher concentrations (>0.5 mM) of PVP showed a much reduced or slower solubility.

UV-VIS spectroscopy was used as a first indication for the presence of silver nanoparticles. Figure 4-9 shows the UV-VIS spectra obtained for the silver nanofluids, which were stabilized using PVP at different concentrations (0.1 mM and 0.5 mM), as well as the absorption peak for PVP. It is noted that PVP does not absorb light in the region where silver nanoparticles are known to absorb. The characteristic peak due to the surface plasmon resonance of silver nanoparticles was observed at 414 nm (Figure 4-9) when a lower concentration of PVP (0.1 mM) was used. The absorption peak obtained for silver nanoparticles stabilized by 0.5 mM PVP was red-shifted and appeared at 430 nm, which indicates the presence of larger particles.

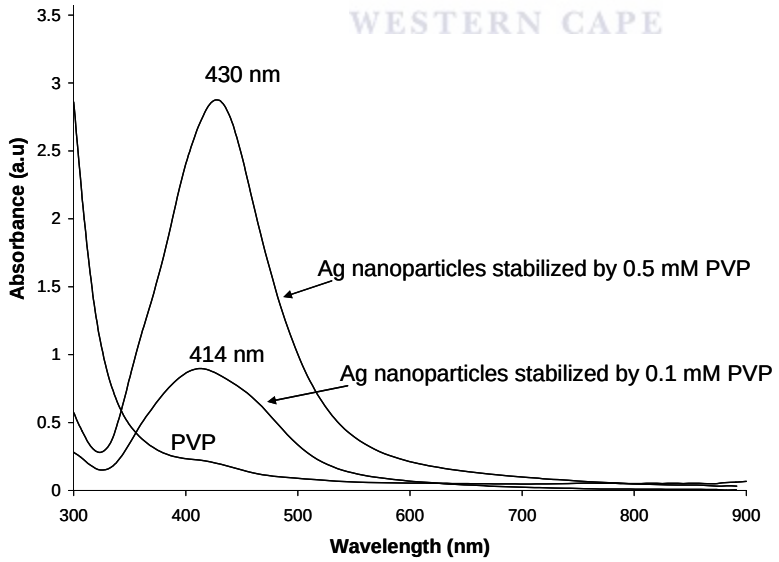

Figure 4-9: UV-VIS spectra obtained for silver nanofluid stabilized by PVP at different concentrations (0.1 mM and 0.5 mM). The spectrum obtained for PVP shows no absorption in the region where silver nanoparticles are known to absorb.

Table 4-1 shows the particle size distributions obtained when different concentrations of PVP were used to stabilize silver nanoparticles.

Table 4-1: Particle size distributions obtained for 0.3 vol.% silver nanofluids using different concentrations of PVP. Experimental details are given in Table 3-2 (sample numbers 3.5.1.6 and 3.5.1.7).

PVP concentration (mM)	Particle size distribution (nm)
0.1	10.96 ± 8.71
0.5	16.75 ± 9.93

Particle size distribution of 10.96 ± 8.71 nm and 16.75 ± 9.93 nm were obtained when 0.1 mM and 0.5 mM PVP were used to stabilize the silver nanoparticles respectively. The particle size distribution for the silver nanoparticles stabilized by 0.5 mM PVP was much broader compared to the silver nanoparticles stabilized by a lower concentration PVP, which could possibly explain the red-shift observed in the UV-VIS spectrum (Figure 4-9). The differences in size distributions observed could be due to silver mirror formation at lower concentrations (0.1 mM in Table 4-1) of PVP and hence less silver was available for particle formation, resulting in a low concentration of smaller particles.

4.1.6 Influence of surfactant (nonionic, ionic and zwitterionic) behaviour on silver nanoparticle formation

Small nanoparticles can be obtained by employing either surfactants that bind more tightly to the nanoparticle surface or larger molecules providing greater steric hindrance (bulkier surfactants). Stable dispersions are those where favorable interactions exist between the capping agents and the base fluid. This provides an energetic barrier to counteract the van der Waals attractions between nanoparticles [114].

The effects of three different kinds of capping agents have been investigated on the protecting abilities of silver nanoparticles namely, Poly(vinylalcohol) (PVA), Poly(dipropylene glycol) phenyl phosphate and 3-(N,N-Dimethyldodecylammonio)propanesulfonate (SB12/Sulfobetaine). In contrast to PVP, these surfactants needed elevated temperatures before complete dissolution.

- **EFFECT OF NONIONIC SURFACTANT: Polyvinylalcohol**

For comparison purposes, silver nanoparticles were prepared and stabilized by Poly(vinylalcohol) PVA in ethylene glycol. PVA is a hydrophilic, biocompatible polymer [115] which is often used for stabilizing magnetic particles for biomedical applications [90]. It has many uses amongst which is as a surfactant for the formation of polymer encapsulation of nanobeads.

Figure 4-10 (A) shows the UV-VIS spectrum obtained for PVA-stabilized silver nanoparticles. A relatively broad absorption peak at ~423 nm, with a FWHM of 153 nm compared to the FWHM of 97 nm for PVP-stabilized silver nanoparticles, was visible indicating the presence of larger particles. A similar spectrum was obtained by Joshi et al. [37]. In their studies, various molecular weights (14,000, 30,000 and 125,000) of PVA were used to stabilize the silver nanoparticles, and all the UV-VIS spectra obtained were broad in nature.

A very wide size distribution is responsible for the broad UV-VIS peak obtained for the PVA-stabilized silver nanofluid. Since only one peak was observed in the absorption spectrum, the particles are expected to be spherical in shape. The TEM micrograph in Figure 4-10 (B) supported the results from UV-VIS.

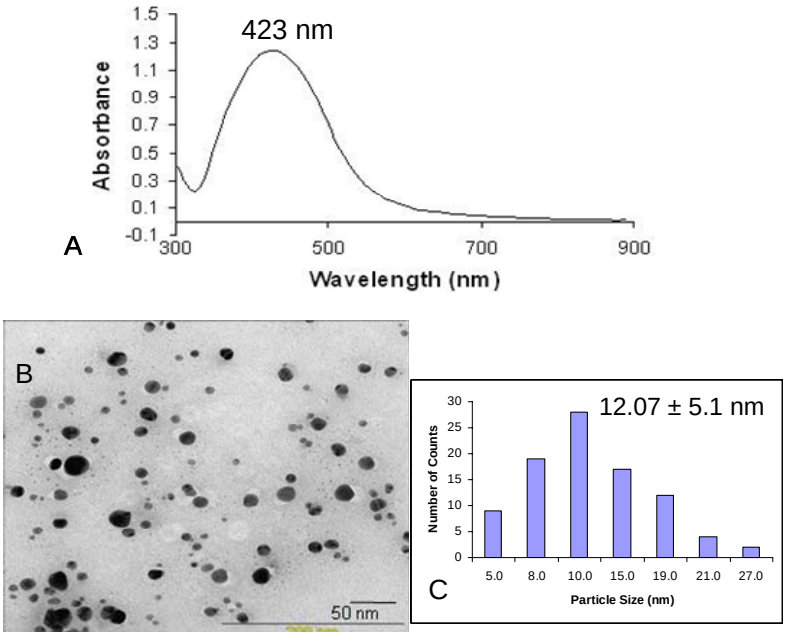

Figure 4-10: (A) UV-VIS spectrum obtained for 0.01 vol.% silver nanoparticles stabilized by 0.01 M PVA. (B) TEM micrograph of 0.01 vol.% silver nanoparticles stabilized by PVA (0.01 M) with (C) corresponding particle size distribution.

A larger average particle size with size distribution of 12 ± 5.1 nm (Figure 4-10 (C)) was obtained for PVA-stabilized silver nanoparticles compared to the 6.2 ± 5.8 nm obtained for PVP-stabilized silver nanoparticles produced using similar molar ratios of silver to surfactant (See 3.1.2 in Table 3-2 and 3.1.15 in Table 3-3). Particles are mainly spherical and well-distributed, similar to PVP-stabilized silver nanoparticles.

It has been found that PVA of high molecular mass (MW~145000) is able to produce stable silver nanoparticles [116], however, from the TEM micrograph presented in this work, the particles appear much more uniformly dispersed using lower molecular weight PVA than that reported in literature for stabilization with higher molecular weight PVA. It is believed that ions which are not yet reduced, adsorb onto atoms or small clusters formed in the initial stages of the reaction and that at this moment, PVA cannot prevent aggregation resulting in a broad size distribution [37]. Dékány et al. compared the stabilizing effects of PVP and PVA during the preparation of their silver sols using hydroquinone and sodium citrate as reducing agents. They found that

PVP provides a more effective steric stabilization and reduced the growth rate of silver nanoparticles [117], which can be supported with the results presented here.
Since the approach taken to synthesize nanoparticles often has an impact on particle size, shape and dispersity, the simple method using ethylene glycol as both the solvent and reducing agent, provides easy access to spherically-shaped silver nanoparticles dispersed in ethylene glycol.

- **EFFECT OF IONIC SURFACTANT: Poly(dipropylene glycol) phenyl phosphite**

Poly(dipropylene glycol) phenyl phosphate is a long carbon chain containing phosphate. The phosphate groups are believed to provide stabilization by complexing with silver ions during the reduction process, and hence reduce agglomeration [118].

Silver nanoparticles were prepared in ethylene glycol and stabilized by Poly(dipropylene glycol) phenyl phosphate. Since the solubility of most reagents differs from each other, some require a little activation energy in order to increase their dissolution rate. Energy in the form of heat was supplied in order to enhance the dissolution rate of Poly(dipropylene glycol) phenyl phosphate in ethylene glycol. Experimental procedures are discussed in section 3.5.1 and reaction conditions are presented in Table 3-3.

Figure 4-11 shows the TEM micrographs obtained. Particles ranging from the nanometer to the micrometer range were visible. This is due to agglomeration since the mobility of particles increases with an increase in temperature [119]. Hence, the chances of collision amongst particles to form bigger particles are much higher. This also shows that Poly(dipropylene glycol) phenyl phosphate is not a suitable capping agent for silver nanoparticles due to its inability to cap the particles during nucleation, resulting in much bigger particles compared to those obtained when PVP and PVA was used. In addition, the reaction required some energy in the form of heat to enhance the dissolution rate of Poly(dipropylene glycol) phenyl phosphate in ethylene

glycol in order to ensure all the surfactant is in solution before silver nanoparticle formation takes place.

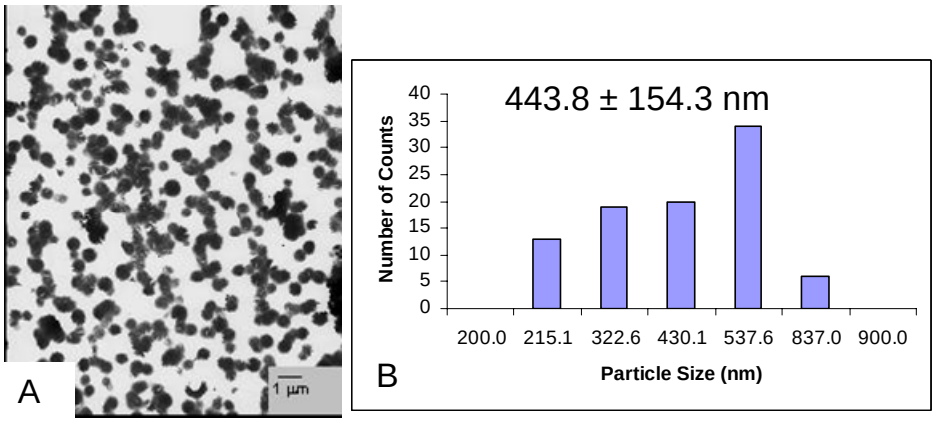

Figure 4-11: (A) TEM micrograph of 0.01 vol.% silver nanofluid stabilized by Poly(dipropylene glycol) phenyl phosphate (12 mM) with (B) corresponding particle size distribution.

It would therefore appear that the type of surfactant plays an important role in particle formation and size. Thus far, PVP seems to be most capable for stabilizing small silver nanoparticles, followed by PVA, then Poly(dipropylene glycol) phenyl phosphite.

- **EFFECT OF ZWITTERIONINC SURFACTANT: 3-(N,N-Dimethyldodecylammonio)propanesulfonate**

3-(N,N-Dimethyldodecylammonio)propanesulfonate, or most commonly known as Sulfobetaine or SB12, is a strongly hydrophilic zwitterionic surfactant and highly soluble in polar solvents. Zwitterionic or amphoteric surfactants have both anionic and cationic dissociations and therefore can act as an acid and a base at the same time.

Bönnemann et al. [120], in their preparation of heterogeneous hydrogenation catalysts, synthesized Pt hydrosols, with average size of 3 nm using SB12 as a protecting agent. With the aim of preparing small silver nanoparticles, the possible route was investigated using SB12 as a capping agent.

UV-VIS spectroscopy was used to monitor the reaction at different temperatures, since no reaction was observed at room temperature. Silver nanoparticles normally give rise to a distinct peak at around 400-420 nm due to the surface plasmon resonance (SPR). However, the UV-VIS results in Figure 4-12 showed that the unique SPR peak has been blue-shifted. This could be due to the adsorption of the surfactant on the silver surface, which increases the electron density and hence results in a blue-shift of the peak position [121].

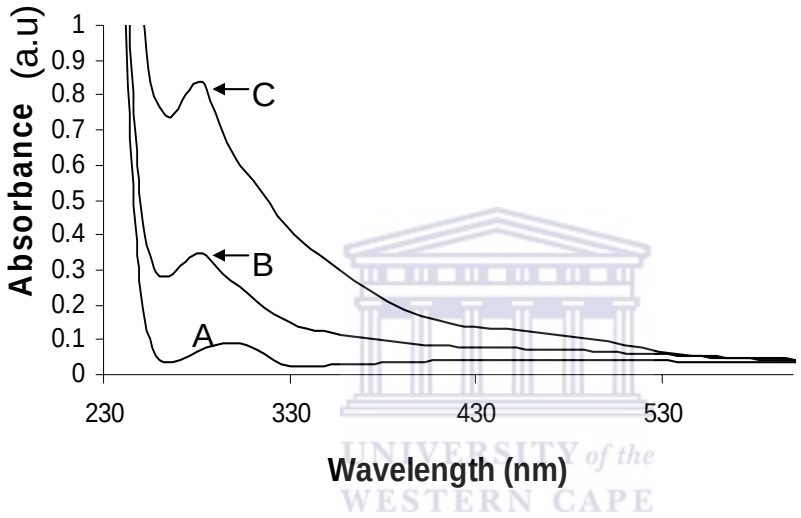

Figure 4-12: UV-VIS spectra of 0.01 vol.% Ag nanofluid stabilized by 3-(N,N-Dimethyldodecylammonio)propanesulfonate (12 mM) obtained at different times and temperatures during the reaction (A) 50 °C = 3 hrs from start of reaction, B) 150˚C = 2 hrs later and C) RT = next day.

During the final stages of the reaction (at RT), a slightly red-shifted broad peak was obtained, which could possibly be due to the presence of some bigger particles. High temperatures normally elevate the mobility of particles and hence results in particle collisions, adhesion and subsequent coalescence. Particle coalescence is the means by which the system tries to attain the thermodynamic equilibrium by reducing its total surface energy. Consequently, a wide range of shapes may also result arising from the coalescence of individual quasi-spherical particles. TEM was employed to confirm

the presence of nanoparticles. From Figure 4-13, silver nanoparticles have been obtained. A very broad particle size distribution of 15.30 ± 11.07 nm was obtained.

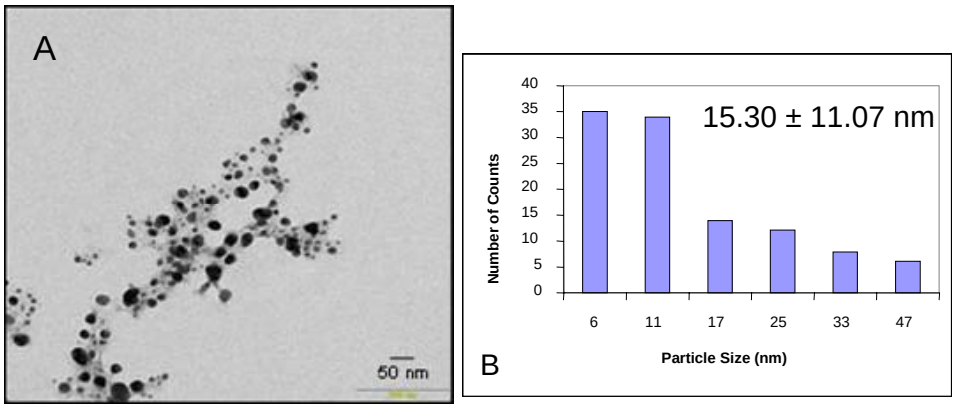

Figure 4-13: (A) TEM micrograph of 0.01 vol.% Ag nanoparticles (at time D=152 °C) stabilized by 3-(N,N-Dimethyldodecylammonio)propanesulfonate (12 mM) with (B) corresponding particle size distribution.

The stabilizing ability of 3-(N,N-Dimethyldodecylammonio)propanesulfonate, as capping agent for silver nanoparticles, is therefore comparable to PVP. However, much higher temperatures were required to obtain silver nanoparticles compared to the Ag-PVP system.

4.1.7 Surfactant free method to silver nanofluids: Use of Fe(III)

It is believed that iron prevents silver nanoparticles etching by removing oxygen from the surface of the seeds during growth of the particles [88]. In addition, since ethylene glycol is normally synthesized and stored in steel vessels, it often contains iron as a contaminant. Therefore it is essential to know the effect of its presence in the synthesis of silver nanoparticles. In this section, the effect of iron during the synthesis of silver nanoparticles, in the absence of stabilizer was investigated. All experimental details pertaining to this section is given in section 3.5.1 and Table 3-3 (Sample numbers 3.5.1.18 - 3.5.1.23).

Effect of Fe(III) concentration during silver nanoparticle formation at different temperatures

- High temperture

Introducing a high concentration (0.02 M) of Fe (III) into the system at 100 °C, resulted in some changes in the UV-VIS spectrum (see Figure 4-14 (A-i)). The spectrum was recorded against a Fe (III) background in order to see the peaks due to silver nanoparticles more clearly. A strong absorption peak appeared around 472 nm and a smaller peak at 418 nm. The small peak at 418 nm could be due to free silver (0) nanoparticles. The strong absorption peak centered at 472 nm could also be due to silver nanoparticles. It is slightly red-shifted probably due to their interaction with iron oxide in solution.

Results from TEM showed that a mixture of differently shaped particles was obtained. Figure 4-14 (B) shows that cube-shaped particles and quasi-spherical particles were obtained. Xia et al. [88] have obtained nanocubes and nanowires by changing the concentration of iron ions in their polyol synthesis of silver nanoparticles in ethylene glycol. It is believed that Fe(II) reacts with and removes the adsorbed atomic oxygen that would otherwise etch twinned seeds and block the self-catalytic addition of silver atoms [88]. Quasi-spherical nanoparticles have lower possible surface energy than cubical nanoparticles and are therefore favoured by thermodynamics. It is important to control the growth kinetics of a seed to ensure the birth of a shape which does not represent an energy minimum. According to Grulke et al., the growth kinetics of a solution-phase synthesis are influenced by (i) the concentration of metal precursor, (ii) the rate of reduction which essentially depends on the concentration and power of the reductant, (iii) the presence of a capping agent, and (iv) the specific adsorption of the capping agent to a specific crystallographic plane [88]. Since no capping agent was used the presence of agglomerates and also quasi-spherical particles are accounted for. The rings obtained in the diffraction pattern (Figure 4-14 (C)) confirm the presence of silver metal particles having FCC structure.

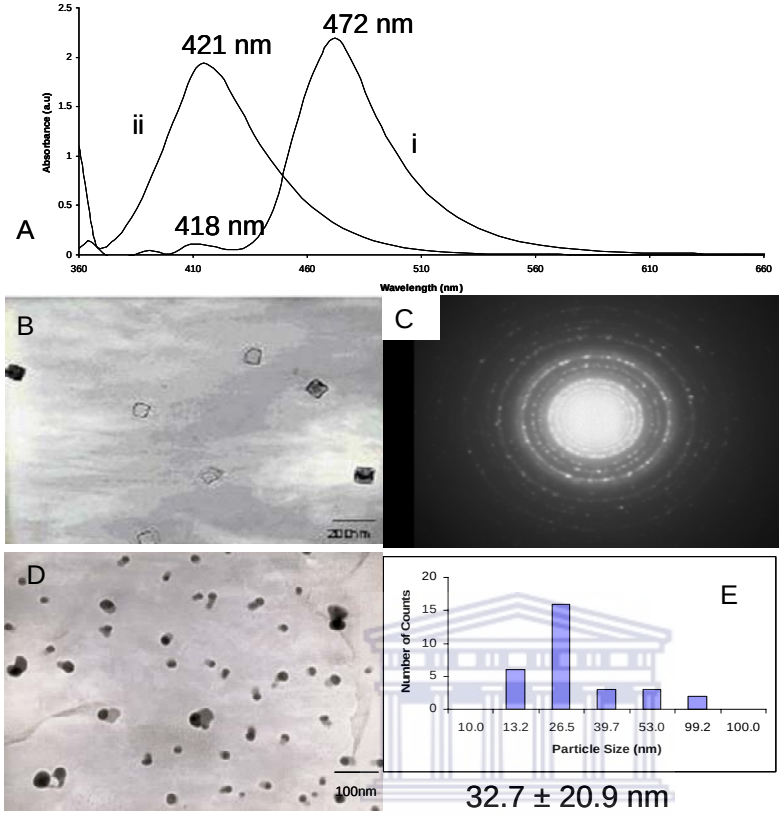

Figure 4-14: (A) UV-VIS spectra for 0.02 vol.% Ag nanofluids containing (i) 0.02 M and (ii) 0.008 M Fe (III). The UV-VIS spectra were recorded against a Fe(III) background. (B) TEM micrograph of 0.02 vol.% Ag nanofluid containing 0.02 M Fe(III) prepared at 100 °C in the absence of stabilizer showing silver nanocubes and quasi-spherical silver nanoparticle, with (C) corresponding diffraction pattern, (D) TEM micrograph of 0.02 vol.% Ag nanofluid containing 0.008 M Fe(III), prepared at 100 °C in the absence of stabilizer with (E) corresponding particle size distribution.

When a much lower concentration of ferric nitrate precursor was used, spherical and quasi-spherical particles could be observed. Figure 4-14 (D) shows the TEM micrograph and corresponding particle size distribution (Figure 4-14 (E)) obtained for the 0.02 vol.% silver nanofluid containing 0.008 M Fe(III), prepared at 100 °C. Since the reaction conditions were too mild to reduce the ferric ions to zerovalent Fe, the particles are probably a mixture of silver and iron oxide nanoparticles. The presence

of Fe (III) was confirmed by addition of potassium thiocyanate to the suspension, which resulted in a blood red color.

Therefore, an irregular growth of silver nanoparticles and an obvious aggregation, which could be due to partially removed oxygen from the silver surfaces [88], was observed when a low concentration of Fe(III) was added to the silver system. Particle size ranged from 10-40 nm.

- Room temperature

When the reaction was performed at room temperature, only spherical and quasi-spherical nanoparticles were obtained at low and high concentrations of Fe(III) respectively (Figure 4-15 A-B). Therefore, the presence of small amounts of Fe(III) in the silver nanofluids result in the formation of spherically-shaped silver nanoparticles compared to the quasi-spherical particles formed when higher concentrations of Fe(III) was used.

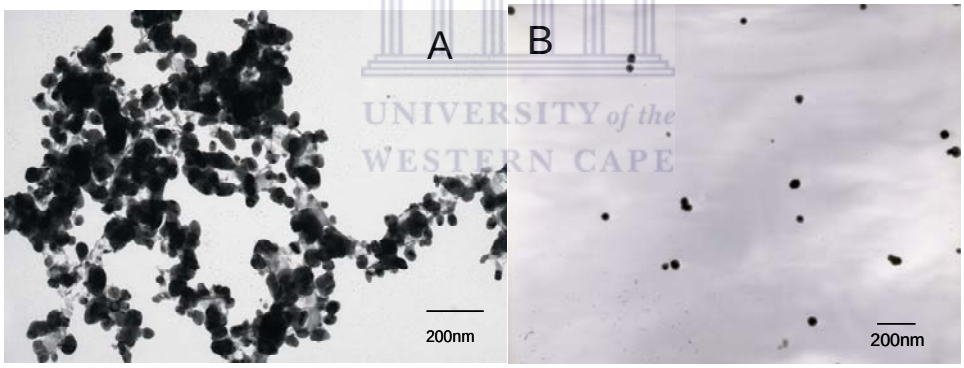

Figure 4-15: TEM micrographs of silver nanofluids containing different concentrations of Fe(III): (A) 0.02 vol.% Ag nanofluid containing 0.02 M Fe(III) and (B) 0.02 vol.% Ag nanofluid containing 0.008 M Fe(III), prepared at room temperature.

Since an obvious aggregation is visible in most of the TEM micrographs of silver nanofluids containing Fe(III), PVP was added in order to see the effect of the surfactant on the nanofluid system. In the presence of PVP, small, well-dispersed spherical particles were obtained (Figure 4-16).

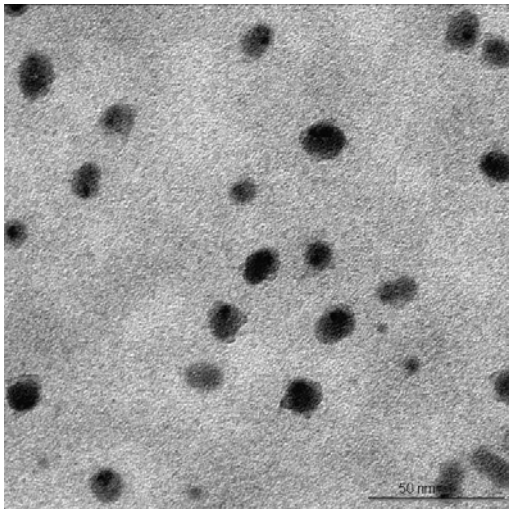

Figure 4-16: TEM micrograph of 0.02 vol.% silver nanofluid containing 0.008M Fe (III) and 0.01 M PVP.

The surfactant therefore plays a vital role during nanoparticle formation in order to obtain small, well dispersed spherically shaped particles.

Effect of sequence in the preparation of silver nanofluids in the presence of Fe(III)

The order in which reactants are introduced into a reaction often plays a role in the outcome of the products. Here the effect of sequence is demonstrated in the room temperature synthesis of silver nanofluids, in the presence of Fe(III).

Figure 4-17 (A) shows the UV-VIS spectrum obtained for the silver nanofluids containing iron ions, which was introduced drop wise to the reaction flask (See Table 3-3 for summary of experimental details). Silver nanoparticles were obtained since the characteristic peak due to the surface plasmon resonance of silver nanoparticles appeared at 412 nm (Figure 4-17 (A)).

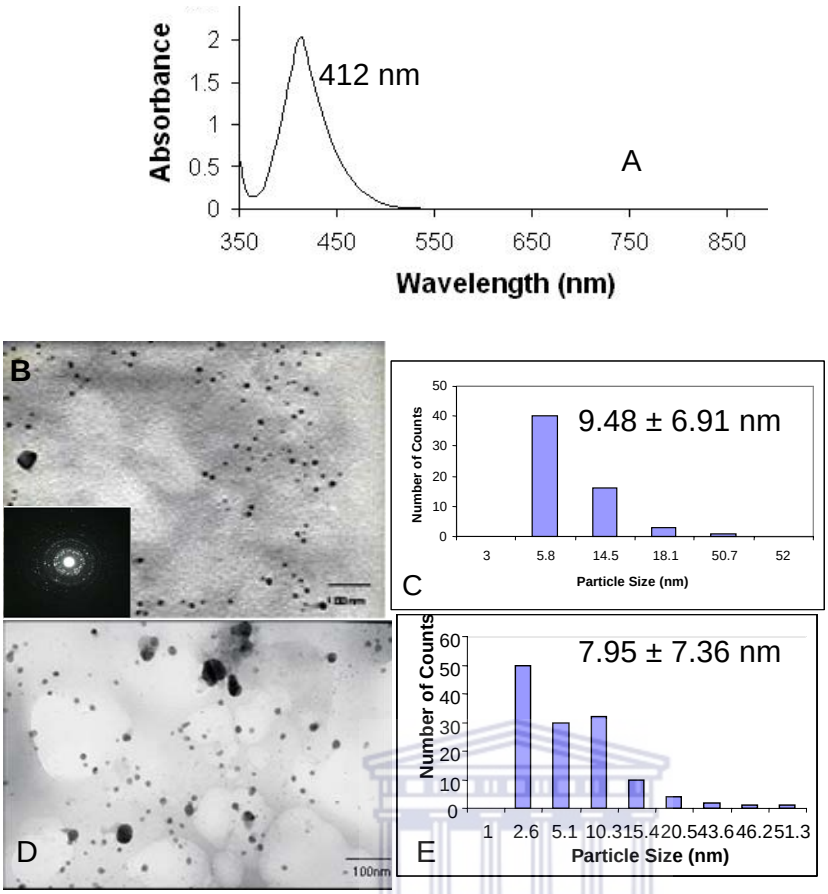

Figure 4-17: (A) UV-VIS spectrum obtained for 0.03 vol.% Ag nanofluid containing 0.002 M Fe (III). (B) TEM micrograph and corresponding diffraction pattern of Ag nanofluid containing Fe(III) prepared by drop wise addition of Fe(III) with (C) corresponding particle size distribution. (D) TEM micrograph of Ag nanofluid containing Fe(III) prepared by introducing all the reactants at once, with (E) corresponding particle size distribution. Both reactions were prepared at room temperature.

The well-defined surface plasmon band with a maximum absorbance at 412 nm (Figure 4-17 (A)) also implicates well dispersed, small nanoparticles with sizes <10 nm. TEM micrographs showed that this method of slow addition of one dissolved reactant (ferric nitrate in ethylene glycol) into another dissolved reactant (silver nitrate in ethylene glycol) resulted in spherical and quasi-spherical particles (Figure 4-17 (B)). A broad range of particle sizes were obtained, yielding a particle size distribution of 9.48 ± 6.91 nm. The observed particles are indeed silver nanoparticles, which were confirmed by EDS analysis. The 99.09% silver obtained by EDS analysis

corresponds to a series of single particles. The corresponding diffraction pattern also shows that the sample is polycrystalline.

Introducing the reactants all at once into the reaction flask resulted in mostly spherically shaped particles (Figure 4-17 (D)). The particles appeared well-dispersed A few agglomerates are also visible. A particle size distribution of 7.95 ± 7.36 nm was obtained, which shows that a broad range of sizes were obtained.

All the abovementioned TEM micrographs of silver nanofluids containing Fe(III) showed the presence of nanoparticles. However, the nanoparticles in the TEM micrographs could possibly be a mixture of both silver and iron (III) oxide particles. In order to investigate if iron (III) oxide particles are indeed obtained in the nanometer range during this particular synthesis pathway, a reaction was performed in the absence of the silver salt. PVP was added as a capping agent. Figure 4-18 shows the TEM micrograph obtained for the PVP-stabilized Fe-nanofluid.

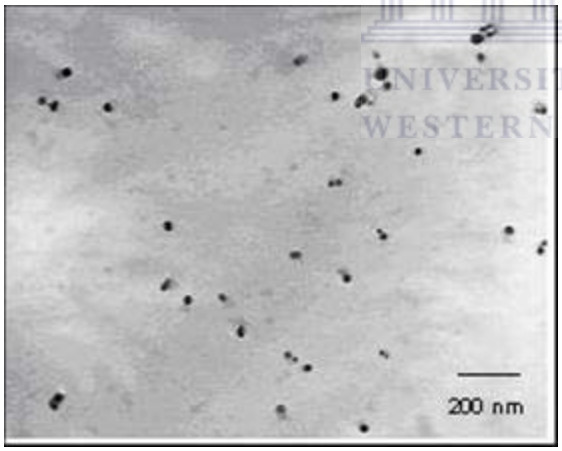

Figure 4-18: TEM micrograph of PVP-stabilized Fe-nanofluid

Particles appeared to be large, but well dispersed. This could be due to the low concentrations used. Particle size ranged from 10-20 nm. It is unlikely that zerovalent iron was obtained since the reactions conditions used in this work were too mild and also, iron nanoparticles are pyrophoric and extremely reactive, which has traditionally made them difficult to study [122]. Hence, the TEM micrographs for all the silver

nanofluids containing Fe(III) represent a mixture of silver and iron (III) oxide nanoparticles. EDS analysis on a series of single particles confirmed the presence of silver and iron.

It appears that there is no significant difference in the sequence used to prepare silver nanofluids in the presence of Fe(III) However, a slightly smaller average size of silver nanoparticles was obtained when the reactants were introduced all at once to the reaction flask, compared to the slow addition of reactants.

4.1.8 Study of viscosity of silver nanofluids in ethylene glycol

Heat transfer fluids provide an environment for adding or removing energy to systems, and their efficiencies depend on their physical properties, such as thermal conductivity, viscosity, density, and heat capacity. Since the density and heat capacity were found not to change much compared to the base fluids [79], due to the low volume fraction of the particles and moderate temperature change, only viscosity and thermal conductivity were investigated.

The viscosity of a suspension depends to a large degree on the particles in the suspension. If favourable interactions occur between the particles, then this would lead to a higher maximum packing fraction with less void spaces between the particles.

In this section, the viscosity of silver nanofluids with the following influences thereon will be presented:

- Silver concentration
- Water
- Temperature

Influence of silver concentration on the viscosity of silver nanofluids

The nanofluids containing silver nanoparticles stabilized by PVP showed Newtonian behavior, whereby the viscosity remained constant with an increase in shear rate (Figure 4-19). This could imply that true colloidal solutions have been obtained.

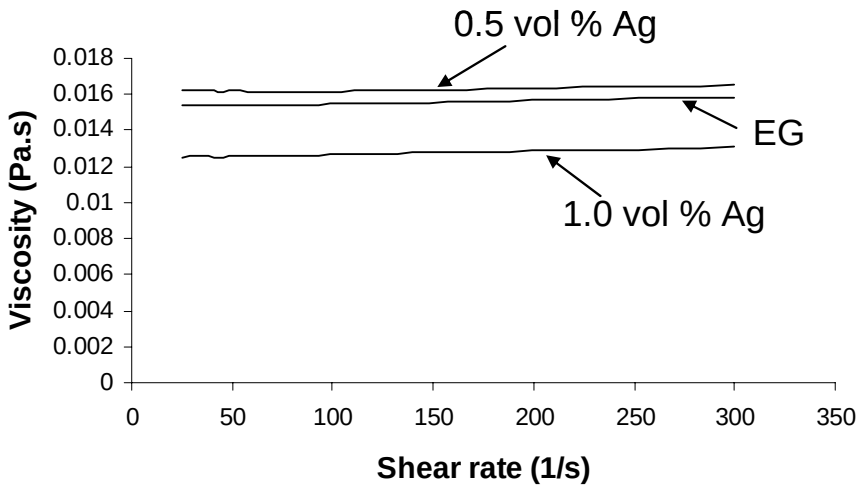

Figure 4-19: Viscosity data showing the effect of silver concentration and the Newtonian behavior of nanofluids and pure ethylene glycol (EG).

There was no noticeable difference between the viscosity of ethylene glycol and the nanofluid containing 0.5 vol.% silver nanoparticles. The viscosity of the nanofluid containing 1.0 vol.% silver nanoparticles was much lower than the viscosity of ethylene glycol. Wang et al. [[2]; and references therein] measured the viscosity of water-based nanofluids containing Al_2O_3 nanoparticles and found that nanofluids have lower viscosities when particles are more dispersed. Therefore, based on their findings in would appear that the 1.0 vol.% silver nanofluid contain well-dispersed silver nanoparticles.

Influence of Water on the viscosity of silver nanofluids

Since ethylene glycol is used as a drying agent for some processes, such as in the dehydration of natural gas [123], its ability to absorb moisture should not be ignored. The effect of water on the viscosity of ethylene glycol was investigated where extra care was taken to use ethylene glycol from a freshly opened bottle. Various amounts of water were added to ethylene glycol and the viscosity was measured. Figure 4-20 shows the viscosity data obtained for the mixtures containing water and ethylene glycol. The viscosity decreases by ~16% with every 5% water present. This is expected since the viscosity of water is much lower than that of ethylene glycol.

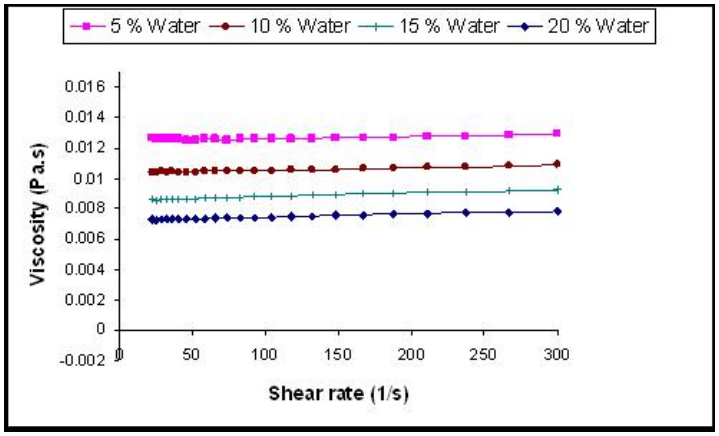

Figure 4-20: Viscosity graphs obtained for ethylene glycol containing known amounts of water.

Influence of temperature on the viscosity of silver nanofluids

The effect of temperature on viscosity was investigated. Most liquids become less viscous as the temperature is raised [124]. This is because, as the temperature increases, the average kinetic energy of the molecules in a liquid increases [125]. The greater average kinetic energy of the molecules more easily overcomes the attractive forces that tend to hold the molecules together. A nanofluid system containing silver nanoparticles and Fe(III) was subjected to a temperature increase to 60 °C and the viscosity measured. Figure 4-21 shows the effect of the temperature increase on the viscosity of the nanofluid containing silver nanoparticles and Fe(III). A drastic decrease in viscosity with an increase in temperature was observed (Figure 4-21), a similar phenomenon to a typical liquid without any suspended nanoparticles. This could possibly imply that the nanofluids are indeed true colloidal solutions.

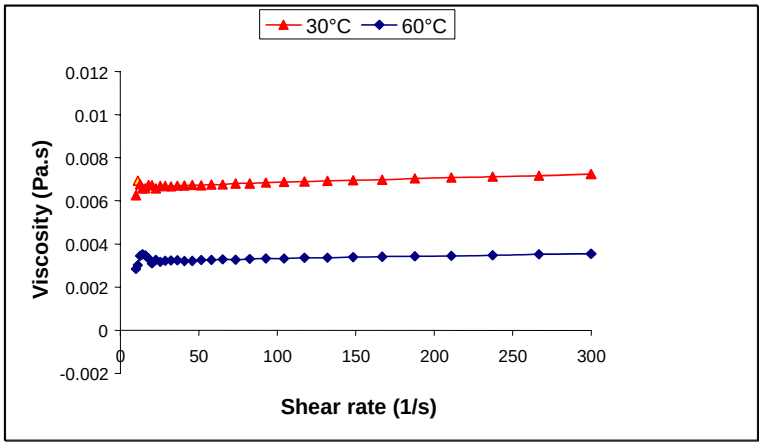

Figure 4-21: Viscosity data obtained for 0.03 vol.% silver nanofluid system containing 0.002 M Fe(III) as a function of temperature

4.1.9 Thermal conductivity of silver nanofluids in ethylene glycol

Since studies of nanofluid thermal conductivity have been more prevalent than studies of other heat transfer properties, this discussion is limited to thermal conductivity, i.e. heat transfer by conduction in stationary fluids.

Current mechanisms cannot explain the thermal conductivity enhancement observed in nanofluids. Keblinski et al. [2] suggested four possible mechanisms to explain the thermal increase observed in nanofluids. Brownian motion was discarded since thermal diffusion occurred much faster than Brownian diffusion and hence the increase in thermal conductivity could not be explained with this theory.

Kwak et al. [14] studied the viscosity and thermal conductivity of ethylene glycol-based nanofluids containing CuO nanoparticles and suggested that an enhancement in thermal conductivity is attainable only when particle volume fraction is below a dilute limit of 0.002. It is therefore clear that different theories exist as to the enhancement in thermal conductivities observed in nanofluid systems.

In this section, the thermal conductivity of silver nanofluids with the following influences thereon will be presented:

- Silver concentration

- Water
- Absence of stabilizing surfactant

Influence of silver concentration on thermal conductivity

The effect of silver concentration for the PVP-stabilized nanofluid systems was investigated. According to most literature, the thermal conductivity of nanofluids increases as the concentration of particles increases [14,34,76].

In this work the thermal conductivity of the freshly prepared nanofluids did not show any noticeable increase of thermal conductivity irrespective of the concentration. The thermal conductivity did however increase as function of time (see Figure 4-22).

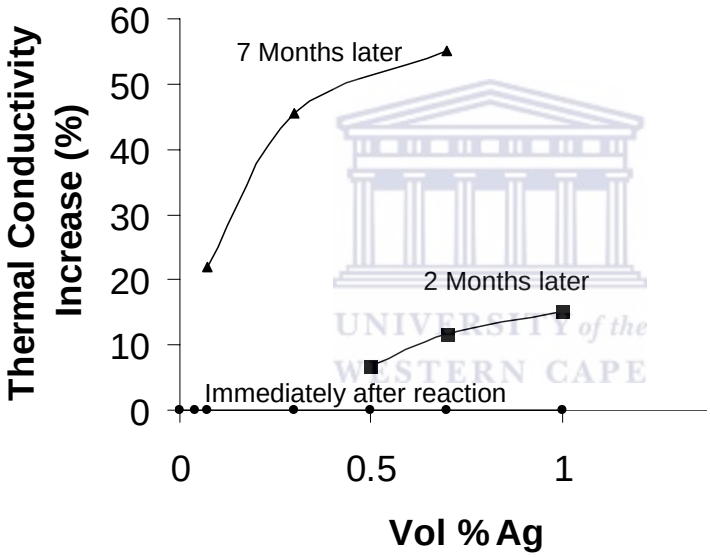

Figure 4-22: Thermal conductivity increase as a function of Ag concentration. Thermal conductivity was found to increase with time.

Knowing the hydroscopic nature of ethylene glycol [126], the water content of the stored samples was determined via Karl Fischer titration. Simultaneously the thermal conductivity of EG with different water content was measured (see Figure 4-23)

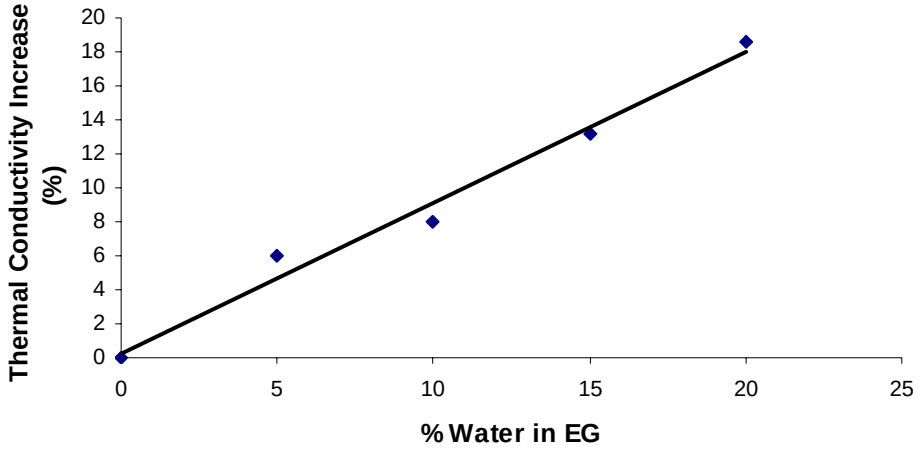

Figure 4-23: Thermal conductivity increase as a function of water present

It appeared that the increase in thermal conductivity was entirely based on the increasing water content with time. Samples at this stage were stored in vials covered with parafilm.

Although UV-VIS (Figure 4-1) and TEM (Figure 4-8) results confirmed the presence of small silver nanoparticles and Karl Fischer results showed no trace of water, no increase in thermal conductivity was observed, even with an increase in silver concentration. Therefore, the role the surfactant plays during the heat transfer process was investigated.

Influence of the absence of the stabilizing surfactant on thermal conductivity

In order to investigate the effect of the surfactant on the thermal conductivity, the reaction was performed without the stabilizing polymer. An increase of 5.2% was observed in the absence of PVP (Figure 4-24).

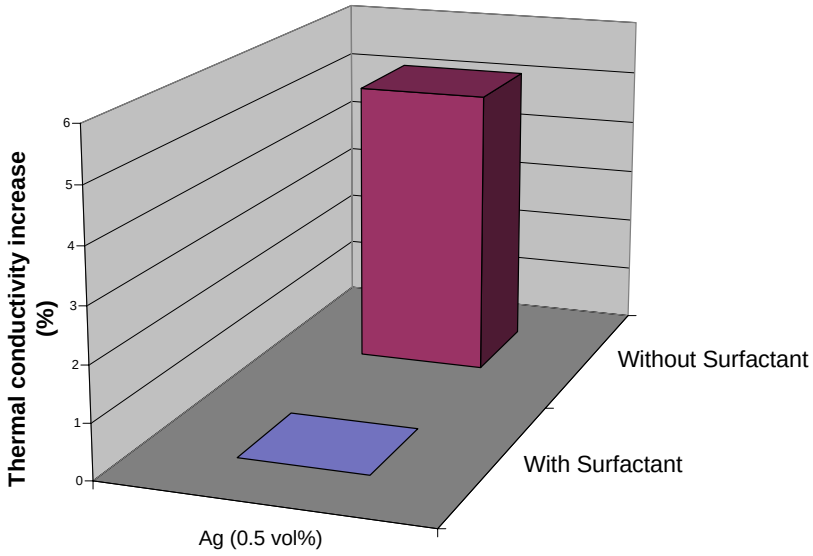

Figure 4-24: Thermal conductivity increase of silver nanofluids with and without surfactant

Macroscopic theories assume that heat is transported by diffusion [13]. In crystalline solids, phonons and electrons are responsible for carrying heat away. When the size of the nanoparticles in a nanofluid becomes less than the phonon mean-free path of ~250-300 nm [127], phonons move ballistically without any scattering rather than diffuse across the nanoparticles, and hence an increase in thermal conductivity is observed. Phonons are essentially quantized lattice vibrations and therefore any defects within the crystal structure can act as scattering centers for thermal waves (phonons) and electrons. The interface between two different materials constitutes an interruption in the regular crystalline lattice on which phonons propagate and therefore can be regarded as a defect, and thus is an obstacle to heat flow.

It is suggested that the capping agent form an insulating layer around the silver nanoparticles, hence causing a 'defect'/interruption in the phonon propagation pathway and therefore inhibit the phonons and electrons from transporting heat energy effectively. Therefore, in the absence of the surfactant, a thermal conductivity increase was possible since there was no obstruction in the pathway of the heat carriers.

Ethylene glycol not only has reducing properties, but can also act as a stabilizer to prevent aggregation of particles at low concentrations. At high concentrations such as 1.0 vol.% Ag, silver mirrors are obtained, which is a clear indication of precipitation. TEM micrographs clearly show well-dispersed particles and the corresponding diffraction pattern confirmed the crystalline nature of the particles (Figure 4-25), which were prepared in the absence of a surfactant. Some amorphicity is also visible in the SAD pattern. This is probably due to the formvar subtrate of the TEM-grid.

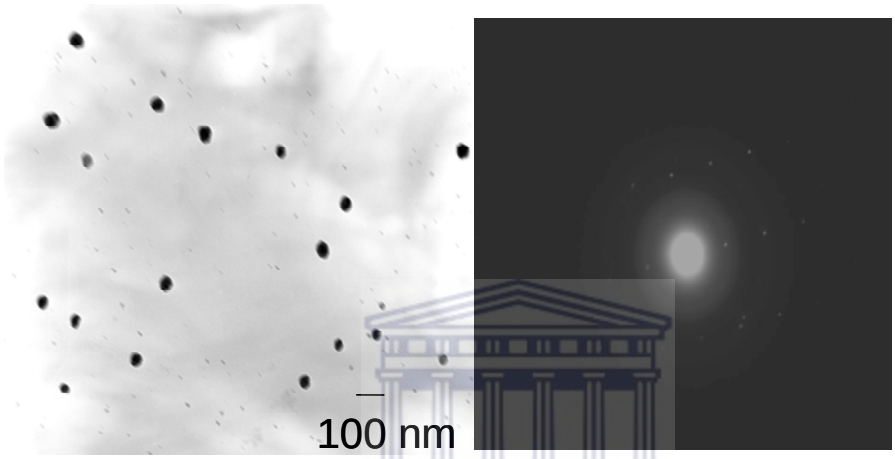

Figure 4-25: TEM micrograph of ethylene glycol stabilized silver nanoparticles and the corresponding diffraction pattern

The particles were however, much bigger in size, with an average diameter of 50 nm, compared to the 16 nm PVP-stabilized silver nanoparticles at the same concentration of silver. In order to obtain small metallic nanoparticles, surfactants are needed to cap particles after nucleation and protect them while growing into small metal clusters. Thus, the presence of a surfactant plays a positive role during particle formation, but not in the heat transfer process.

In this work it is suggested that the surfactant acts as an insulator around the particles, prohibiting heat transport to neighboring particles. Eastman et al. [3] added an acid to stabilize their particles and thus obtained a large increase in the effective thermal conductivity of their 0.3 vol.% Cu nanofluids. However, Putman et al. [128] did not

observe significant enhancement in their Au nanofluids with particle size of 4 nm and contradicted the results obtained by Patel et al. [10]. This may explain the disparities between different experimental data since many researchers used surfactants and others used acids, which could possibly have an effect on the pH of the nanofluid. Investigations on the effect of surface charge state of the nanoparticles in suspension on the thermal conductivity was done by Lee et al. [96]. Their results showed that the pH value of the nanofluid strongly affected the thermal performance of the fluid. In this work it has been shown that the surfactant is the inhibiting force in the enhancement of thermal conductivity of suspensions containing silver nanoparticles.

So far, there are no general mechanisms to explain the difference in thermal conductivities observed and no reliable theory to predict the thermal conductivity of nanofluids. However, many different factors have been considered such as Brownian motion, solid-liquid interfacial layer, ballistic phonon transport, and surface charge state. The thermal conductivity of the nanofluid has been shown, through experimental investigations, to depend on parameters such as the thermal conductivities of the base fluids and nanoparticles, the volume fraction, surface area, nanoparticle shape and temperature. In addition, from the results of this research, the surfactant also plays a significant role towards thermal conductivity enhancement.

The role of the surfactant has never been identified as a crucial parameter by previous researchers. Therefore this work adds significant information to the science of nanofluids. Surfactants do play a major role in thermal conductivity enhancement.

The Maxwell- and the Wasp model were used to determine which could best predict the thermal conductivity of the nanofluids prepared without surfactant. However, the Wasp and the Maxwell model are identical for spherical particles and therefore only the results from the Maxwell model is shown below. The volume fraction of the particles at the end of the reaction is assumed to be the same as the calculated expected volume fraction.

From the Maxwell model,

$$k_{\text{eff,Maxwell}} = \frac{k_p + 2k_l + 2(k_p - k_l)\phi}{k_p + 2k_l - (k_p - k_l)\phi} k_l$$

where k_p = 429 W/m-K is the thermal conductivity of the silver particle, k_l = 0.250 W/m-K is the thermal conductivity of ethylene glycol and ϕ = 0.005 is the silver particle volume fraction of the suspension, a value of 0.250 W/m-K was obtained for k_{eff}, which deviated from the experimental value of 0.263 W/m-K. The thermal conductivity enhancement of the nanofluid without surfactant is far greater than what is predicted based on the Maxwell model. The observed increase of thermal conductivity can, to the best knowledge of the author, not be predicted by any published model.

4.1.10 Conclusions

Ethylene glycol based nanofluids containing silver nanoparticles have been prepared at room temperature using PVP as the stabilizer.

The effect of a wide wavelength spectrum of visible light was investigated and results showed that light accelerates the reduction process and yields growth of small, spherical silver nanoparticles.

Investigations into the effect of silver concentration showed that much lower concentrations of silver nanoparticles yields particles that are more dispersed and smaller in size with size distributions of 15.50 ± 6.98 nm for 0.5 vol.% silver nanoparticles and 6.2 ± 5.8 nm obtained for 0.01 vol.% silver nanoparticles, both stabilized by PVP.

Different capping agents were also tried and results showed that PVP and PVA proved to be the best capping agents for stabilization of silver nanoparticles. A larger average particle of 12 ± 5.1 nm was obtained for PVA-stabilized silver nanoparticles compared to the 6.2 ± 5.8 nm obtained for PVP-stabilized silver nanoparticles

produced using similar molar ratios of silver to surfactant and silver concentrations of 0.01 vol.%.

The effect of iron was also investigated as a surfactant free method to silver nanofluids since it is believed that iron removes oxygen from the surface of the seeds during the growth of the particles. In addition, since ethylene glycol is normally stored in steel vessels during production, iron is always found as an impurity in ethylene glycol. Different particle shapes have been obtained with the introduction of iron to the reaction system.

The viscosity of the PVP-stabilized silver nanofluids (1.0 vol.%) was much lower compared to the base fluid, indicating that the particles are well-dispersed. All the prepared nanofluids showed Newtonian behaviour, implying true colloidal solutions have been obtained.

No thermal conductivity increase was observed irrespective of the silver concentration. The role of the surfactant was investigated and it was found to have a considerable impact on the thermal conductivity of the nanofluid. A thermal conductivity increase of 5.2% was observed when the reaction was performed in the absence of stabilizer. It is suggested that the surfactant forms an insulating coating around the particles, inhibiting phonons and electrons from transferring heat away effectively. The thermal conductivity enhancement of the nanofluid without surfactant is far greater than what is predicted based on the Maxwell model. The observed increase of thermal conductivity can, to the best knowledge of the author, not be predicted by any published model and falls into a whole new area of research.

4.2 Nanofluids based on silver nanoparticles dispersed in Newtonian liquid such as mineral oil

The approach developed for silver nanofluid in ethylene glycol was used for the preparation of silver nanofluid system in mineral oil. The mineral oil based nanofluids containing suspended silver nanoparticles discussed in this section forms

part of an article that has already been published [7]. The rest of the article appears in Appendix (8.1).

4.2.1 Studies of synthesis conditions of silver nanoparticles stabilized by anionic surfactant such as Korantin SH in mineral oil

Silver nanoparticles were prepared in mineral oil using a thermal decomposition method. Different concentrations of silver nanoparticles in mineral were prepared with various concentrations of surfactant, as indicated in Section 3.5.2.

4.2.1.1 Structural studies on mineral oil based silver nanofluids

Elemental analysis (EA) was performed on the mineral oil based nanofluids containing silver nanoparticles in order to determine whether the expected vol.% silver nanoparticles was indeed obtained at the end of the reaction. Some precipitation were visible towards the end of the reaction, therefore it was decided to investigate exactly how much silver nanoparticles were suspended in the mineral oil at the end of the reaction. Results from EA (Table 4-2) shows that the amount of Ag lost through precipitation increases with an increase in silver concentration. This agrees well with the visual observation of a larger precipitate with an increase in concentration after reaction was complete. Nanoparticles suspended in a base liquid are constantly in random motion under the influence of several acting forces, such as Brownian and Van der Waals forces. With such high concentration suspensions and under the influence of external and internal forces, the probability for interparticle collisions is greater and hence may lead to aggregation. Furthermore, sedimentation may occur under gravitational forces if the clusters grow large enough.

Table 4-2: Elemental analysis (EA) results for variable silver and surfactant concentrations for Korantin SH-stabilized silver nanoparticles suspended in mineral oil.

Vol.% Ag Expected	Ratio Ag:Kor	EA result (mg Ag/ml)	Calculated Vol.% Ag lost
0.3	1:1	20.4	0.1
0.011	1:7	0.0975	0.0100
0.011	1:2	0.0819	0.0102
0.011	1:1	0.76	0.004

When a large number of atoms are in close proximity to each other, the available energy levels form a nearly continuous band wherein electrons may undergo transitions. Metal nanocrystallites such as silver nanoparticles have close lying bands and therefore outer electrons are free and ready to move at the beckoning of an electric field [129]. When the conduction band electrons interact with an electromagnetic field, the electrons start to oscillate coherently. This phenomenon is called surface plasmon resonance. A typical UV-VIS absorption spectrum of Korantin SH stabilized silver colloid in mineral oil is shown in Figure 4-26.

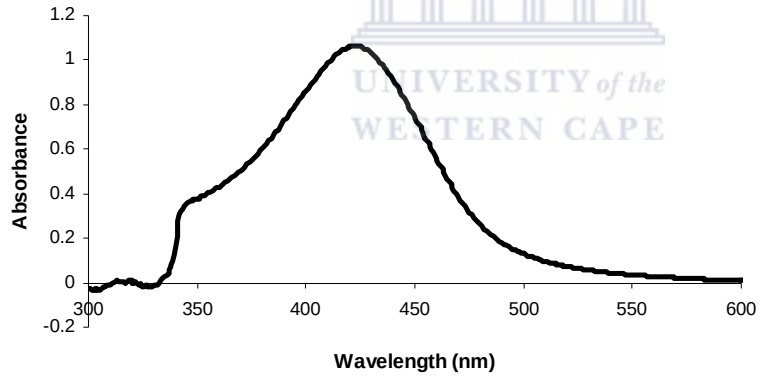

Figure 4-26: UV-VIS spectrum of 0.011 Vol.% Ag-colloid stabilized by Korantin SH (Diluted to 0.5 mM)

The surface plasmon absorption maximum occurs at 420 nm with a FWHM of 80 nm, which is characteristic of spherical silver nanoparticles and in good agreement with literature [130]. This implies that the colloid system is monodisperse with a narrow size distribution. TEM results further supports this result (Figure 4-27).

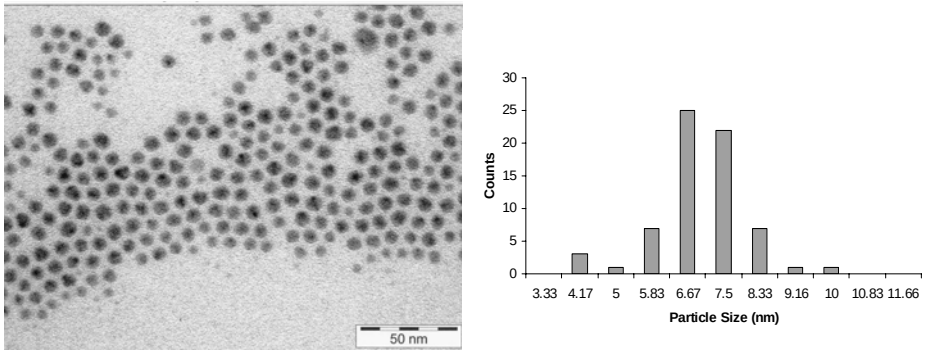

Figure 4-27: (A) TEM micrograph of Korantin SH-stabilized Ag-colloid and (B) corresponding particle size distribution

The TEM micrograph in Figure 4-27 (A) shows that the monodisperse nanocrystals are self-assembled into superlattice structures. This phenomenon has not been observed in the case of the silver nanoparticles suspended in ethylene glycol. Figure 4-27 (B) provided evidence for the tight size distribution of the silver nanoparticles suspended in mineral oil, which was necessary for the superlattice formation. A particle size distribution of 9.5 ± 0.7 nm was obtained Figure 4-27 (B). This is a more narrow size distribution compared to the 5-20 nm in diameter silver particles prepared by Yase et al. [131]. The particles presented here are well separated from each other, thereby demonstrating the interaction between the particles and the surfactant.

Effect of Korantin concentration on particle size

A much lower concentration of Korantin (Ag:Korantin = 4:1) was used to determine the degree of aggregation. Figure 4-28 (A) shows the resulting TEM micrograph of a Korantin stabilized silver colloid with a reduced surfactant ratio. Some smaller and larger particles are visible. The particle size distribution was 8.18 ± 4.4 nm (Figure 4-28 (B)).

(A) 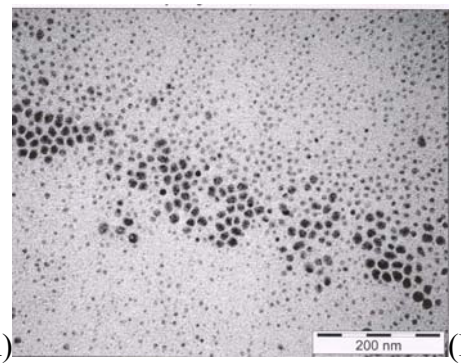

(B) 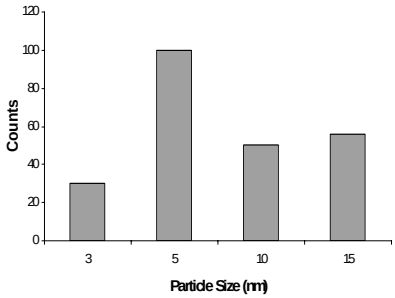

Figure 4-28: TEM micrograph of (A) Korantin SH-stabilized Ag-colloid with (B) corresponding particle size distribution.

Although at much lower concentration of surfactant a broader size distribution was obtained, particles remained well separated.

It has been reported that long chain carboxylic acids form close-packed monolayers on the surface of silver nanoparticles [132].

Yu-Tai Tao reported that the two oxygen atoms of the carboxylate bind to the silver surface nearly symmetrically, and the molecular chain extends in a trans zigzag conformation [133]. In order to gain insight into the interaction between Korantin and the silver surface, FTIR was employed.

Due to the lower concentration of the prepared samples (see Table 4-2) the absorption spectrum of the Korantin-stabilized Ag-colloid was similar to that of mineral oil. Furthermore, mineral oil consists of a high concentration of hydrocarbons, which absorbs in the same region as some of the functional groups of Korantin and hence covers many peaks in the absorption spectrum. However, the most noticeable difference in these complex spectra (Figure 4-29) was the –COO- and the –NCOO- stretching frequencies.

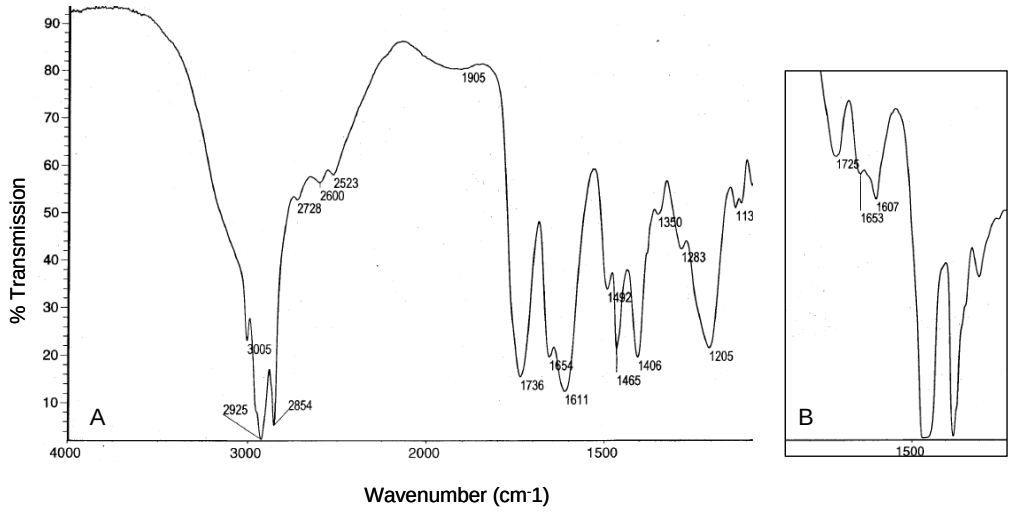

Figure 4-29: FTIR spectra of (A) Korantin SH in mineral oil, without silver nanoparticles, and (B) Korantin SH-stabilized silver nanoparticles suspended in mineral oil.

The strong band at 1736 cm−1 was assigned to the C=O stretching vibration (νC=O) of free Korantin. A shift was observed to lower frequency (1725 cm−1) once the surfactant coordinated itself to the silver surface via the two oxygen atoms. In addition, a slight shift in the amide I band (1611 cm−1) was observed to lower frequency (1607 cm−1). It is therefore possible that the amide also coordinates to the silver surface [134].

Combining all the results thus far, colloidal silver nanoparticles were successfully synthesized directly in mineral oil. The reaction could be explained as follows: In the presence of Korantin, at mild temperature conditions, the silver lactate used was oxidized to pyruvic acid, which in turn caused the silver ions to be reduced to silver (0). It should also be noted that a much shorter reaction time was observed when the reaction was performed in air. Hence in this case, the presence of oxygen plays an active role in silver nanoparticle formation [135]. Upon reduction, the carboxylate head group of Korantin adsorbed onto the silver surface thereby preventing aggregation. This assumption could also provide an indirect explanation to the amount of silver nanoparticles lost through precipitation (Table 4-2), since the oxidation of silver lactate into pyruvic acid could have lead to a lowering of the pH. At lower pH the charge on the particles are weaker and therefore the interactions

between the surfactant and the silver nanoparticles would be weaker and hence lowers the stability of the dispersions [19]. At high surfactant concentration the pH is even lower and hence more unstable dispersions are obtained.

4.2.1.2 Influence of silver concentration on nanofluid formation

The formation of silver particles of different concentration (0.3 vol.% and 0.011 vol.% Ag) was followed by absorbance measurements.

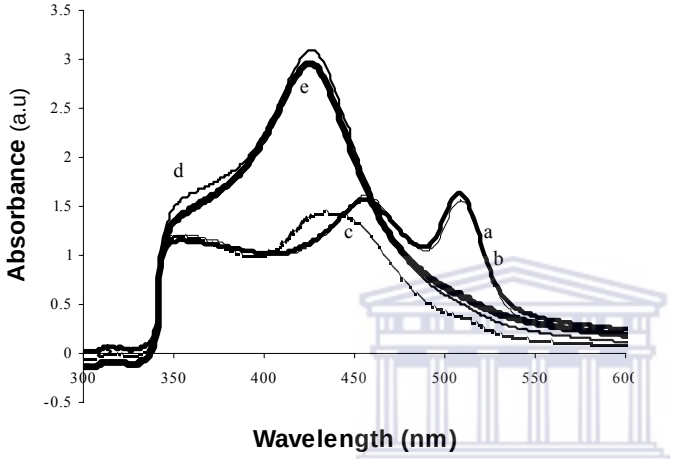

Figure 4-30: UV-VIS spectra of 0.3 vol.% silver nanoparticles at different times during the reaction; (a) and (b) correspond to samples taken at room temperature (after 15 minutes) and at 60 °C (1/2 hr later) respectively, whereas (c) and (d) correspond to samples taken at 90 °C, 40 minutes and 90 minutes later respectively; (e) was collected at room temperature 1-2 days later.

Initially, more than one absorption band was visible (Figure 4-30 (a) and (b)). This is an indication of the polydispersity of the system at that stage. According to Mie's theory, small spherical nanocrystals should exhibit a single surface plasmon band whereas larger metal colloid dispersions can have broad or additional bands in the UV-VIS range. This is due to excitation of plasmon resonances or higher multipole plasmon excitation [136,137]. At 90ºC (Figure 4-30 (c)), the asymmetrical peak blue-shifted as smaller particles started to form. It is therefore suggested that at the beginning of the reaction larger particles were formed, which were later decomposed into smaller particles. Approximately 1½ to 2 hours later at 90ºC, only one symmetric absorption peak was observed at the wavelength characteristic for spherical Ag-

nanoparticles with a narrow size distribution (Figure 4-30 (d)). This was confirmed with TEM (see Figure 4-27). After stirring for 1-2 days at room temperature (Figure 4-30 (e)), no further change was observed which implies that the reaction reached completion.

Figure 4-31 shows the UV-VIS spectra obtained during the Ag-colloid formation studies with a lower concentration of silver.

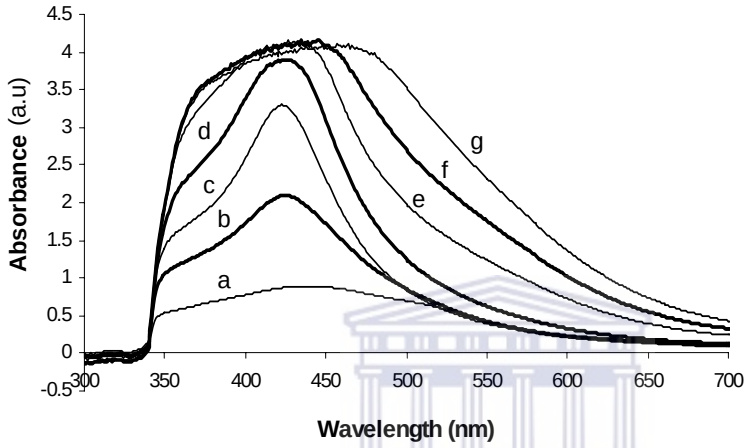

Figure 4-31: UV-VIS spectra of 0.011 vol.% silver nanoparticles in mineral oil at different times during the reaction at 90 °C; (a) 20 min, (b) 1 hour, (c) 2 hours, (d) 4 hours, (e) 5 hours, (f) 6 hours (g) the next day (room temperature).

From the spectra (Figure 4-31 (a-c)), it is would appear that the reaction should be stopped no later than 2 hours (Figure 4-31 (c)) once the abovementioned temperature is reached. This will ensure a narrow size distribution of spherical silver nanoparticles, since from (d) to (g) a gradual increase in the FWHM was observed due to agglomeration.

4.2.1.3 Stability studies of mineral oil based silver nanofluids

To detect the stability of the Korantin-stabilized silver nanoparticles in mineral oil, the absorption spectra were recorded at different times.

From Figure 4-32, no obvious difference was detected in the shape and position of the absorption peak during the initial two weeks (Figure 4-32 a-d).

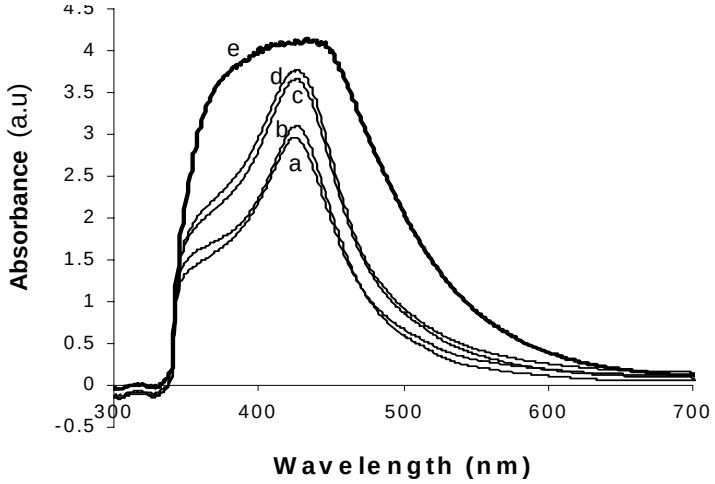

Figure 4-32: Stability studies of Korantin SH-stabilized silver nanoparticles where (a) and (b) corresponds to freshly prepared and a 2-day old sample respectively. Samples (c) and (d) refer to time intervals of 1 and 2 weeks respectively. Sample (e) was collected and measured 1 month later, upon standing.

However, an increase in intensity is observed which could be due to the formation of larger particles. The prepared silver nanoparticle suspensions were stable for about 1 month since at that time the symmetrical peak broadened showing the onset of agglomeration (Figure 4-32 (e)), which shows a decrease in stability.

4.2.2 Conclusions

Mineral oil based nanofluids containing silver nanoparticles with a narrow size distribution (9.5 ± 0.7 nm) were prepared by a one step process. The particles remained well separated even when a much lower surfactant concentration was used. Furthermore, a higher concentration of surfactant yields monodisperse spherical silver particles with a narrow size distribution. However, high concentration silver leads to a higher loss of silver during reaction, probably due to Brownian motion. The particles are stabilized by Korantin, which coordinates to the silver surface via the

two oxygen atoms forming a dense layer around the particles. The silver suspensions were stable for about 1 month.

4.3 Synthesis, structure and studies of physico-chemical properties of silver nanoparticles in transformer oil

Mineral oil, a by-product in the distillation of petroleum to produce gasoline, consists mainly of alkanes and cyclic parrafins. Transformer oil is usually a highly-refined mineral oil. Some of the properties which make transformer oil unique to other oils are the high stability at high temperatures and excellent electrical insulating properties.

The approach developed for silver nanofluid in ethylene glycol and mineral oil was used for nanofluid system in transformer oil. Oil-based nanofluids are not well documented in literature.

In this work, nanofluids containing silver nanoparticles suspended in transformer oil have been prepared via one step methods with and without stabilizer. Two hydrophobic surfactants namely oleylamine and oleic acid were used for stabilization purposes. However, only the results obtained from oleylamine-stabilized nanofluids are reported here since no significant difference was noted in the stabilizing ability of the two surfactants as well as the thermal conductivity increases observed. Two different synthesis pathways have been employed namely high temperature and hydrogen reduction pathways. Herein, the results from these two synthesis pathways are presented and discussed in sections 4.3.1 and 4.3.2 respectively. Since transformer oil has been used to prepare oil-based nanofluids, the dielectric strength has been measured and the results presented and discussed in section 4.3.3.3.

4.3.1 Study of oil based Ag-nanofluid synthesized by using a high temperature method: Particle formation and structure

Nanoparticle synthesis at high temperatures may lead to agglomeration of particles since the mobility of the particles is enhanced and frequent collisions between particles are unavoidable [138]. Since no reaction occurred at lower temperatures and silver mirrors and precipitation were obtained at high temperatures, a suitable

surfactant and a reaction temperature of 130 °C, based on trial and error, was chosen to minimize particle aggregation and mirror formation during synthesis.

Figure 4-33 shows the UV-VIS spectrum obtained for the 0.01 vol.% silver nanofluid prepared using the high temperature method (130 °C). A well-defined peak due to the presence of silver nanoparticles was obtained at 423 nm.

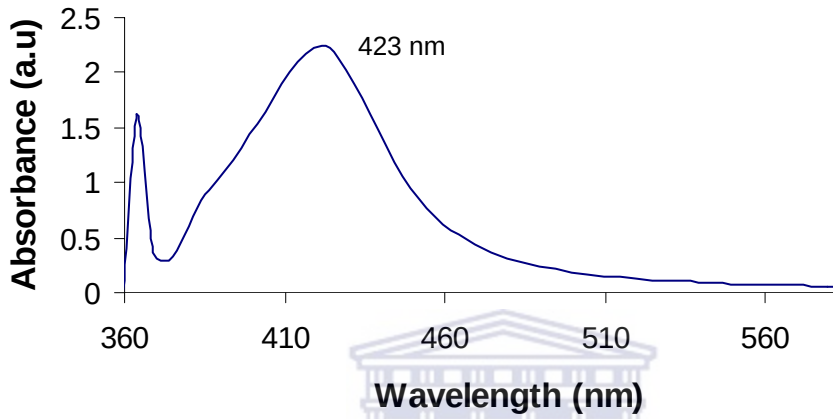

Figure 4-33: UV-VIS spectrum of 0.01 vol.% silver nanofluid prepared by mechanical agitation at 130 °C and stabilized by oleylamine.

Particle size and morphology was investigated using TEM. Figure 4-34 shows the TEM micrograph obtained for oleylamine stabilized silver nanoparticles in transformer oil with corresponding particle size distribution. TEM revealed the presence of small silver nanoparticles with particle size distributions of 3.58 ± 1.61 nm. The particles were mainly spherical. Chen et al. [139] obtained much bigger particles (11.6 ± 3.8 nm) during their synthesis of oleylamine-stabilized silver nanoparticles in mineral oil at much higher temperatures (180 °C) than was used in this work (130 °C).

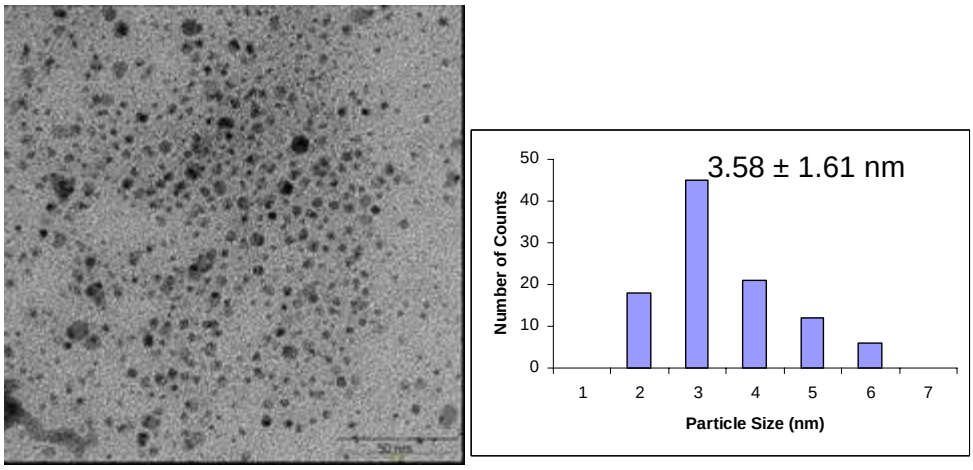

Figure 4-34: TEM micrograph and corresponding particle size distribution of Ag nanofluid prepared using high temperature.

Silver nanoparticles have been successfully synthesized using a simple method of applying high temperatures to the reactants in oil. The size of the particles were much smaller compared to those obtained in the ethylene glycol-based nanofluids since ethylene glycol is a much stronger reducing agent compared to oil, resulting in much faster reactions and higher particle growth rates at room temperature.

4.3.2 Oil based Ag-nanofluid synthesized by using a hydrogen reduction method

Hydrogen reduction pathways have mostly been used to prepare noble metal nanoparticles for use as catalysts. One of the major advantages of using hydrogen reduction is the formation of unwanted by-products since oxygen is excluded during the reaction. Hydrogen was used as a reducing agent for a possible route to small silver nanoparticles in oil.

Influence of reaction time on silver nanoparticle formation in transformer oil

In order to establish the optimum reaction duration, hydrogen was bubbled for 1 hour into the reaction mixture containing silver salt and oleylamine, while sonicating in a 40 °C ultrasonic water bath. All experimental details are summarized in Table 3-4. The TEM micrograph of the oleyamine stabilized silver nanoparticles is shown in Figure

4-35 (A). It would appear that, from the TEM micrograph, the reaction time was insufficient as only a small amount of particles were visible. The particles appear to be in a state of agglomeration.

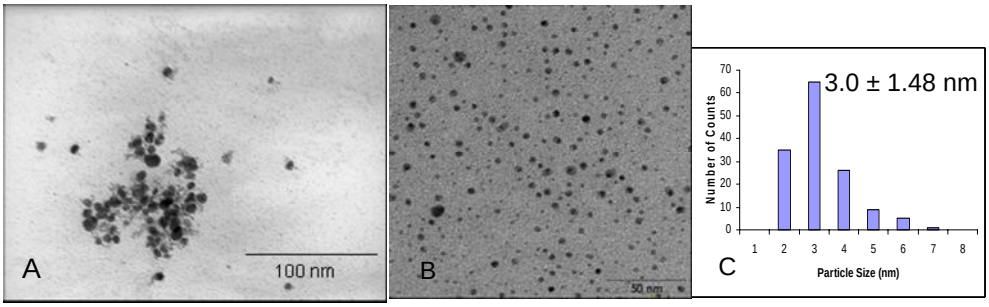

Figure 4-35: TEM micrographs of silver nanofluids prepared by hydrogen reduction (A) for 1 hour reaction time and (B) 6 hours reaction time with (C) corresponding particle size distribution

It was decided to increase the reaction time to 6 hours, while keeping all other parameters constant to ensure that most of the silver salt is reduced. Figure 4-35 (B) shows the TEM micrograph obtained and corresponding particle size distribution (Figure 4-35 (C)) for the oleylamine-stabilized Ag-nanofluid prepared by hydrogen reduction. The particles were mainly spherical with a particle size distribution of 3.0 ± 1.48 nm. It would appear that sufficient reducing agent was present to reduce the silver ions, giving rise to small silver particles.

Hydrogen as a reducing agent is a much cleaner synthesis pathway to obtain metal nanoparticles, where undesirable by-products are eliminated. Its effect is clearly visible in the TEM micrographs. Particles are more uniformly dispersed compared to those prepared by the thermal method where high temperatures were used. This is probably due to the fact that, in methods where high temperatures are used, particles moves faster with the increase in temperature and hence could lead to frequent collisions between particles, resulting in some bigger particles in addition to the smaller particles.

Silver nanoparticles have been successfully prepared in oil by a hydrogen reduction pathway, yielding small metal clusters with uniform particle sizes.

4.3.3 Investigations of physico-chemical properties of silver nanofluids in transformer oil

4.3.3.1 Study of viscosity of silver nanofluids

The rheological properties of the oleylamine-stabilized Ag-nanofluid prepared by hydrogen reduction method, was investigated. Figure 4-36 shows the viscosity curves for the base oil and oleylamine-stabilized Ag-nanofluid. The nanofluids showed Newtonian behaviour, where viscosity remained constant with an increase in shear rate. An increase in viscosity was observed with the addition of stabilized silver nanoparticles.

Dispersions, especially with very low concentrations, which display Newtonian behaviour have no (or only few and very weak) interactions between the particles. In addition, no sedimentation was observed and a totally homogeneous suspension was obtained. It can thus be concluded that true colloidal systems have been obtained.

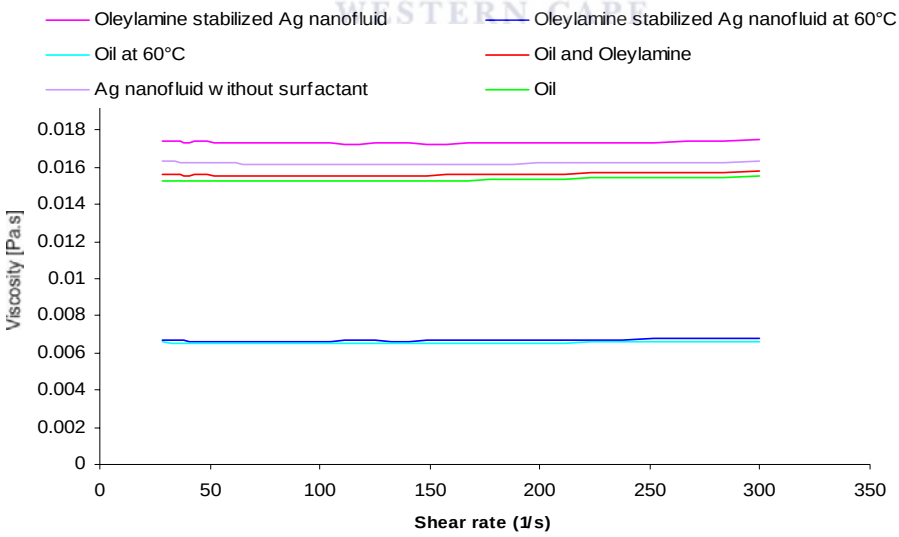

Figure 4-36: Viscosity curves obtained for Ag nanofluids and oil, showing the effect of temperature and surfactant.

Figure 4-36 also shows the viscosity curves obtained for oleylamine stabilized silver nanofluid and the silver nanofluid without surfactant. The nanofluid containing stabilized silver nanoparticles was found to have a slightly higher viscosity than the nanofluid containing silver nanoparticles without surfactant due to the presence of surfactant, since a slight increase in viscosity was observed when oleylamine was added to oil compared to that of the base oil. Figure 4-36 also shows the viscosity curve obtained for oleylamine-stabilized Ag nanofluid at 60˚C. Most liquids become less viscous as the temperature is raised [124]. A drastic drop in viscosity was observed for both the oil and the oleylamine stabilized silver nanofluid when the analysis was performed at 60˚C. Since a molecule moves only if it acquires at least a minimum energy, the probability that a molecule has at least a minimum energy Ea is proportional to $e^{-Ea/RT}$, so the mobility of the molecules in a liquid should follow this type of temperature dependence. The coefficient of viscosity η is inversely proportional to the mobility of the particles, so it's expected that

$$\eta \propto e^{Ea/RT}$$

This expression implies that the viscosity should decrease exponentially with increasing temperature. The intermolecular forces between the molecules of a liquid govern the magnitude of Ea, however, calculations of it are extremely difficult and still largely unsolved [68].

Furthermore, at higher temperature, the viscosity of the nanofluid containing oleylamine-stabilized silver nanoparticles is practically the same as the base oil in contrast with the nanofluid at room temperature (see Figure 4-36).

4.3.3.2 Study of thermal conductivity of silver nanofluids

No difference between the two surfactants was observed with regard to stabilizing ability as well as thermal conductivity increases observed. The thermal conductivity results of the oleylamine-stabilized Ag-nanofluids are reported here. Similar to the ethylene glycol based nanofluids, no increase in thermal conductivity was observed, even though the suspensions were stable and particles were ~3 nm and well dispersed

(Figure 4-34 and Figure 4-35). The relation between the surfactant and the thermal conductivity was investigated.

Influence of the absence of surfactant on the thermal conductivity of silver nanofluids

The synthesis of the nanofluid systems were repeated without the surfactant and the thermal conductivity measured. Figure 4-37 shows the thermal conductivity results obtained for the nanofluid with and without surfactant.

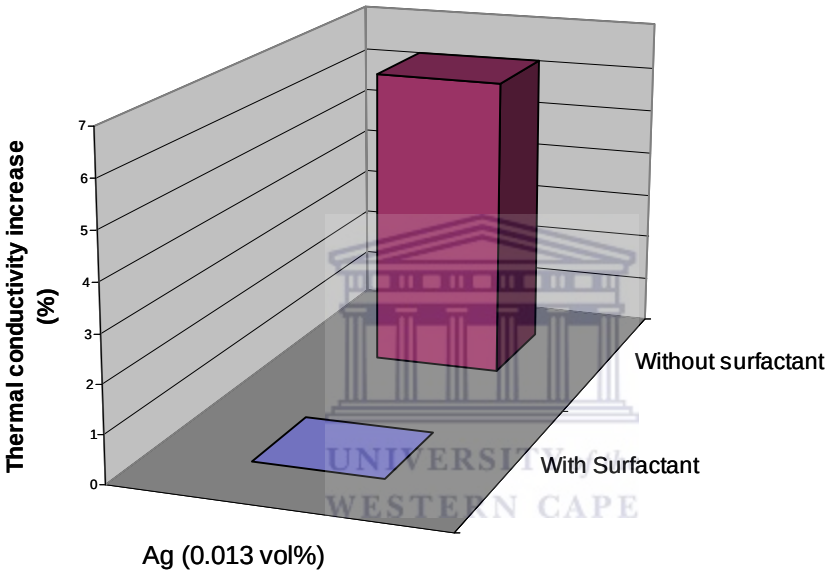

Figure 4-37: Graph showing the effect of surfactant on thermal conductivity of 0.01 vol.% silver nanofluids, prepared with and without surfactant.

In the absence of the surfactant, an increase in thermal conductivity was observed, clearly indicating that the surfactant may act as an insulator around the particles. This finding was also observed for the ethylene glycol-based nanofluids. Figure 4-38 shows the effect of silver concentration on thermal conductivity of silver nanofluids prepared without surfactant.

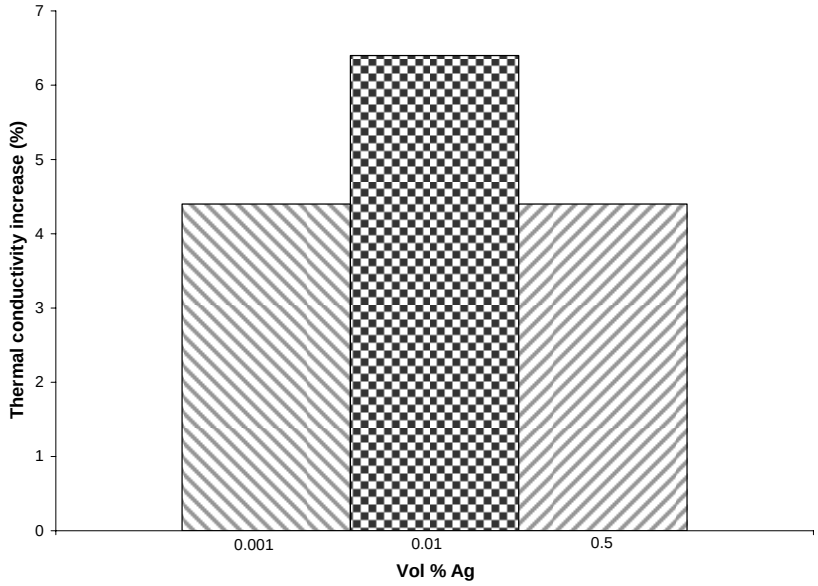

Figure 4-38: Graph showing the effect of silver concentration on thermal conductivity of silver nanofluids prepared without surfactant.

The highest increase in thermal conductivity was observed in the case of the 0.01 vol.% silver nanofluid (Figure 4-38). At higher silver concentration such as 0.5 vol.% silver, the increase of thermal conductivity was lower than for the nanofluid with 0.01% Ag. This unexpected result may be caused by excessive precipitation of Ag to the extent that the actual Ag in solution was lower than for the nanofluid with 0.01%. Since the surfactant is used to prevent particle aggregation during growth of the nuclei, performing the synthesis without surfactant may lead to particle aggregation. The TEM micrographs in Figure 4-39 (A-B) shows that the particles are in the process of agglomerating and that much bigger particles are obtained when no surfactant is used, yet an increase in thermal conductivity was observed.

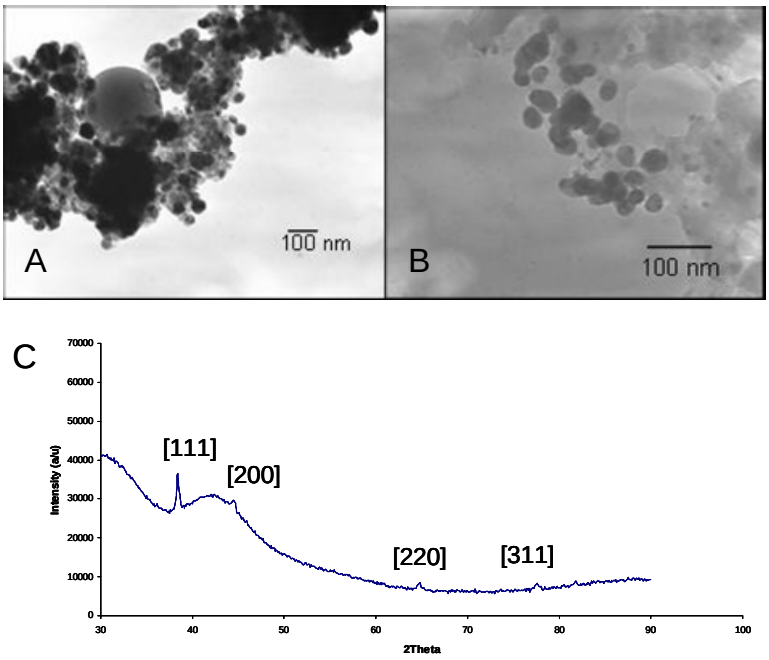

Figure 4-39: (A-B) TEM micrographs of 0.01 vol.% silver nanoparticles prepared with oil as reducing agent in the absence of surfactant and (C) XRD pattern of 0.01 vol.% silver nanoparticles prepared in oil without surfactant.

Results from XRD confirmed that the silver nanoparticles were crystalline (Figure 4-39 (C)). The diffraction peaks can be indexed to those of pure face-centered cubic (FCC), corresponding to the (111), (200), (220), and (311) planes respectively.

The surfactant, with a thermal conductivity comparable to oil, and much lower compared to silver nanoparticles, coats the particle surface to prevent particle agglomeration but also inhibit phonons from transporting heat. The coating around the particle could be seen as a defect in the crystalline lattice of the nanoparticle on which phonons propagate, causing a resistance to heat flow.

As already explained in section 4.1.9, Maxwell model will not predict any noticeable difference for volume fractions >0.05 up until the fraction of Ag in oil. The fractions of silver in the samples prepared under this section are much lower. The observed increase of thermal conductivity can, to the best knowledge of the author, not be

predicted by any published model and currently falls into a whole new area of research.

4.3.3.3 Study of the dielectric strength of transformer oil-based silver nanofluids

Since the transformer oil-based nanofluids could find possible application in transformers, the breakdown voltages of these cooling fluids were determined. Transformer oil is an electrically insulating oil which basically functions as a cooling medium to dissipate heat generated within the transformer windings. Insufficient cooling will lead to disintergration of the insulation layers around the wires and eventually to short-circuit or explosion of the transformer. It is important that the oil maintains good electrical properties such as high dielectric strength while resisting thermal degradation and oxidation. The dielectric strength of transformer oil is defined as the maximum electric field strength that the oil can withstand intrinsically before breaking down. Any significant reduction in the dielectric strength may indicate that the oil is not capable of performing the vital function in offering sufficient electrical insulation.

The dielectric strength of the transformer oil-based nanofluids containing 0.06 vol.% silver nanoparticles was measured for possible application in transformers. The results are summarized in Table 4-3 below.

Table 4-3: Dielctric strength results obtained for transformer oil-based nanofluid containing 0.06 vol.% silver nanoparticles.

Sample	Dielectric Strength (kV)	Water (ppm)	Acidity (mg/KOH/g oil)
Transformer oil (heat treated, without silver nanoparticles)	56	30	0.01
Transformer oil-based nanofluid containing oleylamine (0.08 M)-stabilized silver nanoparticles	28	69	0.09
Transformer oil-based nanofluid containing silver nanoparticles without surfactant	51	34	0.06

From Table 4-3, some changes were observed in the dielectric strength of the oil when silver nanoparticles were added, with and without surfactant. The dielectric strength was greatly reduced with the introduction of oleylamine-stabilized silver nanoparticles compared to the pure oil (Table 4-3). The low dielectric strength of the prepared nanofluid could mainly be due to the presence of moisture and the slight increase in acidity levels, as shown in Table 4-3 above. However, silver nanoparticles without added surfactant only caused a small loss in dielectric strength, which could also be due to the presence of moisture and a slight increase in acidity (Table 4-3).

4.3.4 Conclusions

Oil based nanofluids containing silver nanoparticles stabilized by oleylamine were successfully prepared using two different pathways. Both the high temperature pathway and the hydrogen reduction pathway yielded small silver nanoparticles with particle size distributions of 3.58 ± 1.61 nm and 3.0 ± 1.48 nm respectively. All the nanofluids showed Newtonian behaviour, implying true colloidal systems.

As in the case of the ethylene glycol-based nanofluids, no thermal enhancement was observed and yet again the surfactant was found to be responsible. A 6.4% increase was observed for a 0.01 vol.% silver nanofluid when the reaction was performed without the stabilizing agent. The dispersion of the particles was somehow affected since particles appeared much closer and in the process of agglomerating, resulting in much bigger particles with sizes ranging from 30-100 nm. The thermal conductivity enhancement of the oil based nanofluid without surfactant is far greater than what is predicted based on the Maxwell model. The greatly reduced dielectric strength observed with the introduction of oleylamine stabilized silver nanoparticles showed that the prepared nanofluid is not favorable for use in high voltage transformers. However, silver nanoparticles prepared without a surfactant could possibly be used in transformers since only a slight decrease in dielectric strength was observed for the suspension of silver nanoparticles in oil compared to the base oil.

5 CHAPTER FIVE: NANOFLUIDS BASED ON SILVER NANOPARTICLES IN NON-NEWTONIAN LIQUIDS – RESULTS AND DISCUSSION

The same approach as in Chapter 4 was used for nanofluid synthesis in transformer oil with carbon nanotubes and silica doping.

Multi-walled carbon nanotubes (CNTs) are tubular structures which are composed of multilayered concentric cylinders of single graphene sheets and are many microns in length but with nanometer-sized diameters ranging from around 0.4 nm [140] for inner tubes and 10 ± 30 nm for the outermost tubes. It would appear that carbon nanotubes would be the ideal fibers for heat transport because of their high aspect ratios and also because their thermal conductivity is comparable to the in-plane conductivity of graphite and approaches or even exceeds that of natural diamond, the best room temperature thermal conductor [13].

Silica is a group IV metal oxide, which has good abrasion resistance, electrical insulation and high thermal stability. Fumed silica has chain-like particle morphology. When introduced to liquids, the chains bond together via weak hydrogen bonds forming a three dimensional network, trapping liquid and effectively increasing the viscosity.

The heat management of transformer units determines a great part of the transformer cost and are of great importance since the development of so called “hotspots” can have disastrous consequences. Hotspots can be formed when the heat generated in the coil cannot be removed quickly enough. The high temperatures will attack the insulation layers on the coil. It is obvious that proper heat management should prevent hot spots or general overheating of the transformer. Installing additional radiators or enhancing the oil flow using forced convection do enhance heat

management, but require alterations to the transformer. Applying nanofluids, based on transformer oil, with enhanced thermal conductivity is another option to improve heat management. The capacity and/or the life span of the transformer may increase by just changing the oil.

By introducing carbon nanotubes or silica to transformer oil, similar trends in the enhancement of thermal conductivity may also be obtained in these systems, as was seen with silver nanoparticles suspended in transformer oil.

5.1 Synthesis and Physico-Chemical properties of silver nanoparticles dispersed in transformer oil doped with carbon nanotubes

Carbon nanotubes have some limitations to the solution-phase manipulation and processability since they are incompatible with most solvents and stabilizers [141]. Hence, poor dispersion is one of the main issues around carbon nanotube suspensions. However, it is possible to overcome the problem by acid-treating/oxidizing the carbon nanotubes. It is well known that the most effective oxidation method is treatment in a mixture of HNO_3 and H_2SO_4. The acid-treatment not only allows for oxidation to take place, but also aids in the purification of the nanotubes.

The carbon nanotubes used in most of the experiments in this work, were from a commercial source. However, carbon nanotubes have been prepared in-house (see Appendix (8.2)) for comparison purposes. The CNTs were acid treated and dispersed in oil using different surfactants. In an attempt to increase the thermal properties of the oil-based nanofluids containing carbon nanotubes even further, silver nanoparticles were deposited on the acid treated CNTs.

Nanoparticles, particularly Pt, supported on CNTs have been prepared by various research groups [142,143,144,145,146] for use as catalysts. Refluxing of carbon

nanotubes introduces acid sites on the surface of the nanotubes. The acid sites are composed of functional groups such as COOH and OH, which can act as nucleation centres for metal ions. The decoration of nanotubes by Au, Pt and Ag have been reported by Rao et al. In their work, silver nanoparticles were supported on carbon nanotubes by refluxing the nanotubes with the silver salt and nitric acid. [147].

However, the one-step synthesis and deposition of silver nanoparticles on carbon nanotubes in transformer oil have not been reported before. Herein the results are reported from the one-step method used to decorate carbon nanotubes by silver nanoparticles directly in transformer oil.

5.1.1 Influence of carbon nanotube doping on Physico-Chemical properties of transformer oil

The most common method for producing carbon nanotubes is by chemical-vapor-deposition (CVD). Certain parameters, such as the type of catalyst and carbon source used during nanotube synthesis, could influence the final properties of the nanotubes in terms of purity and size. Choi et al. [4] for example, used xylene as the primary carbon source and ferrocene to provide the iron catalyst to prepare multi-walled carbon nanotubes, which was then suspended into a synthetic poly(α-olefin) oil.
$LaNi_5$ is an intermetallic compound that is rich in nickel and is normally used for hydrogen storage applications [148]. In this study, $LaNi_5$ served as the Ni catalyst and LPG, which is cheap and readily available, was used as a carbon source.

5.1.1.1 Structural studies of carbon nanotubes dispersed in transformer oil

TEM was used to study the size and morphology of the homemade and commercially obtained carbon nanotubes. Figure 5-1 presents the TEM micrographs of the homemade and commercial carbon nanotubes before acid treatment. A broad size distribution was observed in the case of the homemade nanotubes since a mixture of

nanotubes was obtained with diameters of ~10 nm for the smaller sized nanotubes and ~70 nm for the larger nanotubes.

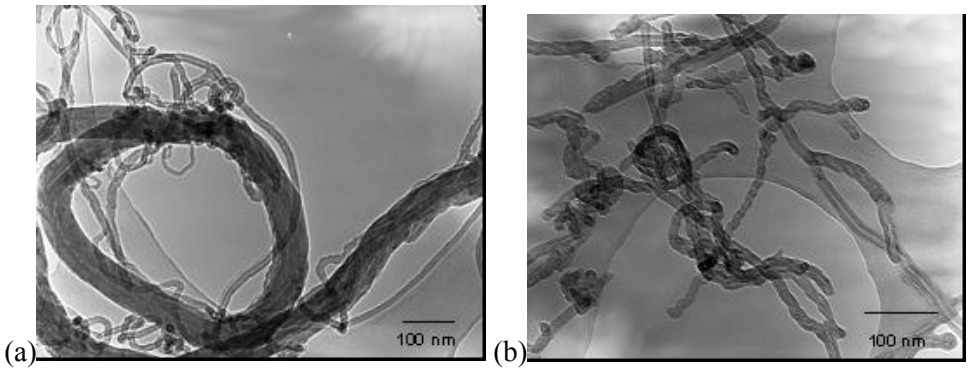

Figure 5-1: TEM micrographs of raw (a) homemade, prepared by CVD using $LaNi_5$ as catalyst and LPG as carbon source and (b) commercial CNTs before acid treatment

For comparison purposes, the TEM micrograph of the commercial nanotubes used in this study (Cheap Tubes, Inc.) is also shown in Figure 5-1. The nanotubes were generally shorter and straighter. Hence, a more uniform size distribution was obtained in the case of the commercial nanotubes with an average tube diameter of 18.4 nm, yielding a much higher aspect ratio of ~1630 compared to the homemade nanotubes with broad size distribution and lower aspect ratio of ~500-1000. The nanotubes prepared by Choi et al. [4] had an average diameter of ~25 nm and an aspect ratio of 2000. This is a clear indication that the size of the nanotubes is dependent on the method of preparation, which in turn includes the type of catalyst and carbon source.

The crystalline phases of the carbon nanotubes were determined by XRD. The XRD patterns in Figure 5-2 show that the homemade carbon nanotubes and the commercial carbon nanotubes show similar peaks to CVD-prepared carbon nanotubes that have been annealed. Annealing is usually done to improve the crystallinity of CVD-prepared nanotubes [149]. Several graphite peaks can be distinguished, among which the strongest d(002) reflection at $2\theta = 26°$.

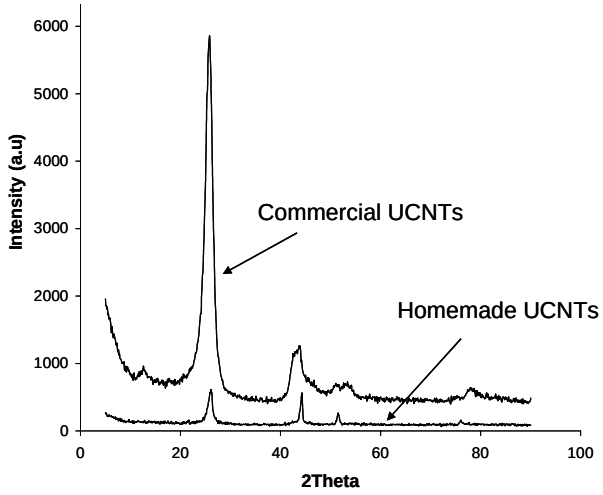

Figure 5-2: XRD patterns of the homemade CNTs, prepared by CVD using $LaNi_5$ as catalyst and LPG as carbon source, and commercial nanotubes before acid-treatment.

The nanotubes were subjected to acid-treatment in order to purify and introduce some oxygen containing groups for better dispersion.

Structural studies of carbon nanotubes after acid treatment

Acid treatment of nanotubes not only removes all the amorphous material but also allow for functionalization of the nanomaterial surface. This in turn allows for better dispersion or a means for stabilizers to attach to the nanomaterial surface. Stabilizers are often used to either stabilize materials in the nanometer range or improve their dispersion behaviour. Oleic acid and oleylamine was used as stabilizers and to enhance the dispersion characteristics of the nanomaterial. No noticeable difference was observed in the stabilizing ability of the surfactants since similar sedimentations were observed after 1 week upon standing. Figure 5-3 shows the TEM micrograph of a homemade, acid treated sample stabilized by oleic acid. The hollow core of the nanomaterial is clearly visible from the TEM micrograph in Figure 5-3. Hence, the nanotubes are in fact carbon nanotubes.

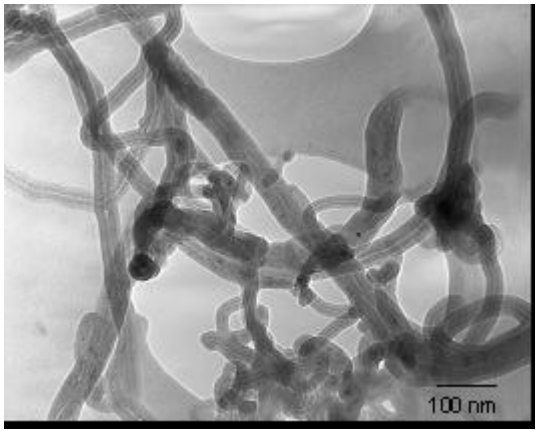

Figure 5-3: TEM micrograph of homemade, acid treated (refluxed 4 hours in a mixture of concentrated sulphuric and nitric acids (1:1 by volume sulphuric: nitric acid)), CNTs stabilized by oleic acid in transformer oil

To establish whether the graphitic structure of the CNTs is affected by the acid treatment during the oxidation process, XRD measurements were carried out on the acid treated commercial carbon nanotubes. After oxidation, all graphite peaks are still visible in the XRD spectrum (Figure 5-4). This observation demonstrates that the graphitic structure of the CNTs is unchanged after treatment, which is expected since the acid treatment only attacks the outer layer of MWCNTs.

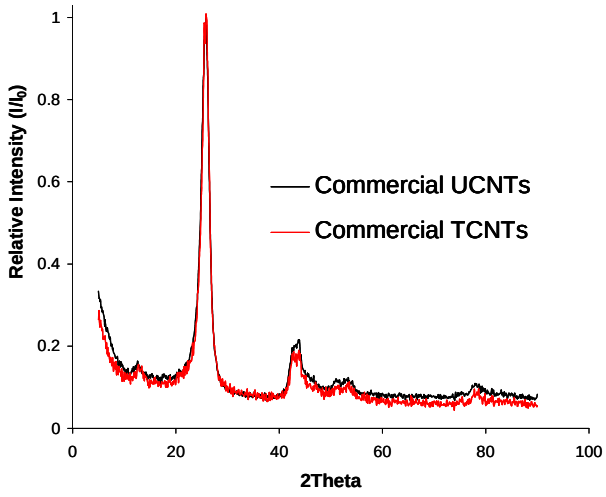

Figure 5-4: XRD patterns of untreated and acid-treated commercial carbon nanotubes, showing that the graphitic structure is retained after acid treatment.

Functional groups introduced during chemical treatment of CNTs were confirmed by Fourier Transformation Infrared (FTIR) spectroscopy. Figure 5-5 shows the infrared spectrum of carbon nanotubes before and after pretreatment in the 2400 - 500 cm^{-1} range. Comparing the two curves, it appears that the pretreatment, i.e. during the oxidation process, can lead to some organic functional groups on the surface of carbon nanotubes.

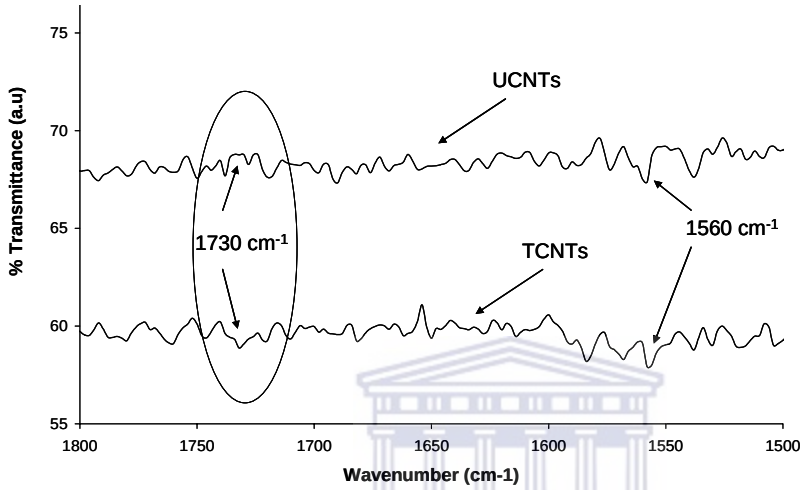

Figure 5-5: Infrared spectra of carbon nanotubes before (UCNTs) and after acid-treatment (TCNTs) showing the presence of the carbonyl group at 1730 cm^{-1} after acid treatment.

The treated carbon nanotubes (TCNTs) showed an additional peak at 1730 cm-1 which is assigned to carbonyl (C=O) stretching band. The peaks observed at ~1560 cm-1 in both the TCNTs and untreated carbon nanotubes (UCNTs) corresponds to the carbon skeleton.

In order to gain some more insight into the purity of the carbon nanotubes, TGA was performed from RT to 900˚C in air.

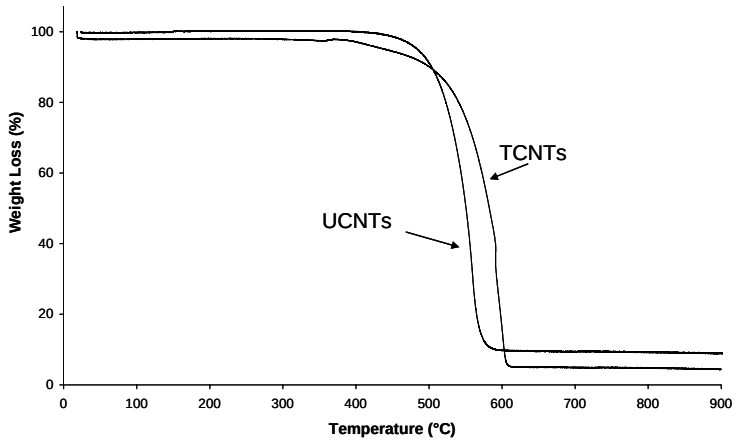

Figure 5-6: TGA thermograms obtained for commercial CNTs before (UCNTs) and after (TCNTs) acid treatment with heating rate of 5˚C/min.

Figure 5-6 shows the TGA thermograms obtained for carbon nanotubes before and after acid treatment. Some of the metal impurities were removed during the acid treatment as much less residue was observed in the thermograms after acid treatment, compared to before the acid treatment step. In addition, the temperature of combustion is an indication of the carbon nanotube's degree of crystallinity. The results suggest that the acid treatment increases the crystallinity.

Figure 5-7 shows the decomposition patterns obtained for the acid-treated homemade and commercial CNTs. The TGA study of the CNTs showed that its onset temperature for the weight loss in air occurred at 500 ˚C (Figure 5-7) and are completely oxidized around 650 ˚C. It is also noted that the commercial carbon nanotubes oxidized at a lower temperature compared to the homemade nanotubes. Smaller diameter nanotubes are believed to oxidize at lower temperatures due to a higher curvature strain. Since ~30 % of residue from the homemade CNTs remained beyond the decomposition range observed for carbon nanotubes, it implies that the homemade nanotubes contained much more impurities compared to the commercial CNTs, probably from the starting materials used to provide the catalyst.

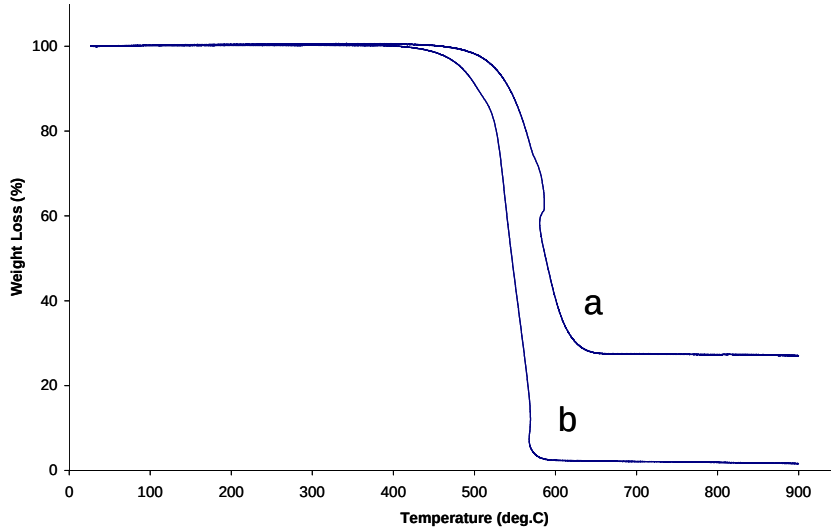

Figure 5-7: TGA thermograms obtained for acid-treated (a) homemade and (b) commercial CNT's with heating rate of 5 ˚C/min.

EDS analysis of $LaNi_5$ showed that La constitutes ~18 wt% and Ni ~ 43 wt% of the total composition (Table 5-1). The energy spectrum is given in Appendix (8.2).

Table 5-1: Quantitative EDS data for the total surface of $LaNi_5$

Element Line	*Net Counts*	*Weight %*	*Atom %*
Al K	991	3.19	8.44
Mn K	2770	7.66	9.96
Co K	2242	8.03	9.73
Ni L	4330	43.16	52.51
La L	8258	17.54	9.02
Ce L	5166	13.81	7.04
Pr L	970	2.31	1.17
Nd L	1697	4.31	2.13
Total		100.00	100.00

ICP analysis was performed in order to determine the mass % of La and Ni lost during acid-treatment. Table 5-2 shows the results obtained from ICP analysis. The results not only proved that the acid treatment is more selective towards etching La compared to Ni, but also showed that ~7 % of La is still present (Table 5-2) after acid treatment. Therefore, a mixture of impurities consisting of La, Mn, Co, Ce, Pr, Nd, as shown in Table 5-1, is responsible for the 30 % residue observed during thermal decomposition patterns (Figure 5-7). It has been shown that La enhances CNT yield

[150] and therefore this method of preparing the catalyst may be of use for methods to produce bulk quantities, kg's or more.

Table 5-2: ICP results showing the mass % of La and Ni lost during acid-treatment.

Time of Acid Treatment (min)	Mass % La Lost	Mass % Ni Lost
15	10.17	0.403
30	10.88	0.360
60	11.39	0.396

As mentioned before, oleic acid was used as a stabilizer and a means to improve the dispersion behaviour of the CNTs. Figure 5-8 shows the decomposition pattern obtained for the commercial carbon nanotube stabilized by oleic acid. The large weightloss observed at 130 -250 ˚C could be due to the surfactant as well as some moisture, followed by nanotubes oxidation until ~600 °C. No residue was observed in the decomposition pattern, which implies that the sample was free of metallic impurities. Since surfactants aids in the dispersion of carbon nanotubes, it is possible that during this process, some of the surface impurities were left behind.

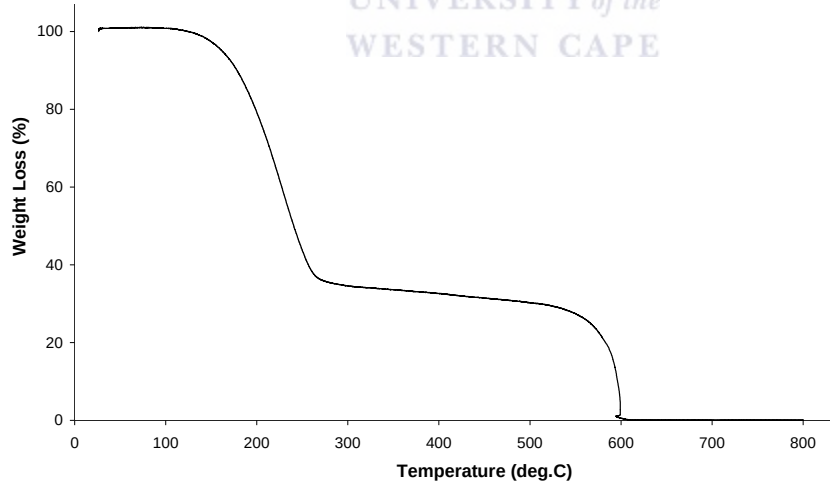

Figure 5-8: TGA thermogram obtained for commercial CNTs stabilized by oleic acid with heating rate of 5 ˚C/min.

Based on the results obtained, the homemade carbon nanotubes and the commercially obtained carbon nanotubes differ from each other by their aspect ratios as well as the purity.

5.1.1.2 Investigations of thermal conductivity of carbon nanotubes dispersed in transformer oil

Since both the homemade and commercial carbon nanotubes have been prepared using different catalysts and carbon sources and hence have different levels of impurities, one can expect that the two carbon nanotube samples will have different thermal conductivities.

In literature, significant increases in thermal conductivity have been observed in suspensions of carbon nanotubes, which, in addition to high thermal conductivity, have a very high aspect ratio [2]. The thermal conductivity of multi-walled carbon nanotubes, at room temperature, is about 20,000 times greater than that of engine oil [13]. It is therefore expected that there will be a significantly enhanced thermal conductivity in these fluids containing suspended CNTs than the conventional heat transfer fluids.

Since impurities could hold a negative or positive effect on some material properties, the effect it has towards thermal conductivity enhancement was investigated. Figure 5-9 shows the difference in thermal conductivity observed for suspensions containing the homemade and commercial CNTs, prepared without surfactant. At 0.4 wt% carbon nanotube loading, a 2.7 % and 5.4 % increase in thermal conductivity was observed for the homemade and commercial carbon nanotubes respectively. When the loading was 1.0 wt %, a 3.6 % and 7.3 % increase in thermal conductivity was observed for the homemade and commercial carbon nanotubes respectively (Figure 5-9). The nanofluids containing the commercial nanotubes showed, in general, roughly double the thermal conductivity increase (Figure 5-9), possibly due to the uniform size of the CNTs and the higher aspect ratio as well as the degree of purity found in the commercial carbon nanotubes (see TGA results in Figure 5-7). The level

of defects in nanotubes, caused mostly by the presence of impurities which could either be found in the structure or on the surface of the carbon nanotubes, can act as scattering centers for phonons and hence limit the thermal flow. In addition, the higher aspect ratios obtained for the commercial carbon nanotubes allowed for rapid heat flow over longer paths without the need to cross an interface. The thermal conductivity was found to increase nonlinearly with an increase in carbon nanotube loading. Although much larger increases in thermal conductivity of surfactant-free multi-walled carbon nanotube suspensions have been presented in literature [4], several other studies have shown smaller enhancement in thermal conductivity: Xie et al. [11] obtained a 10-20 % increase in thermal conductivity at 1.0 vol.% carbon nanotubes in organic liquid and water suspensions.

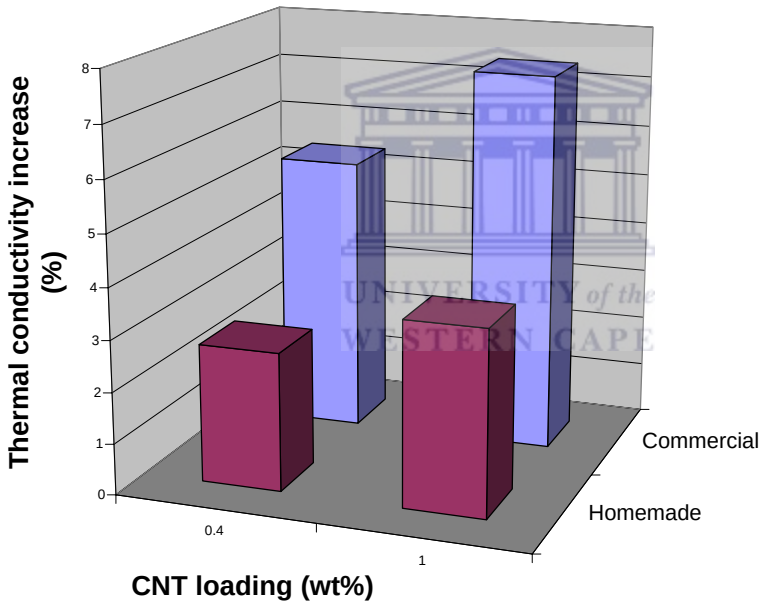

Figure 5-9: Thermal conductivity increase observed between untreated homemade and commercial nanotubes.

Before the prominent insulative role of the surfactants on the nanoparticle had been identified, it was not clear why Ag-based nanofluids did not show any increase of the thermal conductivity. In an attempt to find an explanation, CNT-based nanofluids

which were the first nanofluids showing an increase in thermal conductivity, were mixed with Ag nanoparticles.

5.1.2 Physico-Chemical properties of nanofluids based on silver nanoparticles dispersed in transformer oil modified with carbon nanotubes

Oleic acid and oleylamine was used as stabilizers and to enhance the dispersion characteristics of the nanomaterials. However, the results obtained for oleylamine-stabilized silver nanofluids containing carbon nanotubes are presented here since no noticeable difference was observed in the stabilizing ability of the surfactants. Similar average particle sizes and distributions were obtained for both oleic acid -and oleylamine-stabilized silver nanoparticles.

5.1.2.1 Synthesis and structural properties of nanofluids

Silver nanoparticles were successfully supported on CNTs by using a one-step thermal method. Figure 5-10 shows the TEM micrographs of silver supported on homemade (Figure 5-10 (A)) and commercial (Figure 5-10 (C)) CNTs with corresponding particle size distributions (Figure 5-10 (B, D)).

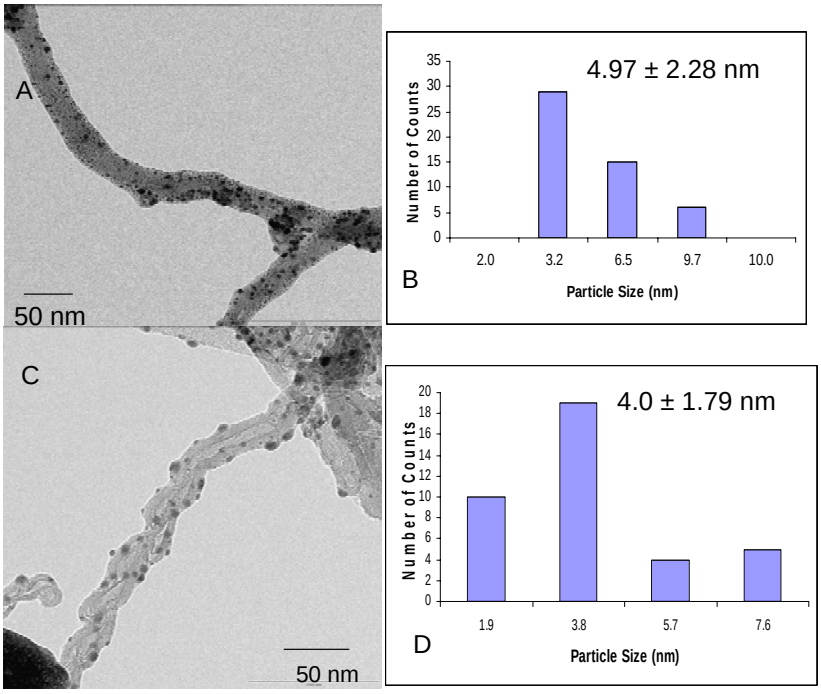

Figure 5-10: TEM micrographs and corresponding particle size distribution graphs of silver supported on (A-B) homemade carbon nanotubes and (C-D) commercial carbon nanotubes.

A silver particle size distribution of 4.97 ± 2.28 nm and 4.0 ± 1.79 nm was obtained in the case of the homemade and commercial nanotubes respectively. In both cases, particles appeared well-dispersed on the nanotube surface.

In order to support the TEM results showing the deposition of silver nanoparticles on the carbon nanotube surfaces, TGA was performed and the decomposition curve of the unsupported nanotubes compared with that of the silver supported nanotubes. Figure 5-11 shows the thermograms obtained for CNTs stabilized by surfactant and surfactant-stabilized silver nanoparticles supported on carbon nanotubes.

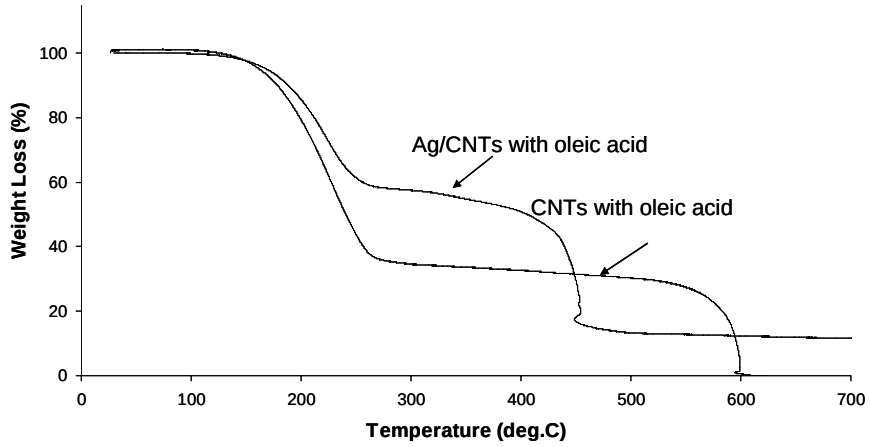

Figure 5-11: TGA thermograms obtained with heating rate of 5˚C/min. for silver supported on acid-treated commercial CNTs stabilized by oleic acid and acid treated commercial CNTs stabilized by oleic acid.

The mass loss from around 130 -250 ˚C is likely due to the decomposition of the surfactant in both samples. Following the decomposition of the surfactant, another mass loss percentage was observed, which is attributed to the oxidation of carbon nanotubes. Without silver supported on the nanotubes, the decomposition range for the nanotubes is from ~250-600 ˚C. However, with silver supported on the carbon nanotubes, a change was observed in the decomposition range for the nanotubes. The nanotubes were fully oxidized around 474 ˚C, leaving a residue which could be due to the presence of oxidized silver nanoparticles (Figure 5-11). The oxidizing temperature of decorated carbon nanotubes decreases because transition metals are known to catalyze the oxidation of carbon nanotubes. Furthermore, the DSC curve for CNTs without silver nanoparticles showed only one exothermic peak at 592 °C (Figure 5-12) due to the oxidation of carbon nanotubes, in good agreement with the TGA curve shown in Figure 5-11.

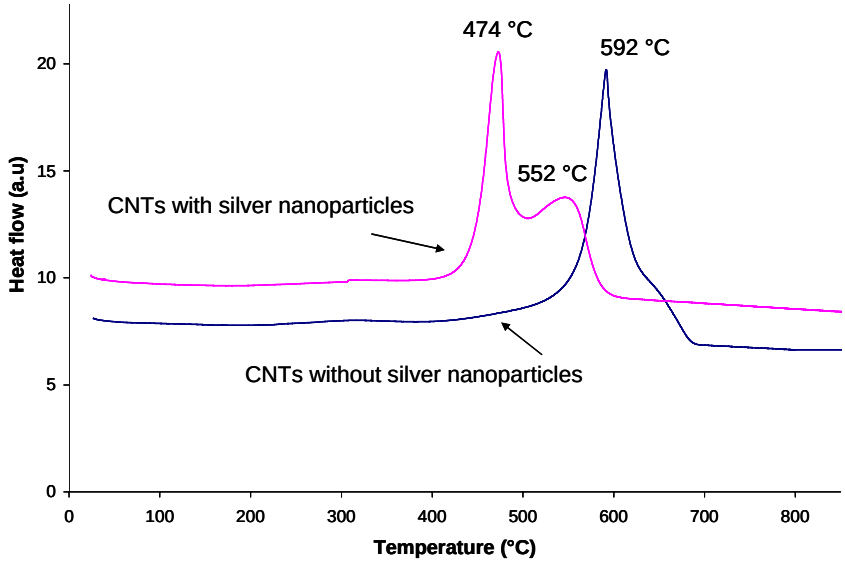

Figure 5-12: DSC curves of commercially obtained CNTs without silver nanoparticles and silver supported on commercial CNTs, stabilized by oleic acid.

Two exothermic peaks were obtained in the DSC curve for silver nanoparticles supported on CNTs, one at 474˚C (due to the oxidation of carbon nanotubes) and the other at ~552˚C (Figure 5-12). The peak at ~552 °C could possibly be due to the oxidation of silver nanoparticles, since the TEM images in Figure 5-10 showed the presence of silver nanoparticles on the surface of the carbon nanotubes, and no mass loss was observed in the TGA thermograms (Figure 5-11) during that temperature range.

5.1.2.2 Rheological properties of nanofluids containing carbon nanotubes

The rheological properties of nanofluids are often overlooked. As mentioned in section 2.1.3.1, the viscosity of a Non-Newtonian fluid will vary with shear rate.

The prepared nanofluids containing CNTs showed Non-Newtonian behavior (Figure 5-13). In addition, the fluids were shear thinning.

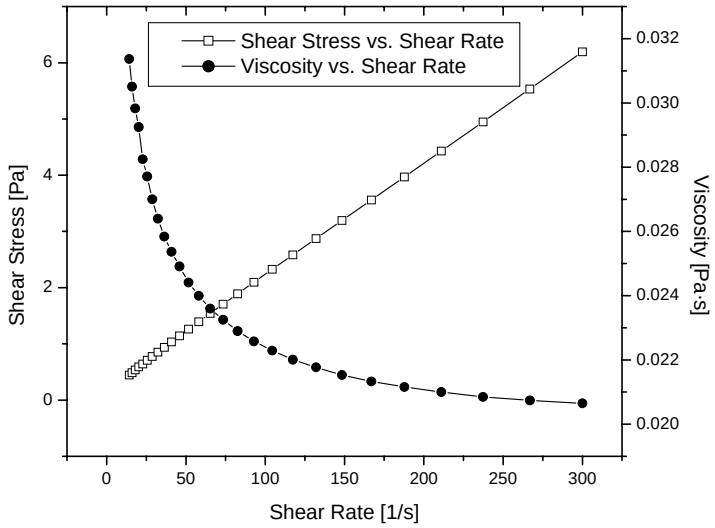

Figure 5-13: Viscosity and flow curve as a function of shear rate, showing that the nanofluid is Non-Newtonian and shear-thinning.

Shear thinning behaviour can be a result of many causes. Firstly, if aggregates are present, the increase in shear rate will cause the agglomerates to break down and hence reduce the amount of solvent immobilized by the particles, causing a lowering in the apparent viscosity of the system [151].

Secondly, asymmetric particles can also give rise to shear thinning behavior since they disturb the flow lines when they are randomly orientated at low-velocity gradients. In addition, particle interaction and solvent immobilization are favoured when conditions of random orientation prevail [151].

The high aspect ratio of carbon nanotubes could also be responsible for the observed flow behaviour. This means that longer tubes will be detangled and oriented by the shearing process which would result in a decrease in viscosity. It would therefore appear that the observed flow behaviour could be due to the high aspect ratio, as already established in section 5.1.1.1.

Figure 5-13 also shows the flow curve of the shear thinning fluid. A linear behaviour of shear stress against shear rate with an apparent yield stress is visible and therefore

the nanofluid follows the Bingham flow model [151]. Therefore, for applications which require heat transfer fluids that flow homogenously, this nanofluid may not be useful.

5.1.2.3 Thermal conductivity of nanofluids

The effect of silver nanoparticles on the thermal conductivity of nanofluids containing commercial CNTs, in the presence of surfactant, is illustrated in Figure 5-14. The carbon nanotubes without silver nanoparticles showed a 13.3 % increase in thermal conductivity at a loading of 4.0 wt%. The introduction of 0.07 vol.% silver nanoparticles allowed for a further increase of ~6 %. The growth of silver nanoparticles onto dispersed carbon nanotubes leads to further enhancement of the thermal conductivity of the nanofluids containing CNTs.

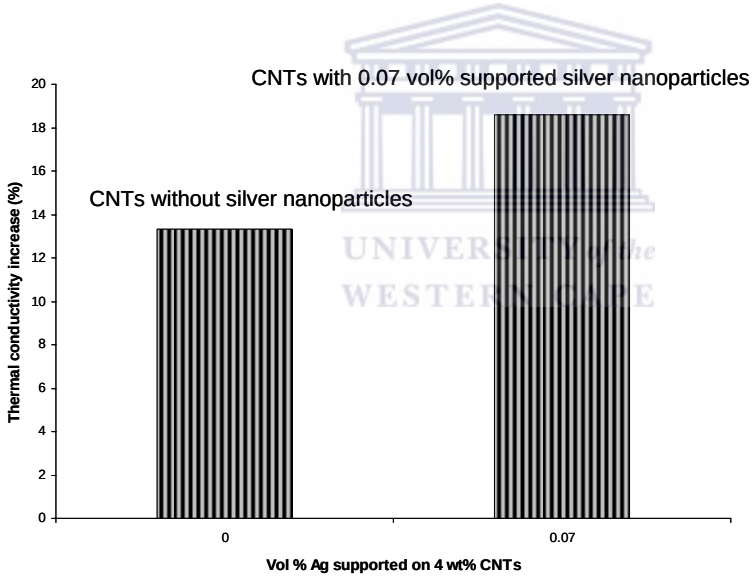

Figure 5-14: Graph showing the effect of 0.07 vol.% supported silver nanoparticles on the thermal conductivity of nanofluids containing carbon nanotubes, prepared at 130 °C in the presence of oleylamine as stabilizer.

Since the nanofluids were prepared in the presence of surfactant, it would appear that the results obtained here contradict previous results obtained for nanofluids containing unsupported, surfactant-stabilized silver nanoparticles, where no increase

in thermal conductivity was observed. A possible justification for the differences in thermal conductivity observed based on surfactant coordination to the silver and nanotube surface, is therefore given. Previous results for nanofluids containing surfactant-stabilized silver nanoparticles have shown that if the surfactant is coordinated to the silver nanoparticles, no increase in thermal conductivity was observed. Therefore it is unlikely that silver nanoparticles are coordinated to the carbon nanotube surface through the surfactant, as shown in Figure 5-15 (Scenario A).

Since the surfactant is used to improve the dispersion behaviour of the nanotubes, by coordination of the nitrogen atoms of oleylamine to the oxygen groups on the surface of the carbon nanotubes [152], it is believed that oleylamine and silver nanoparticles may compete for the oxygen groups to coordinate to the carbon nanotube surface. Since oleylamine is a long-chain (18-C) surfactant, some of the CNT-coordinated surfactant may create a shield for CNT-coordinated silver nanoparticles and hence results in surfactant free silver nanoparticles on the surface of the carbon nanotubes (Figure 5-15 (Scenario B)).

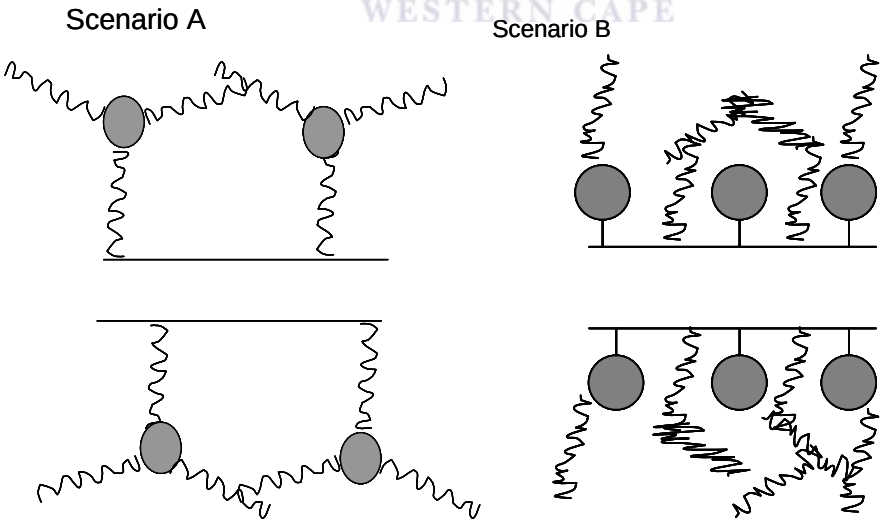

Figure 5-15: Schematic diagram showing Scenario (A): the unlikely coordination of silver nanoparticles, by means of the surfactant (oleylamine), to the carbon nanotubes surface; Scenario (B): Proposed coordination of silver nanoparticles and oleylamine to the oxygen groups on the carbon nanotube surface. A shielding effect is created for the silver nanoparticles due to the bulky surfactant

and hence surfactant free silver nanoparticles are present on the carbon nanotube surface, creating alternative phonon pathways.

This also leads to an increase in surface area of the carbon nanotubes. Since it has been shown in the case of surfactant-stabilized silver nanoparticles in both ethylene glycol and transformer oil, that the surfactant was responsible for inhibiting the heat transfer process, the enhanced thermal conductivity observed in the case of silver nanoparticles supported on CNTs could be due to alternative phonon pathways created by the presence of surfactant free silver nanoparticles on the surface of the carbon nanotubes.

5.1.2.4 Dielectric Strength of nanofluids

Due to the poor dispersion of carbon nanotubes, surfactant is necessary in order to obtain stable suspensions. Therefore, carbon nanotube-based nanofluids were prepared in the presence of a surfactant. Carbon nanotubes have very high electrical conductivity. Introducing carbon nanotubes and silver nanoparticles, which are also electrically conductive, into transformer oil could lead to drastic changes in the breakdown voltage of the transformer oil. The dielectric strength of transformer oil-based nanofluids containing surfactant-stabilized silver nanoparticles supported on carbon nanotubes was measured. The results are summarized in Table 5-3 below.

Table 5-3: Dielctric strength results obtained with corresponding water and acidity levels for transformer oil-based nanofluid containing silver nanoparticles and carbon nanotubes, in the presence of a surfactant.

Sample	Dielectric Strength (kV)	Water (ppm)	Acidity (mg/KOH/g oil)
Transformer oil (heat treated)	56	30	0.01
Transformer oil-based nanofluid containing oleylamine-stabilized silver nanoparticles	28	69	0.09
Transformer oil-based nanofluid containing oleylamine-stabilized silver nanoparticles and carbon nanotubes	2	-	-

The dielectric strength was greatly reduced with the introduction of silver nanoparticles and carbon nanotubes compared to the pure oil and also stabilized silver nanoparticles in oil (Table 5-3). The reduction in dielectric strength could be due to the nanofluid suspension reaching its percolation threshold, which implies the critical concentration where the silver nanoparticles and carbon nanotubes become close enough to form a continuous conductive pathway and hence increasing the electrical conductivity quite sharply. For future applications it would be important to study the dielectric properties in more detail and possibly find solutions to the discrepancies in the results observed. However, it would require more intensive research in this particular field.

5.1.3 Conclusions

Oil-based nanofluids containing silver nanoparticles supported nanotubes were successfully prepared using a one-step high temperature pathway. Particles were uniformly dispersed on the nanotube surface. All the nanofluids containing nanotubes were shear-thinning, showing non-Newtonian behaviour and following the Bingham flow model, which implies that the nanofluid has a yield value.

The nanofluids containing the commercial carbon nanotubes showed in general a much higher thermal conductivity than the homemade nanotubes. The lower aspect ratio of the homemade nanotubes, which was confirmed by TEM, can justify the difference.

The thermal conductivity was found to increase significantly with the introduction of the silver nanoparticles even though Ag has a much lower thermal conductivity (429 W/m-K) than carbon nanotubes (3000 W/m-K). In addition, the nanofluids were prepared in the presence of a surfactant, which was previously shown to inhibit any increase in thermal conductivity. The proposed competition between oleylamine and silver nanoparticles for the oxygen groups on the surface of the carbon nanotubes could cause a shielding effect created by the bulky nature of the surfactant. This

shielding effect leaves surfactant free silver nanoparticles on the surface of the nanotubes. This could make provision for alternative phonon pathways and hence an enhancement in thermal conductivity was observed for the nanofluid containing silver nanoparticles supported on carbon nanotubes. The dielectric strength of the oil was drastically reduced. The greatly reduced dielectric strength observed showed that the prepared nanofluid, containing silver nanoparticles supported on carbon nanotubes, is not favorable for use in high voltage transformers, and should find its application elsewhere.

5.2 Synthesis and Physico-Chemical properties of silver nanoparticles dispersed in transformer oil doped with silica

The high thermal and chemical stability of silica makes it an attractive additive in heat transfer systems. In this section, the results from various nanofluid systems containing silica and silver nanoparticles supported on silica are discussed. Detailed experimental procedures of all samples are discussed in section 3.6.2. Low concentrations of silver were used due to the poor dissolution of silver salt in the oil. All the nanofluids were prepared without any surfactant.

5.2.1 Synthesis and structural studies of silver nanoparticles dispersed in transformer oil modified with silica

Particle size and morphology was studied using TEM. Figure 5-16 (A) shows the TEM micrograph of commercially obtained silica in oil. Silver nanoparticles of varying concentrations were then synthesized and supported on 0.07 wt% silica in a single step. Figure 5-16 (B-C) shows the TEM micrograph of 0.06 vol.% silver nanoparticles supported on 0.07 wt % silica with corresponding particle size distribution. Well-dispersed silver nanoparticles were successfully deposited on the silica surface. Particles are spherical in shape with a particle size distribution of 5.5 ± 2.4 nm (Figure 5-16 (B-C)).

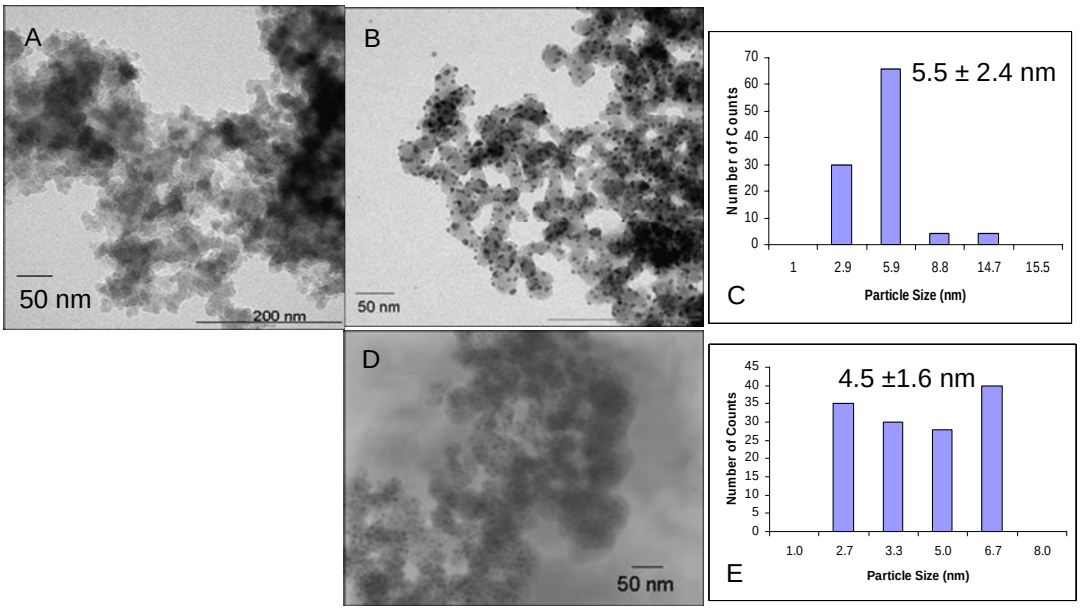

Figure 5-16: (A) TEM micrograph showing commercially obtained silica dispersed in oil, (B) TEM micrograph showing the well dispersed silver particles (0.06 vol.%) supported on the silica (0.07 wt%) with (C) corresponding particle size distribution graph, (D) TEM micrograph showing the well dispersed silver particles (0.06 vol.%) supported on the silica (0.07 wt%) after 4 months with (E) corresponding particle size distribution graph

The nanofluid system was stable since after 4 months, the same scenario of well-dispersed silver particles supported on silica was observed (Figure 5-16 (D)). No free particles were visible in the TEM micrograph and it would appear that all the silver nanoparticles stayed intact on the surface of silica. Particles are mainly spherical in shape with a particle size distribution of 4.5 ± 1.6 nm (Figure 5-16 (E)).

The XRD pattern obtained for silver nanoparticles supported on silica consisted of many sharp peaks which revealed the crystalline nature of the material (Figure 5-17). The crystallite sizes were determined by means of the Scherrer formula. Considering the [111] direction in the XRD spectrum, a value of d = 9.52 nm was found. The value obtained from TEM micrographs was much lower (Figure 5-16).

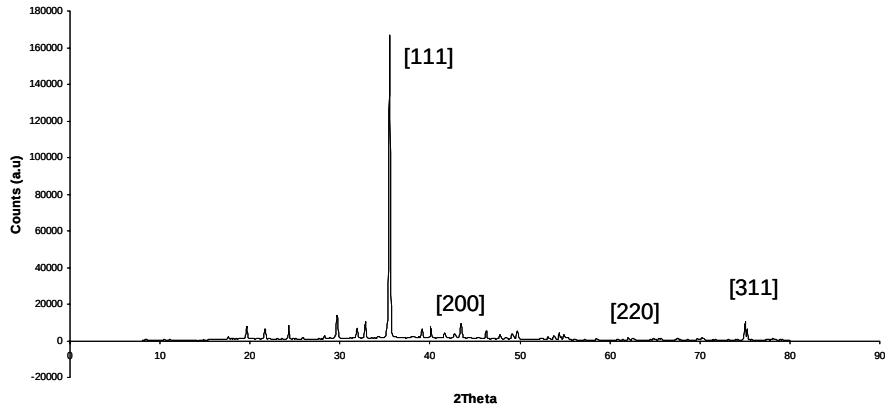

Figure 5-17: XRD pattern obtained for 0.06 vol.% Ag supported on 0.07 wt% silica

The disagreement between the crystal size obtained from TEM and XRD data is due to the fact that in the x-ray pattern, mainly the large nanocrystals contribute to the Bragg peaks. In addition, the Scherrer formula is based on size limited bulk structure. Hence, relating particle size to the peak width cannot be used with great accuracy for particles of very small size [153].

Investigation of the optical properties provided a UV-VIS spectrum with more than one peak (Figure 5-18).

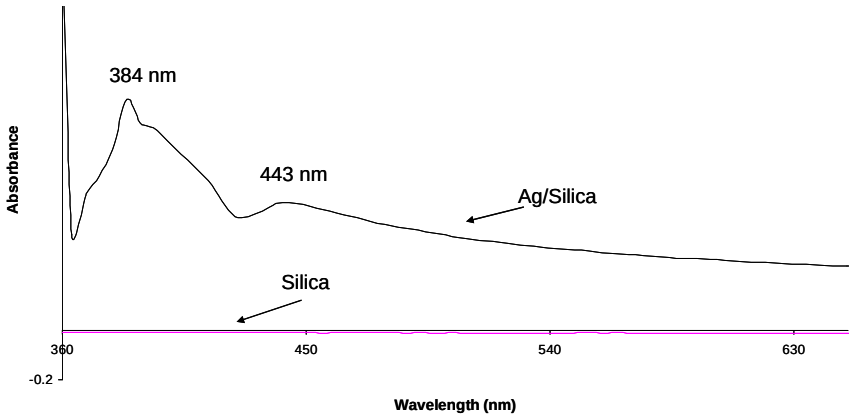

Figure 5-18: UV-VIS spectra obtained for silica without silver nanoparticles and Ag nanoparticles supported on silica

It is noted that silica has no absorption peak in ultraviolet spectrum (Figure 5-18). The Ag supported nanofluid system however, gave rise to two peaks at 384 nm and 443 nm, which were also very broad. The exact position of this plasmon band is extremely sensitive to particle size and shape and to the optical and electronic properties of the medium surrounding the particles. Silica is electronically inert (it does not exchange charge with the silver particles), but its refractive index is different from that of silver. Hence, since all the particles appeared to be spherical and mono-dispersed on the silica support, the observed spectrum could be as a result of the electronic properties of the surrounding medium.

5.2.2 Rheological properties of nanofluids

Silica (especially fumed silica), is known for its ability to increase the viscosity of organic media and nonpolar liquids, such as mineral oil and other hydrocarbons, by forming interparticle linkages arising from the net attractive forces between particles. When such linkages are formed extensively and span the sample volume, the result is a colloidal gel (i.e., a three-dimensional network of particles) [154].

Since silica forms a colloidal gel at high concentrations, a yield value is expected. This is due to intermolecular forces (Van-der-Waals). This includes dipole-dipole interactions between the particles and between the particles and the surrounding base fluid. In general, samples which display yield points tend to flow inhomogeneously and only begin to flow when the external force acting on the material is larger than the internal structural forces [151].

Figure 5-19 shows the viscosity curves for different nanofluid systems. Both suspensions containing 1.4 wt% silica showed shear-thinning behaviour at low shear rates, after which they showed idealviscous behaviour (Figure 5-19). Shearing probably caused the three-dimensional network to disintegrate, resulting in a decrease in the interaction forces amongst the particles and hence lowered the flow resistance. In addition, the suspension containing Ag supported on silica showed a lower viscosity compared to the nanofluid containing silica without Ag. This could be due

to the immobilization of silver nanoparticles on the silica, preventing the formation of the three-dimensional network that silica is known to form otherwise [154].

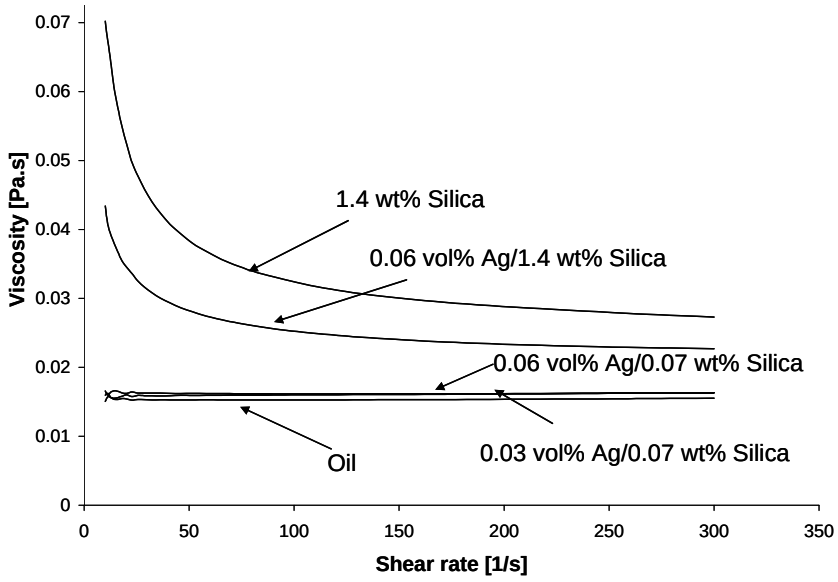

Figure 5-19: Viscosity curves for 1.4 wt% silica in oil, 0.06 vol.% Ag/1.4 wt% silica, 0.06 vol.% Ag/0.07 wt% silica, 0.03 vol.% Ag/0.07 wt% silica and oil. The nanofluid suspensions containing silver nanoparticles supported on 0.07 wt% silica showed Newtonian behaviour and the two viscosity curves were identical and slightly more viscous than the oil.

However, when a lower concentration of silica was used, a different picture was revealed in the viscosity curves. Both suspensions containing different concentrations of silver nanoparticles supported on 0.07 wt% silica showed Newtonian behaviour (Figure 5-19). This is possibly due to the much lower concentration of silica that was causing the particles to be far apart and hence, no significant interaction forces occurred between the particles, which allowed it to have a negligible effect on the viscosity. Figure 5-20 shows the behaviour of silica-based nanofluids in terms of the applied shear stress and resultant shear rate. The trend line of the correlation was calculated and the equation of the relation was investigated. The flow curves revealed that both suspensions containing 1.4 wt% silica had yield values and therefore followed the Bingham flow model (Figure 5-20). A similar result was obtained for the carbon nanotube system.

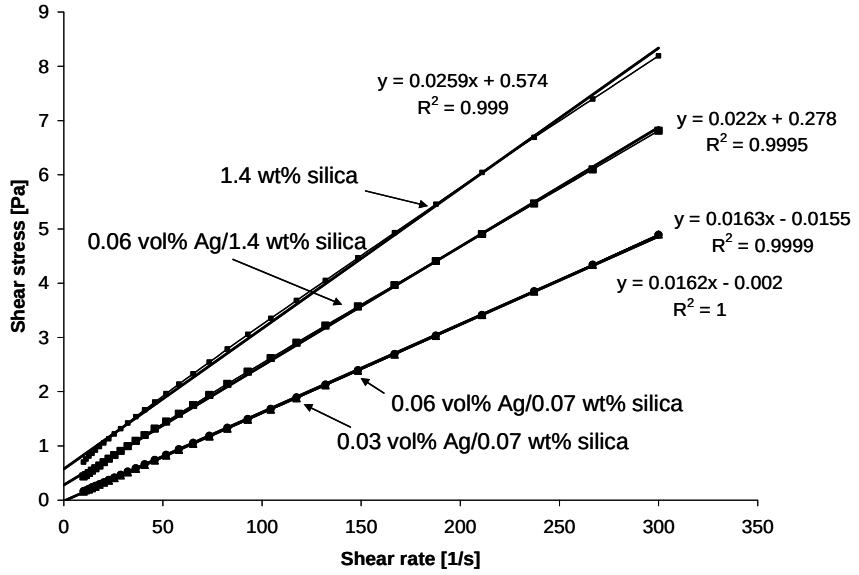

Figure 5-20: Flow curves for 1.4 wt% silica in oil, 0.06 vol.% Ag/1.4 wt% silica, 0.06 vol.% Ag/0.07 wt% silica and 0.03 vol.% Ag/0.07 wt% silica.

Figure 5-20 also shows the flow behaviour of 0.06 vol.% Ag/0.07 wt% silica and 0.03 vol.% Ag/0.07 wt% silica. As was shown in Figure 5-19, Newtonian behaviour was revealed and this was confirmed in the flow curve (Figure 5-20) showing no yield value and therefore follows the ideal Newtonian flow model. The two suspensions, although different concentrations of silver were used, had identical flow behaviour. Since the silver nanoparticles are fixed on the silica, the resulting flow behavior observed is therefore due to the silica and not due to the silver nanoparticles.

5.2.3 Thermal conductivity of nanofluids

The thermal conductivity of nanofluids containing various concentrations of silica in oil, and silica with supported silver nanoparticles in oil were measured. All the nanofluids were prepared in the absence of surfactant. A summary of the reaction conditions is given in Table 3-6. The effect of silica and silver concentration towards thermal conductivity enhancement was investigated.

- ***Influence of silica concentration without silver nanoparticles on thermal conductivity***

Due to the electrical insulation that silica offers, silica nanofluids can be very important to certain industries where cooling is required for example in high voltage applications. With a slightly higher thermal conductivity (1.4 W/m-K) than transformer oil (0.110 W/m-K), nanofluids containing silica is likely to enhance the heat transfer properties of transformer oil. Oil-based nanofluids with varying concentrations of silica were prepared and the thermal conductivity measured.

Figure 5-21 shows the thermal conductivity increase as a function of silica concentration. A 1.7% increase in thermal conductivity was observed with 0.5 wt% silica and a 3.5% increase for 1.8 wt% silica in oil. The highest concentration of silica under investigation was 4.4 wt% and resulted in a 5.2% increase in thermal conductivity (Figure 5-21). However, the higher the concentration of silica, the more gel-like the suspensions. The nanofluid containing high concentration of silica showed shear-thinning behaviour with a yield value (as was shown in Figure 5-19 and Figure 5-20). For further investigations, a silica wt% of 0.07 was chosen to ensure a homogeneous suspension.

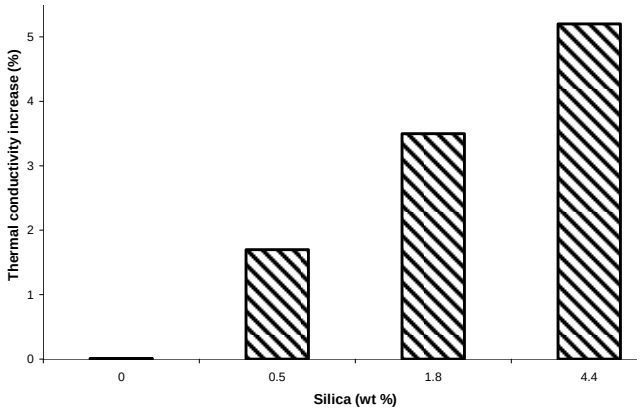

Figure 5-21: Thermal conductivity increase as a function of silica concentration

In order to bring about a further enhancement in thermal conductivity, silver nanoparticles were synthesized and deposited onto silica in one single step. Various concentrations of silver nanoparticles were deposited on 0.07 wt% silica.

- ***Influence of silver concentration on thermal conductivity in nanofluids containing silver nanoparticles supported on 0.07 wt% silica***

The effect of silver nanoparticle concentration on the thermal conductivity of nanofluids, containing silver nanoparticles supported on 0.07 wt % silica, is shown in Figure 5-22. The thermal conductivity was found to increase with an increase in silver concentration. A thermal conductivity increase of 15% was obtained when only 0.06 vol.% Ag was supported on 0.07 wt% silica. It would appear that particles need to be close enough for thermal transport to take place between them, and supporting the particles on a support provides good grounds for a stable heat transfer system.

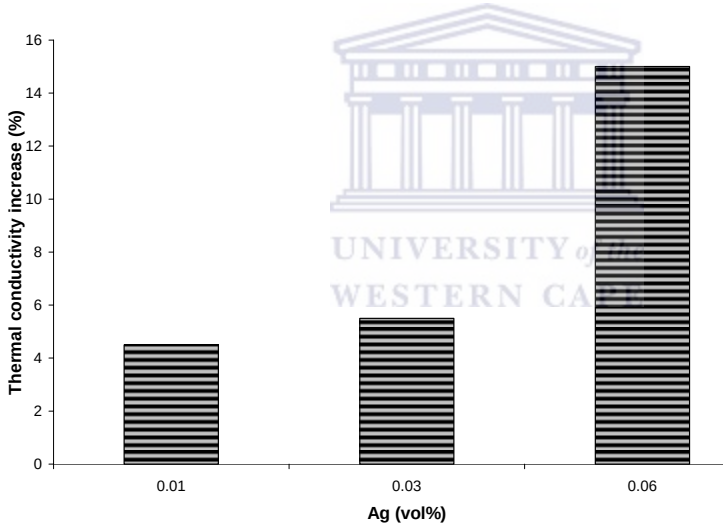

Figure 5-22: Thermal conductivity increase as a function of Ag concentration, supported on 0.07 wt % silica. Due to the poor dissolution of silver salt in oil, a maximum concentration of 0.06 vol.% silver was used.

When silver nanoparticles are fixed on a support (Figure 5-23; Scenario B), the chances of a phonon reaching another particle is far greater and hence an enhancement in the heat transfer process is observed as opposed to free particles in a suspension at varying distances from each other (Figure 5-23; Scenario A).

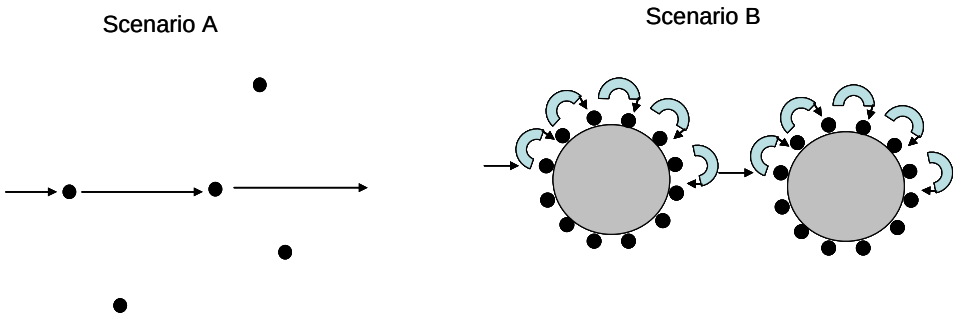

Figure 5-23: Schematic diagram showing (Scenario A) the nanofluid system containing unsupported silver nanoparticles at varying distances apart and (Scenario B) silver nanoparticles fixed at short distances from each other on the silica support.

In addition, free particles in a suspension are in constant motion due to Brownian motion and hence the chances of particles colliding to form bigger agglomerates are much greater than when a stable system is created by supporting the particles on a suitable support. In previous TEM results for silver nanoparticles suspended in oil without a surfactant, larger silver nanoparticles were observed, however, the size of the agglomerated particles were less than the phonon mean free path of ~250-300 nm [127], and therefore an enhanced thermal conductivity was obtained. Silica is not only a good support for silver nanoparticles, but is itself capable of transferring heat away. So essentially, it will not inhibit the heat transfer process as evidenced by the thermal conductivity results obtained for silica in oil.

Since the prepared nanofluids could possibly be used in transformer applications, the dielectric strength of the nanofluids had to be investigated.

5.2.4 Dielectric Strength of nanofluids

The dielectric strength is the most important electrical property when dealing with transformer oils. These oils are designed to provide electrical insulation under high electric fields. If the maximum electric field strength is reached, breakdown occurs and hence the oil would experience failure of its insulating properties. Therefore, a high dielectric strength is a prerequisite for good quality transformer oil.

The dielectric strength of the transformer oil-based nanofluids containing silica and silver supported on silica were measured for possible application in transformers. The results are summarized in Table 5-4 below.

Table 5-4: Dielctric strength results obtained for transformer oil-based nanofluid containing silica and silver supported on silica.

Sample	Dielectric Strength (kV)	Water (ppm)	Acidity (mg/KOH/g oil)
Transformer oil (heat treated)	56	30	0.01
Transformer oil-based nanofluid containing silica	34	36	0.01
Transformer oil-based nanofluid containing dried silica	30	34	0.01
Transformer oil-based nanofluid containing silver nanoparticles supported on silica	22	64	0.02

The difference in the dielectric strength observed after the introduction of silica to the oil could possibly be due to water, which is one of the main factors to reduce the breakdown voltage. Since silica is known to absorb moisture, it could possibly be responsible for the increase in water content observed (Karl Fischer results). However, since the nanofluids were prepared at temperatures above 100 °C, an improvement in dielectric strength was expected since the moisture content should be significantly reduced at such high temperatures. However, since silica is porous, moisture trapped within the pores would not be able to escape, even at such temperatures. Temperatures of 600 °C were employed to dry the silica. Some other factors such as the presence of oil-degradation by-products and high temperatures may possibly have aided in the reduction of the dielectric strength. Furthermore, high temperatures could also lead to oxidation of oil which could increase the acidity of the resulting nanofluid due to the presence of carboxylic acids. The acidity and the moisture content of the nanofluids were determined and the results are given in Table 5-4.

From Table 5-4, the acidity of the nanofluids containing silica seems to be within limits compared with the acidity obtained for the pure oil. However, an increase in moisture content was found in the nanofluids containing silica, which could possibly explain the reduced dielectric strength. The highest moisture content was observed in the nanofluid containing silver supported on silica. The reduction in the dielectric strength observed when silver nanoparticles were supported on the silica could be due to both the amount of moisture present and the presence of electrically conductive silver nanoparticles. As mentioned in section 5.1.2.4, more intensive research is necessary in this particular field before these nanofluids can be used in for example high voltage applications.

5.2.5 Conclusions

Oil-based nanofluids containing silica have been successfully prepared using a high temperature pathway. The viscosity of the silica nanofluids were found to be shear-thinning and followed the Bingham flow model at high concentrations (1.4 wt%), which could be because of 3-dimensional network silica is known to form. However, at lower silica concentrations (0.07 wt%), the nanofluids were found to be Newtonian, probably due to insignificant interaction between particles at such low concentrations. Thermal conductivity was found to increase with silica concentration.

Oil-based nanofluids containing silver nanoparticles with particle size distribution of 5.5 ± 2.4 nm supported on silica have been successfully prepared using a high temperature pathway. Small silver particles were deposited uniformly on the silica support. Nanofluids containing Ag supported on silica showed a lower viscosity compared to the nanofluid containing unsupported silica. This could be due to the immobilization of silver nanoparticles on the silica, preventing the formation of the three-dimensional network that silica is known to form otherwise. An enhancement in thermal conductivity of 15 % was observed when 0.06 vol.% silver was supported on 0.07 wt% silica. The enhancement in thermal conductivity could be due to the fixed distances of the nanoparticles on the silica support, allowing the phonons to travel

shorter distances from particle to particle compared to free particles at random distances from each other. Thermal conductivity was found to increase with an increase in silver concentration. The dielectric strength measurements showed much reduced electrical insulating properties of the oil, due to the introduction of 0.06 vol.% silver nanoparticles, but requires more intensive research in this particular field before use in high voltage transformer applications. In addition, the longterm stability of these nanofluids is poor since particles start to sediment after 1 month.

6 OVERALL CONCLUSIONS AND RECOMMENDATIONS

Nanofluids based on silver nanoparticles dispersed in Newtonian liquid -ethylene glycol as model system: Synthesis, structure and physico-chemical properties

- The effect of a wide spectrum of light during particle formation was found to play an important role in the formation of small, spherical silver nanoparticles with average size of 6 nm. In the absence of light, nanoparticle formation is slow and various shapes such as smaller spherical particles and large irregular-shaped hexagons, with sizes ranging from 10 – 450 nm are formed.
- The particle size of PVP-stabilized silver nanoparticles was found to increase with silver concentration and particle size distributions of 6.2 ± 5.8 nm, 15.50 ± 6.98 nm, 16.25 ± 8.46 nm and 21.10 ± 3.65 nm was obtained for silver concentrations of 0.01 vol.%, 0.5 vol.%, 0.7 vol.% and 1.0 vol.% respectively.
- PVP and PVA proved to be the best surfactants to stabilize silver nanoparticles since particle sizes were smaller and particles appeared to be more dispersed compared to Sulfobetaine-stabilized -and Poly(dipropylene glycol) phenyl phosphate-stabilized silver nanoparticles. A particle size distribution of 12 ± 5.1 nm was obtained for PVA-stabilized silver nanoparticles compared to the 6.2 ± 5.8 nm obtained for PVP-stabilized silver nanoparticles produced using similar molar ratios of silver to surfactant and silver concentrations of 0.01 vol.%.
- The use of Fe(III) as a surfactant free method to silver nanoparticles was investigated. The addition of ferric nitrate of varying concentrations resulted in particles with different shapes, ranging from cubes to quasi-spherical particles.
- Ethylene glycol-based nanofluids containing silver nanoparticles are Newtonian and have lower viscosities when the particles are well-dispersed.

- The thermal conductivity was measured as a function of silver particle concentration. Surprisingly, no increase in thermal conductivity was obtained even with increasing concentration of silver nanoparticles.
- The surfactant-stabilized silver nanofluids showed an increase in thermal conductivity in time, which, due to the hygroscopic nature of ethylene glycol, was entirely based on the increasing water content.
- The role of the surfactant during the heat transfer process was investigated. It was found that the surfactant is crucial for stabilization in most cases, but also has an unfavourable effect on the thermal properties. The surfactant was found to act as an insulator around the particles. A possible explanation is that the surfactant is seen as a defect in the crystal structure of the nanoparticles and therefore inhibits the phonons and electrons from transporting heat energy effectively. A 5.2 % increase for a nanofluid containing 0.5 vol.% silver nanoparticles was observed when no surfactant was used. Particles, although bigger in size, still remained well-dispersed due to protective ability of EG.
- The thermal conductivity enhancement of the nanofluid without surfactant is far greater than what is predicted based on the Maxwell model. The observed increase of thermal conductivity can, to the best knowledge of the author, not be predicted by any published model and falls into a whole new area of research.

Nanofluids based on silver nanoparticles dispersed in Newtonian liquid such as mineral oil

- Mineral oil based nanofluids containing silver nanoparticles with a narrow size distribution (9.5 ± 0.7 nm) were prepared by a one step process. The particles remained well separated even when a much lower surfactant concentration (molar ratio Ag/Korantin = 4 compared to Ag/Korantin = 1) was used.
- A higher concentration of surfactant yields monodisperse spherical silver particles with a narrow size distribution. However, high concentration silver leads to a higher loss of silver during reaction, possibly due to Brownian motion.
- The particles are stabilized by Korantin, which coordinates to the silver surface via the two oxygen atoms forming a dense layer around the particles.

- The silver suspensions were stable for about 1 month before precipitation was observed.

Synthesis, structure and studies of physico-chemical properties of silver nanoparticles in transformer oil

- The hydrogen reduction method provided smaller and more uniformly dispersed silver nanoparticles, with particle size distribution of 3.0 ± 1.48 nm, compared to thermal methods, which yielded a particle size distribution of 3.58 ± 1.61 nm.
- The nanofluids showed Newtonian behavior, showing the true colloidal nature of the solutions and since particles with sizes less than 5 nm have been obtained, it implies that the nanofluid is, for possible future applications, not likely to clog any flow channels in cooling equipment.
- Similar to ethylene glycol-based nanofluids, no increase in thermal conductivity was observed, even with the presence of very small, well-dispersed silver nanoparticles. Therefore the effect of the surfactant was investigated by performing the reactions in the absence of the surfactant. Particle size increased when no surfactant was used. A 6.4% increase was obtained for nanofluids containing 0.013 vol.% silver nanoparticles *without* a surfactant. Similarly to the ethylene glycol based nanofluid, the results showed that the stabilizer acts as an insulator around silver nanoparticles, inhibiting phonons and electrons in carrying heat away efficiently. This could possibly be due the fact that the surfactant is seen as a defect in the crystalline lattice of the nanoparticle on which phonons propagate, causing a resistance to heat flow. The observed increase in thermal conductivity is remarkable considering the minute volume fraction of Ag. The produced nanofluids outperform all models (Maxwell, Wasp, etc.) currently available in literature.
- The dielectric strength of nanofluids containing silver nanoparticles without surfactant was only slightly reduced to 51 kV (possibly due to the presence of moisture and some acidity) compared to the 56kV of the base oil.
- The transformer oil-based nanofluid containing silver nanoparticles could possibly find use in transformers due to the higher thermal conductivity, the

Newtonian flow behaviour and the only slightly reduced dielectric strength observed in these fluids. However, a limiting factor is the long-term stability of the silver nanoparticles suspended in transformer oil, which carries no guarantee. Therefore, for future applications, more research needs to be conducted on the longterm stability of these nanofluids.

Synthesis and Physico-Chemical properties of silver nanoparticles dispersed in transformer oil doped with carbon nanotubes

- Acid treatment of the nanotubes did not alter the graphitic structure of the nanotubes and removed some of the impurities found in the nanotubes. In turn, it functionalized the tips of the carbon nanotubes with oxygen-containing groups, which probably aided in the attachment of silver nanoparticles to the nanotube surface.
- Silver nanoparticles were supported on CNTs and particle size distributions of 4.97 ± 2.28 nm and 4.0 ± 1.79 nm was obtained for the Ag/homemade and Ag/commercial nanotubes respectively.
- Nanofluids containing CNTs showed shear-thinning behaviour with yield values, implying that slightly more energy will be needed for the fluids to flow in cooling application.

- Thermal conductivity results showed an increase up to 19 % with silver supported nanotubes, showing that silver nanoparticles supported on CNTs can lead to a further enhancement in thermal conductivity (~ 6 % for 0.07 vol.% silver nanoparticles), with the introduction of the silver nanoparticles with much lower conductivity (429 W/m-K) compared to carbon nanotubes (3000 W/m-K). In addition, the nanofluids were prepared in the presence of a surfactant, which was previously shown to inhibit any increase in thermal conductivity. Despite all these factors, an increase in thermal conductivity was observed. This could possibly be due to the proposed competition that exists between oleylamine and silver nanoparticles for the oxygen groups on the surface of the carbon nanotubes. A shielding effect is thereby created due to the bulky nature of the surfactant, leaving surfactant free silver nanoparticles on the surface of the nanotubes. This phenomenon made provision for alternative phonon pathways and hence an enhancement in thermal conductivity was

observed for the nanofluid containing silver nanoparticles supported on carbon nanotubes. For future work, Surface Enhanced Raman Spectroscopy (SERS) studies and computer modelling could be useful for further insight into the actual interaction between the surfactant and the particles.

- The dielectric strength of the oil-based nanofluid containing silver nanoparticles and carbon nanotubes was found to be 2 kV compared to the 56 kV obtained for that of pure oil. The greatly reduced dielectric strength observed showed that the prepared nanofluid, containing silver nanoparticles supported on carbon nanotubes, is not favorable for use in high voltage transformers, and should find its application elsewhere. For future applications, more intensive research is therefore necessary in this particular field.

Synthesis and Physico-Chemical properties of silver nanoparticles dispersed in transformer oil doped with silica

- The thermal conductivity was measured as a function of silica concentration. An increase in thermal conductivity was observed with an increase in silica concentration. A 5.2% increase in thermal conductivity was observed with a loading of 4.4 wt% silica.
- Since heat transfer fluids are to be used under flow conditions, it is essential to know how these fluids will behave then. High concentrations of silica results in shear-thinning fluid behaviour with yield values, much lower concentrations are required in order to obtain homogeneous suspensions with Newtonian behaviour. Hence, at high silica concentrations, some energy will be required before the fluid will flow during cooling applications. However, lower concentrations of silica will not need any additional pumping power.
- Silver nanoparticles were synthesized and supported on silica in one single step. Very small, uniformly dispersed silver nanoparticles were visible on the silica support. A particle size distribution of 5.5 ± 2.4 nm was obtained.
- The thermal conductivity was measured as a function of silver concentration. An increase in thermal conductivity was observed with an increase in silver

concentration. A 15 % increase in thermal conductivity was obtained with only 0.06 vol.% Ag on 0.07 wt% silica. It would appear that one of the main parameters affecting the heat transfer process is the distance between individual particles. Since free particles in a suspension could be randomly orientated or move in random directions at different distances from each other, this could possibly explain the varying increases in thermal conductivity observed, not only in this work, but by other research groups as well. For efficient heat transfer through the nanofluid, particles need to be close to each other so that phonons have a shorter distance to travel during the heat transfer process. Supported silver nanoparticles are in fixed positions close to each other which allows for phonons and electrons to effectively transfer heat through the nanofluid as they move down their paths from particle to particle. Other interesting areas of research such as the temperature dependence of thermal conductivity and the critical heat flux of nanofluids also require further investigations before nanofluids are used in cooling applications.

- The dielectric strength of the pure oil was found to be 56 kV. With the introduction of 0.07 wt% silica, a decrease was observed resulting in a dielectric strength of 34 kV. Supporting silver nanoparticles on the silica resulted in an even further reduction of the dielectric strength, yielding a value of 22 kV. The decrease due to the introduction of silver nanoparticles was slightly lower in the case of supported silver nanoparticles compared with the unsupported silver nanoparticles, stabilized by oleylamine, in transformer oil. The poor insulating properties could be due to considerable moisture levels found in the nanofluids. More intensive research is therefore needed in this particular field before use in high voltage transformer applications, especially since the nanofluids showed some sedimentation upon standing after 1 month.

7 BIBLIOGRAPHY

[1] Choi, S. U. S.;Eastman, J. A.; Patent: US 6221275 B1 (2001)

[2] Keblinski, P.; Eastman, J. A.; Cahill, D. G. *Mater. Today*, June, 2005, 36.

[3] Eastman, J. A.; Choi, S. U. S.; Li, S.; Yu, W.; Thompson, L. J.; *Appl. Phys. Lett.*, 78, 2001, 718.

[4] Choi, S. U. S.; Zhang, Z. G.; Yu, W.; Lockwood, F. E.; Grulke, E. A.; *Appl. Phys. Lett.*, 79, 2001, 2252.

[5] Karabacak, D. M.; Yakhot, V.; Ekinci, K. L.; *Phys. Rev. Lett.*, 98, 2007, 254505-1.

[6] Lee, D. K.; Kang, Y. S.; *ETRI J.*, 26, 2004, 252.

[7] Bönnemann, H.; Botha S. S.; Bladergroen B.; Linkov, V. M.; *Appl. Organomet. Chem.*, 19, 2005, 768.

[8] Zhu, H.; Lin Y.; Yin, Y.; *J. Coloid Interface Sci.*, 277, 2004, 100.

[9] Abid, J. P.; Wark, A. W.; Brevet, P. F.; Girault, H. H.; *Chem. Commun.*, 2002, 792.

[10] Patel, H. E.; Das, S. K.; Sundararajan, T.; Nair, A. S.; George, B.; Pradeep, T.; *Appl. Phys. Lett.*, 83, 2003, 2931.

[11] Xie, H.; Lee, H.; Youn, W.; Choi, M.; *J. Appl. Phys.*, 94, 2003, 4967.

[12] Liu, M.-S.; Lin, M. C.-C.; Huang, I.-T.; Wang, C.-C., *Int. Commun.Heat Mass Transfer*, 32, 2005, 1202.

[13] Eastman, J. A.; Phillpot, S. R.; Choi, S. U. S.; Keblinski, P., *Annu. Rev. Mater. Res.*, 34, 2004, 219.

[14] Kwak, K.; Kim, C.; *Kor.-Austr. Rheol. J.*, 17, 2005, 35.

[15] Hornstein, B. J.; Finke, R. G.; *Chem. Mater.*, 15, 2003, 899.

[16] Masala, O.; Seshadri, R.; *Annu. Rev. Mater. Res.*, 34, 2004, 41.

[17] Edlestein, A. S.; Cammarata, R. C.; Eds. 2001, *Nanomaterials: Synthesis, Properties and Applications*. London: Institute of Physics.

[18] Van Hyning, D. L.; Klemperer, W. G.; Zukoski, C. F.; *Langmuir*, 17, 2001, 3128.

[19] Sondi, I.; Goia, D. V.; Matijevi´c, E.; *J. Colloid Interface. Sci.*, 260, 2003, 75.

[20] Son, S. U.; Park, I. K.; Park, J.; Hyeon, T.; *Chem. Commun.*, 2004, 778.

[21] Mallick, K.; Witcomb, M. J.; Scurrell, M. S.; *J. Mater. Sci.*, 39, 2004, 4459.

[22] Ma, H.; Yin, B.; Wang, S.; Jiao, Y.; Pan, W.; Huang, S.; Chen, S.; Meng, F.; *ChemPhysChem*, 5, 2004, 68.

[23] Nikoobakht, B.; Wang, Z. L.; El-Sayed, M. A.; *J. Phys. Chem. B*, 104, 2000, 8635.

[24] Widegren, J. A.; Finke, R. G.; *J. Mol. Catal. A:* 191, 2003, 187.

[25] Bönnemann, H.; Brijoux, W.;,Brinkmann, R.; Endruschat, U.; Hofstadt, W.; *Angermund K. Rev. Roum. Chim.* 44, 1999, 1003.

[26] Paulus, U. A.; Endruschat, U.; Feldmeyer, G. J.; Schmidt, T.J.; Bönnemann, H.; Behm, R. J.;*J. Catal.*, 195, 2000, 383.

[27] Bönnemann, H.; Angermund, K.; Bühl, M.;, Endruschat, U.; Mauschick, F.T.; Mörtel, R.; Mynott, R.; Tesche, B.; Waldöfner, N.; *J., Phys. Chem. B.* 107, 2003 7507.

[28] Bönnemann, H.; Waldöfner, N.; *Chem. Mater.*, 14, 2002, 1115.

[29] Bönnemann, H.; Brijoux, W.; Brinkmann, R.; WO 99/59713, November 1999.

[30] Slistan-Grijalva, A.; Herrera-Urbina, R.; Rivas-Silva, J. F.; Ávalos-Borja, M.; Castillón-Barraza, F. F.; Posada-Amarillas, A.; *Physica E*, 25, 2005, 438.

[31] Mock, J. J.; Barbic, M.; Smith, D. R.; Schultz, D. A.; Schultz, S.; *J. Chem. Phys.*, 116 (15), 2002.

[32] Kryukov, A. I.; Ziníchuk, N. N.; Korzhak, A. V.; Ya. Kuchmii, S.; *Theor. Exp. Chem.*, 39 (1), 2003, 9.

[33] González, A. L.; Noguez, C.; Ortiz, G. P.; Rodríguez-Gattorno, G.; *J. Phys. Chem. B.*, 109, 2005, 7512.

[34] Xuan, Y.; Li, Q.; *Int. J. Heat Fluid Flow*, 21, 2000, 58.

[35] Bom D.; Andrews R.; Jacques D.; Anthony J.; Chen B.; Meier M.S.; Seleque J.P.; *Nano Lett.*, 2 (6), 2002, 615.

[36] Kreibig, U.; Bour, G.; Hilger, A.; Gartz, M.; *Phys. Status Solidi A*, 175, 1999, 351.

[37] Temgire, M. K.; Joshi, S. S.; *Radiat. Phys. Chem.*, 71 (5), 2004, 1039.

[38] Wang, S.; Kang, S. S.; Nikles, D. E.; Harrell, J. W.; Wu, X. W.; *J. Magn. Magn. Mater.*, 266, 2003, 49.

[39] Patel, K.; Kapoor, S.; Dave, D. P.; Mukherjee, T.; *J. Chem. Sci*.,117 (1), 2005, 53.

[40] Gao, Y.; Jiang, P.; Song, L.; Liu, L.; Yan, X.; Zhou, Z.; Liu, D.; Wang, J.; Yuan, H.; Zhang, Z.; Zhao, X.; Dou, X.; Zhou, W.; Wang, G.; Xie, S.; *J. Phys. D: Appl. Phys*. 38, 2005, 1061.

[41] Bonet, F.; Tekaia-Elhsissen, K.; Sarathy, K. V.; *Bull. Mater. Sci.*, 23 (3), 2000, 165.

[42] Sun, Y.; Gates, B.; Mayers, B.; Xia, Y.; *Nano Lett.*, 2 (2), 2002, 165.

[43] Chimentão, R. J.; Kirm, I.; Medina, F.; Rodríguez, X.; Cesteros, Y.; Salagre, P.; Sueiras, J. E.; *Chem. Commun.*, 2004, 846.

[44] Brust, M. J.; Chem. Soc., *Chem. Comm.*, 7, 1994, 801.

[45] Lo, C-H.; Tsung, T-T.; Chen, L-C.; Su, C-H.; Lin, H-M.; *J. Nanopart. Res.,* 7, 2005, 313.

[46] Hsin, Y.L.; Hwang, K.C.; Chen, F.; Kai, J.; *Adv. Mater.*, 13, 2001, 11.

[47] Sastry, M.; *Pure Appl. Chem.*; 74(9), 2002, 1621.

[48] Warad, H. C.; Ghosh, S. C.; Hemtanon, B.; Thanachayanont, C.; Dutta, J.; *Sci. Technol. Adv. Mater.*, 6, 2005, 296.

[49] Juillerat, F.; Solak, H. H.; Bowen, P.; Hofmann, H.; *Nanotechnol.*, 16, 2005, 1311.

[50] Itri, R.; Depeyrot, J.; Tourinho, F. A.; Sousa, M. H.; *Eur. Phys. J. E*, 4, 2001, 201.

[51] Chen, C-W.; Chen, M-Q.; Serizawa, T.; Akashi, M.; *Adv. Mater.*, 10 (14), 1998, 1122.

[52] Kong, Q.; Chen, X.; Yao, J.; Xue, D.; *Nanotechnol.*, 16, 2005, 164.

[53] Rensmo, H.; Ongaro, A.; Ryan, D.; Fitzmaurice, D.; *J. Mater. Chem.*, 12, 2002, 2762.

[54] Pal, T.; Sau, T. K.; Jana, N. R.; *Langmuir*, 13, 1997, 1481.

[55] Egorova, E. M.; Revina, A. A.; *Colloid J.*, 64 (3), 2002, 301.

[56] Aiken III, J. D.; Finke, R. G.; *J. Mol. Cat. A*, 145, 1999,1.

[57] Liu, J.; Luijten, E.; *Phys. Rev. Lett.*, PRL 93, 2004, 247802.

[58] Karanikas, S.; Louis, A.A.; *Phys. Rev. Lett.*, PRL 93, 2004, 248303.

[59] Gaddy, G. A.; Korchev, A. S.; McLain, Jason L.; Black, J. R.; Mills, G.; Bratcher, M. S.; Slaten, B.L.; *Reversible Formation of Silver Clusters and Particles in Polymer Films*, December 2004, Conference paper, ADA433495.

[60] Chou, K.-S.; Lai, Y.-S.; *Mater. Chem. Phys.*, 83, 2004, 82.

[61] Keblinski, P.; Phillpot, S. R.; Choi, S.; Eastmand, J. A.; *Int. J. Mass Heat Transfer*, 45, 2002, 855.

[62] Tsai, C. Y.; Chiena, H. T.; Ding, P. P.; Chan, B.; Luh, T. Y.; Chen, P. H.; *Mater. Lett.*, 58, 2004, 1461.

[63] Kim, J-K.; Jung, J. Y.; Kang, Y. T.; *Int. J. Refrig.*, 29, 2006, 22.

[64] Lo, C-H.; Tsung, T-T.; Chen, L-C.; *J. Cryst. Growth.*, 277, 2005, 636.

[65] Koo, J.; Kleinstreuer, C.; *Int. Commun. Heat Mass Transfer*, 32, 2005, 1111.

[66] Xuan, Y.; Roetzel, W.; *Int. J. Heat Mass Transfer*, 43, 2000, 3701.

[67] Buyevich, Y. A.; *Fluid Dynamics in Fine Suspension Flow.* In *Advances in the Flow and Rheology of Non-Newtonian Fluids, Part B*. 1st ed. Edited by Siginer, D. A.; De Kee, D.; Chhabra, R. P.; Amsterdam, The Netherlands: Elsevier, 1999, 1237-1297.

[68] Atkins, P. W.; 1994, *Physical Chemistry*, Oxford: Oxford University Press.

[69] Xue, Q.; Xu, W-M.; *Mater. Chem. Phys.*, 90, 2005, 298.

[70] Choi, S. U. S.; Zhang, Z. G.; Yu, W.; Lockwood, F. E.; Grulke, E. A. *Appl. Phys. Lett.*, 79, 2001, 2252.

[71] Hamilton, R. L.; Crosser, O. K.; *I & EC Fundamentals,* 1, 1962, 187.

[72] Koo, J.; Kleinstreuer, C.; *J. Nanopart. Res.*, 6 (6), 2004, 577.

[73] Wang, B-X.; Zhou, L-P.; Peng, X-F.; *Int. J. Heat Mass Transfer*, 46, 2003, 2665.

[74] Yu, W.; Choi, S. U. S.; *J. Nanopart. Res.,* 5, 2003, 167.

[75] Kumar, D. H.; Patel, H. E. Kumar, V. R. R.; Sundararajan, T.; Pradeep, T.; Das, S. K., *Phys. Rev. Lett.*, 93, 2004, 14.

[76] Murshed, S. M. S.; Leong, K. C.; Yang, C.; *Int. J. Therm. Sci.*, 44, 2005, 367.

[77] Putra, N.; Roetzel, W.; Das, S. K.; *Heat Mass Transfer*, 39, 2003, 775.

[78] Trisaksri, V.; Wongwises, S.; Renew. Sust. Energ. Rev., 11, 2007, 512.

[79] Yang, Y.; Grulke, E.A.; Zhang, Z.G.; Wu, G.; *J. Appl. Phys.*, 99, 2006, 114307-1.

[80] Alstaedt, V.; Werner, P.; Sandler, J.; *Polímeros: Ciência e Tecnologia*, 13 (4), 2003, 218.

[81] Song, Y.S.; *Rheol. Acta*, 46, 2006, 231.

[82] Assael, M. J.; Chen, C.-F.; Metaxa, I.; Wakeham, W. A.; *Int. J. Thermophys.*, 25, 2004, 971.

[83] Assael, M. J.; Metaxa, I. N.; Arvanitidis, J.; Christofilos, D.; Lioutas, C.; *Int. J. Thermophys.*, 26, 2005, 647.

[84] Xue, Q. Z.; Physica B, 368, 2005, 302.

[85] The Dow Chemical Company (1995-2007), *Thermal fluids: Pharmaceutical processing*, [Online].Available http://www.dow.com/heattrans/app/pharm.htm

[86] U.S. Department of Enegy, Office of Fossil Energy: National Energy Technology Laboratory, (2007), *Nanofluids for use as ultra-deep drilling fluids*, [Online] Available http://www.netl.doe.gov/

[87] Ma, H. B.; Wilson, C.; Borgmeyer, B.; Park, K.; Yu, Q.; Choi, S. U. S.; Tirumala, M.; *Appl. Phys. Lett*., 88, 2006, 143116.

[88] Wiley, B.; Sun, Y.; Xia, Y.; *Langmuir*, 21 (18), 2005, 8077.

[89] Yang, Y.; Grulke, E.A.; Zhang, Z.G.; Wu, G.; *J. Appl. Phys.*, 99, 2006, 114307-1.

[90] Tartaj, P.; Del Puerto Morales, M.; Veintemillas-Verdaguer, S.; González-Carreño, T.; Serna, C. J.; *J. Phys. D: Appl. Phys.*, 36. 2003, 182.

[91] Sun, L.; Zhang, Z.; Dang, H.; *Mater. Lett.*, 57, 2003, 3874.

[92] Patakfalvi, R.; Oszkó, A.; Dékány, I.; *Colloids Surf. A: Physicochem. Eng. Aspects*, 220, 2003, 45.

[93] He, R.; Qian, X.; Yin, J.; Zhu, Z.; *J. Mater. Chem*. 12, 2002, 3783.

[94] Yin, Y.D.; Li, Z. Y.; Zhong, Z. Y.; Gates, B.; Xia, Y.; Venkateswaran, S.; *J. Mater. Chem*., 12, 2002, 522.

[95] Jiang, L.-P.; Wang, A.-N.; Zhao, Y.; Zhang, J.-R.; Zhu, J.-J.; *Inorg. Chem. Commun.*, 7, 2004, 506.

[96] Lee, M.-H.; Oh, S.-G.; Suh, K.-D.; Kim, D.-G.; Sohn, D.; *Colloids Surf. A: Physicochem. Eng. Aspects*, 210, 2002, 49.

[97] Pastoriza-Santos, I.; Liz-Marzán, L. M.; *Nano Lett*., 2, 2002, 903.

[98] Gargallo, L.; Dadić, D.; Martínez-Piña, F.; *Eur. Polym. J.*, 33 (10-12), 1997, 1767.

[99] Kong, Q.; Chen, X.; Yao, J.; Xue, D.; *Nanotechnol*., 16, 2005, 164.

[100] Cai, M.; Chen, J.; Zhou, J.; *Appl. Surf. Sci*., 226 (4), 2004, 422.

[101] Mandal, S.; Arumugam, S. K.; Pasricha, R.; Sastry, M.; *Bull. Mater. Sci.*, 28, 2005, 503.

[102] Liu, Y.; *J. Coll. Inter. Sci.,* 257, 2003, 188.

[103] Yang, Y. J.; He, L. Y.; *J. Solid State Electrochem.*, 10, 2006, 430.

[104]. Eduardo, J. H.; Lee, C. R.; Elson, L.; Edson, R. L.; *Chem. Phys.*, 328, 2006, 229.

[105] Tilaki, R. M.; Irajizad, A.; Mahdavi, S. M.; *Appl. Phys. A*, 84, 2006, 215.

[106] Huang, H. H.; Ni, X. P.; Loy, G. L.; Chew, C. H.; Tan, K. L.; Loh, F. C.; Deng, J. F.; Xu, G. Q.; *Langmuir*, 12, 1996, 909.

[107] Yan, X.; Liu, H.; Liew, K-Y.; *J. Mater. Chem.*, 11, 2001, 3387.

[108] Nikoobakht, B.; El-Sayed, M. A.; *Chem. Mater.*, 15, 2003, 1957.

[109] Hailstone, R.; *Nature*, 402 (6764), 1999, 856.

[110] Lindfors, L.; Skantze, P., Skantze, U.; Rasmusson, M.; Zackrisson, A.; Olsson, U.; *Langmuir*, 22, 2006, 906.

[111] Wang, H.; Qiao, X.; Chen, J.; Wang, X.; Ding, J.; *J. Mat. Phys*., 94, 2005, 449.

[112] Gao, Y.; Jiang, P.; Liu, D. F.; Yuan, H. J.; Yan, X. Q.; Zhou, Z. P.; Wang, J. X.; Song, L.; Lui, L. F.; Zhou, W. Y.; Wang, G.; Wang, C. Y.; Xie, S. S.; J. Phys. Chem. B, 108, 2004, 12877.

[113] Liz-Marzán, L. M.; *Mater. Today* (2004).

[114] Murray, C. B.; Sun, S., Gaschler, W.; Doyle, H.; Betley, T. A.; Kagan, C. R.; *IBM J. Res. & Dev.*, 45 (1), 2001, 47.

[115] Harris, L. A.; *Chemistry 173* (Virginia Polytechnic Institute and State University, Blacksburg, Virginia, 2002).

[116] Serebryakova, N. V.; Uryupina, O. Y.; Roldughin, V. I.; *Colloid J.* 67, 2005, 79.

[117] Dékány, I.; Patakfalvi, R.; Virányi, Z.; *Colloi. Polym. Sci.*, 283, 2004, 299.

[118] Joshi, R.; Mukherjee, T.; *Radiat. Phys. Chem.*, 76, 2007, 811.

[119] Haynie, D.T.; *Biological Thermodynamics*, Cambridge University Press, 2001, ISBN: 0521795494.

[120] Bönnemann, H.; Wittholt, W.; Jentsch, J. D.; Tilling, A. S.; *New J. Chem.*, 1998, 713.

[121] Capek, I.; *Adv. Colloid Interface Sci.*, 110, 2004, 49.

[122] Huber, D. L.; *Small*, 1 (5), 2005, 482.

[123] Gavlin, G.; Coltsin, B.;United States Patent 546258 (1995).

[124] Wright, P. G.; *Phys. Edu.*, 1977, 323.

[125] Ramsden, E. N.; *A-Level Chemistry*, 4th ed., Nelson Thornes, 2000, ISBN 0748752994.

[126] Kao, M. J.; Tien, D. C.; Jwo, C. S.; Tsung, T. T.; *7th International Symposium on Measurement Technology and Intelligent Instruments,* 442-445 (Institute of Physics, 2005).

[127] Chen, G., *J.; Nanopart. Res.*, 2, 2000, 199.

[128] Putnam, S. A.; Cahill, D. G.; Braun, P. V.; Ge, Z.; Shimmin, R. G.; *J. Appl. Phys.*, 99 (8), 2006, 084308.

[129] Link, S.; Wang, Z. L.; El-Sayed, M. A.; *J. Phys. Chem. B.*; 103, 1999; 3529.

[130] Ghosh, S. K.; Kundu, S.; Mandal, M.; Nath, S.; Pal, T.; *J. Nanopart. Res.*, 5: 2003, 577.

[131] Wang, W.; Chen, X.; Efrima, S. J.; *Phys. Chem. B.*, 103, 1999; 7238.

[132] Abe, K.; Hanada, T., Yoshida, Y.; Tanigaki, N.; Takiguchi, H.; Nagasawa, H.; Nakamoto, M.; Yamaguchi, T.; Yase, K.; *Thin Solid Films*, 327-329, 1998, 524.

[133] Choi, H. J.; Han, S. W.; Lee, S. J.; Kim, K.; *J. Colloid Interface Sci.*, 264: 2003; 458.

[134] Shin, H. S.; Yang, H. J.; Kim, S. B.; Lee, M. S.; *J. Colloid Int. Sci.*, 274, 2004, 89.

[135] Tao, Y.; *J. Am. Chem. Soc.*, 115, 1993; 4350.

[136] Pastoriza-Santos, I.; Liz-Marzán, L. M.; *Pure Appl. Chem.*, 72, 2000, 83.

[137] He, R.; Qian, X.; Yin, J.; Zhu, Z.; *J. Mater. Chem.,* 12, 2002, 3783.

[138] Carotenuto, G.; *Appl. Organomet. Chem.*, 15, 2001, 344.

[139] Chen, M.; Feng, Y-G.; Wang, X.; Li, T-C.; Zhang, J-Y.; Qian, D-J.; *Langmuir*, 23, 2007, 5296.

[140] Dresselhaus, M. S.; Dresselhaus, G.; Jorio, A.; *Annu. Rev. Mater. Res.*, 34, 2004, 247.

[141] Hong, C-Y.; You, Y-Z.; Pan, C-Y.; *Polym.*, 47, 2006, 4300.

[142] Zhao, Z. W.; Guo, Z. P.; Ding, J.; Wexler, D.; Ma, Z. F.; Zhang, D. Y.; Liu, H. K.; *Electrochem. Commun*., 8, 2006, 245.

[143] Takashi, O.; Shinji, I.; Masashi, I.; *Catal. Commun.*, 8, 2007, 701.

[144] Yuan, F.; Ryu, H.; *Nanotechnol.*, 15, 2004, S596.

[145] Matsumoto, T.; Komatsu, T.; Nakano, H.; Arai, K.; Nagashima, Y.; Yoo, E.; Yamazaki, T.; Kijima, M.; Shimizu, H.; Takasawa, Y.; Nakamura, J.; *Catal. Today*, 90, 2004, 277.

[146] Li, W.; Liang, C.; Zhou, W.; Qiu, J.; Zhou, Z.; Sun, G.; Xin, Q.; *J. Phys. Chem. B.*, 107, 2003, 6292.

[147] Satishkumar, B. C.; Vogl, E. M.; Govindaraj, A.; Rao, C. N. R.; *J. Phys. D: Appl. Phys.,* 29, 1996, 3173.

[148] Joubert, J-M.; Černý, R.; Latroche, M.; Leroy, E.; Guénée, L.; Percheron-Guégan, A.; Yvon, K.; *J. Solid State Chem.*, 166, 2002, 1.

[149] Wu, X. B.; Chen, P.; Lin, J.; Tan, K. L.; Int. J. Hydrogen Energy, 25, 2000, 261.

[150] Jiang, Q.; Song, L. J.; Zhao, Y.; Lu, X. Y.; Zhu, X. T.; Qian, L.; Ren, X. M.; Cai. Y. D.; *Mater. Lett.*, 61, 2007, 2749.

[151] Shaw, D. J.; *Colloid and Surface Chemistry*, 1991, Butterworth Heinemann, Oxford, 252.

[152] Chen, M.; Feng, Y-G.; Wang, X.; Li, T-C.; Zhang, J-Y.; Qian, D-J.; *Langmuir*, 23, 2007, 5296.

[153] Cohen, J. B.; *Ultramicroscopy*, 34, 1990, 41.

[154] Raghavan, S. R.; Walls, H. J.; Khan. S. A.; *Langmuir,* 16, 2000, 7920.

8. Appendix

8.1 Approaches in the preparation of stable Cu-colloids

8.1.1 Experimental

Materials
$Cu(acac)_2$ (Sigma-Aldrich) and $Al(octyl)_3$ (Crompton GmbH), were all used as received. Cashew Nut Shell Liquid (CNSL) was extracted in-house from Cashew Nut Shells. THF was dried under argon.

Preparation of Cu-colloid from $Cu(acac)_2$ and $Al(octyl)_3$
All experiments were done in an Argon atmosphere and absolute dry THF as the solvent. $Cu(acac)_2$ (2.6 g, 10 mmol) was dissolved in 700 ml of THF in a 1 L flask. The solution was blue green in colour. $Al(octyl)_3$ (4.4 ml, 10 mmol) in 50 ml THF was added dropwise at room temperature within 4 hours.
The blue colour changed to deep red and traces of shiny elemental Cu was visible. A reddish precipitate settled at the bottom of the flask.

A small amount of the obtained suspension was transferred into two separate flasks for peptization with KorantinSH and Cashew Nut Shell Liquid (CNSL).

Peptization of Cu-colloid with KorantinSH
To approximately 0.10g of the Cu-colloid in 3 ml THF, 0.12g of KorantinSH was added. The reddish brown suspension changed to a wine red solution. A sample was taken for analysis with TEM.

Peptization of Cu-colloid with Cashew Nut Shell Liquid (CNSL)
Approximately 0.08g mg of Cashew nut shell oil was added to 0.05g of the Cu-colloid in 1ml of THF. A wine red solution resulted. A sample was taken for analysis (TEM) to see if particles were still present in the solution.

8.1.2 Results and Discussion

The blue colour of the $Cu(acac)_2$ solution changed to a deep red upon addition of $Al(octyl)_3$ which indicated that copper is reduced from Cu^{2+} to Cu^0. The small trace of shiny elemental copper, which was visible on the flask, was a clear indication that the interaction between the Cu and $Al(octyl)_3$ was not sufficient. Results from elemental analysis showed that 2.54% Cu (from expected 10%) was obtained when a 1:1 ratio was used, whereas the amount of Cu obtained agreed well with expected 5% when a 1:3 ratio was used. Thus, a ratio of 1:3 or above is more favorable for complete reduction. Hence, not all the copper particles was stabilized and hence aggregated at the bottom of the flask.

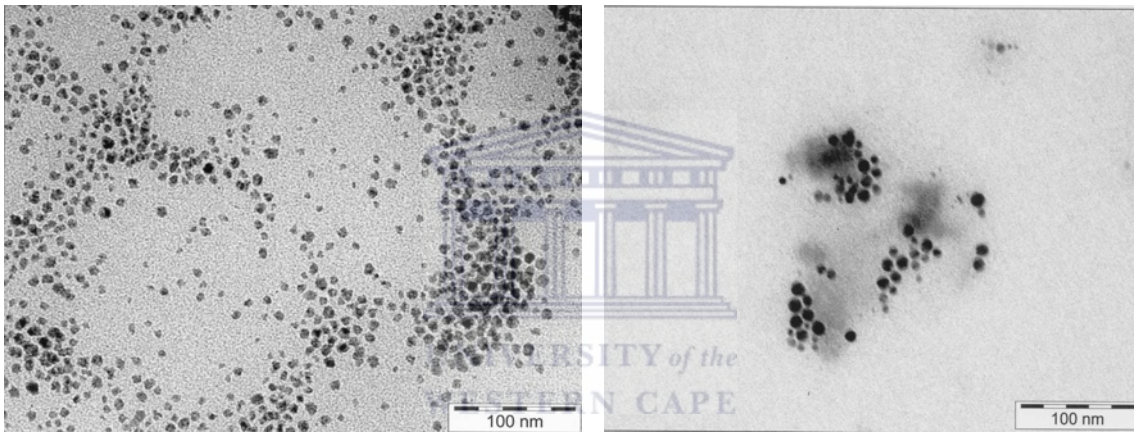

Fig. 8.1.1: TEM micrographs of (a) Korantin stabilized Cu-colloid and (b) cashew stabilized Cu-colloid

However, it was possible to solubilize the precipitate by peptization with Korantin or Cashew Nut Shell Liquid. From the TEM micrographs in Fig. 8.1.1 it is clear that Cu nanoparticles with a uniform particle size were obtained. Particle size of less than 10 nm was obtained in the case where Korantin (Fig. 8.1.1 (a)) was employed. In the case where CNSL was used, some smaller particles and some larger particles are visible with size between 7-15 nm (Fig. 8.1.1 (b)). The influence of the protecting shell is also illustrated since the particles appeared well separated from each other. However, the Cu-colloid is extremely sensitive to air and remains a challenge.

8.2 Preparation of Carbon Nanotubes

- **Synthesis of CNTS**

Carbon nanotubes were prepared by hydrocarbon pyrolysis using LPG as carbon source with $LaNi_5$ as nickel catalyst at 800°C for 1 hour.

- **Oxidation of CNTs (Acid Treatment)**

CNT's was added to a mixture of concentrated nitric acid and sulfuric acid (1:1) and refluxed for 3 hours.

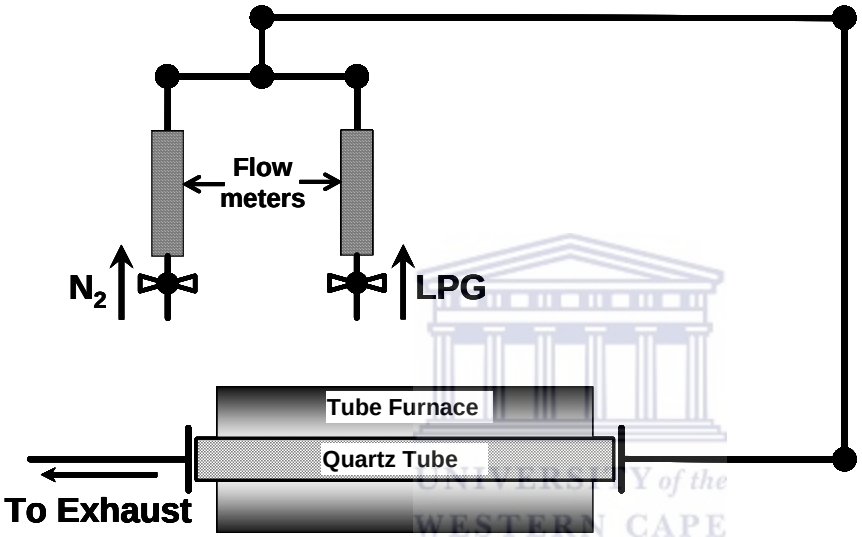

Fig. 8.2.1: Schematic diagram of CVD set-up for LPG pyrolysis

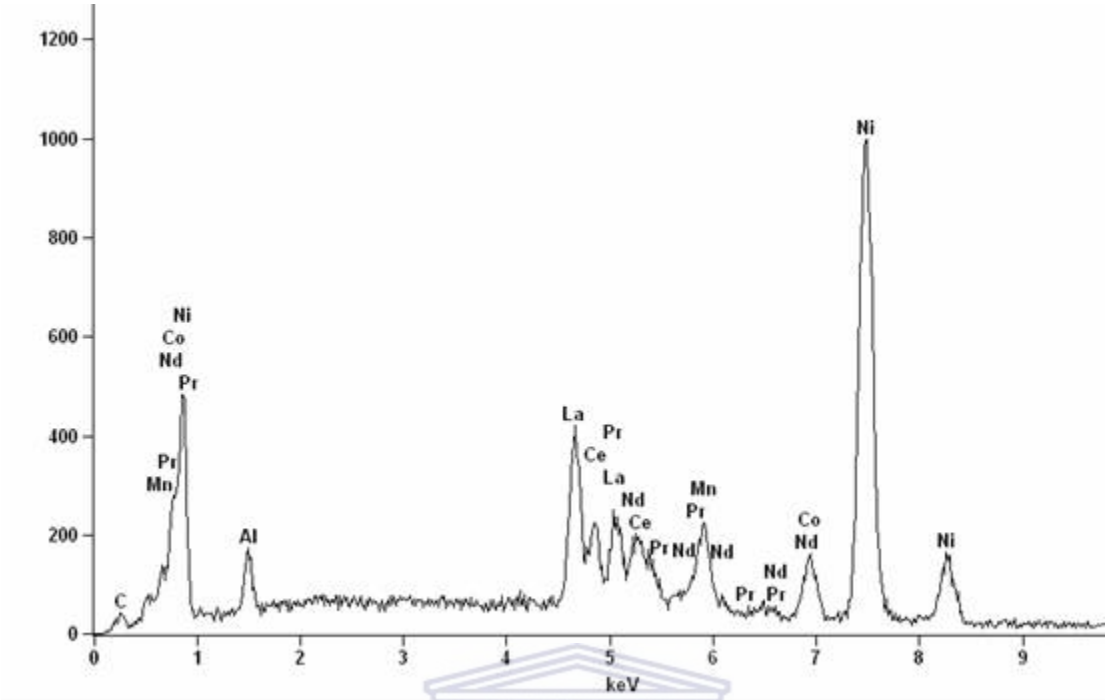

Fig. 8.2.2: Energy spectra of secondary X rays collected from the total surface of $LaNi_5$

8.3 List of Abbreviations

acac	Acetylacetonate
AlR_3	Trialkylaluminium
Ar	Argon
CNSL	Cashew nut shell liquid
CNTs	carbon nanotubes
E	Energy
EA	Elemental analysis
EDS	Energy Dispersive Spectroscopy
EDX	Energy dispersive X-ray analysis
EG	Ethylene glycol
fcc	Face-centered cubic
FTIR	Fourier Transform Infrared Spectroscopy
hrs	Hours
ICP	Inductively coupled plasma spectroscopy
MPI	Max-Planck Institute
MWCNTs	Multi-walled carbon nanotubes
nm	Nanometer
PDPP	Poly(dipropylene glycol) phenyl phosphite
PVA	Polyvinylalcohol
PVP	Polyvinylpyrrolidone
RT	Room temperature
SAD	Selected Area Electron Diffraction
SB12	Sulfobetaine/ 3-(N,N-Dimethyldodecylammonio)propanesulfonate
SCNTs	Single-wall carbon nanotubes
SEM	Scanning electron microscopy
t	Time
T	Temperature
TCNTs	Treated carbon nanotubes
TEM	Transmission electron microscopy
Temp.	Temperature

TGA	Thermogravimetric analysis
UCNTs	Untreated carbon nanotubes
UV-VIS	Ultraviolet-Visible spectroscopy
XRD	X-ray powder diffraction

Symbols

Å	Angstroms
λ	Wavelength
2Θ	Scattering angle

8.4 Glossary of Terms

Aggregation: The direct mutual attraction between particles (atoms or molecules) via van der Waals forces or chemical bonding. When there are collisions between particles in fluid, there are chances that particles will attach to each other and become larger particle. There are 3 major physical mechanisms to form aggregate: Brownian motion, Fluid shear and differential settling.

Aspect ratio: The ratio of the longest Feret's diameter of a particle to the shortest perpendicular one.

Brownian motion: The random motion of minute particles suspended in a fluid and provides a mechanism for diffusion.

Carbon nanotube: Nanotube consisting of one or several graphene sheets rolled up into a seamless tube, forming single-walled (SWCNT) or multi-walled (MWCNT) tubes.

Chemical Vapour Deposition: A top-down production method where vapour is formed in a reaction chamber and condensed onto a solid substrate to form a thin film.

Coalescence: The disappearance of the boundary between two particles in contact, or between one of these and a bulk phase followed by changes of shape leading to a reduction of the total surface area.

Dielectric strength: The maximum electric field strength that the oil (transformer oil) can withstand intrinsically before breaking down.

Hydrophilic: Having an affinity for water.

Hydrophobic: Compounds that do not dissolve easily in water easily and are usually non-polar.

Hydrosol: Sol in which water forms the dispersion medium.

Interface: The plane ideally marking the boundary between two phases.

Ionic surfactant: A surfactant carrying a net charge. If the charge is negative, the surfactant is more specifically called anionic; if the charge is positive, it is called cationic.

Monodisperse: Powder or particle suspension containing primary particles with a narrow size distribution.

Nanofluid: A new class of solid-liquid composite materials consisting of solid nanoparticles (in the range of 1-100 nm) or carbon nanotubes, dispersed in a heat transfer fluid such as ethylene glycol, water or oil.

Nanomaterial: Is categorized as those which have structured components with at least one dimension less than 100 nm.

Nanoparticle: Particle 1 to 100 nm in diameter.

Nanostructured: Having identifiable structure at the nanoscale.

Nanotube: Hollow nanofibre.

Newtonian fluid: A fluid is said to be Newtonian if the viscosity remains constant with an increase in shear rate.

Non-Newtonian fluid: Fluids, whose viscosity changes with an increase in shear rate. Nonionic surfactant: A surfactant with no positive or negative charge.

Ostwald ripening: The growth of larger crystals from those of smaller size which have a higher solubility than the larger ones.

Rheology: The study of the deformation and flow of matter.

Sedimentation: The settling of solid particles from a suspension, either naturally by gravity, or as a result of centrifugation.

Shear-thinning: A non-Newtonian fluid which exhibits higher viscosities at lower shear rates and vice-versa.

Sonication: High-frequency sound waves typically used to aid the dispersion of nanoparticles in a liquid.

Surfactant: A substance which lowers the surface tension of the medium in which it is dissolved, and/or the interfacial tension with other phases, and, accordingly, is positively adsorbed at the liquid/vapour and/or at other interfaces.

Suspension: A liquid in which solid particles are dispersed.

Thermal conductivity: The quantity of heat that will flow through a unit area of a substance in unit time under a unit temperature gradient.

Viscosity: The resistance of a fluid to flow.

Well-dispersed: Fine particles that are evenly distributed in a medium.

Yield stress/value: The external force required before a material will start to flow.

Zwitterionic surfactant: Neutral compounds having formal unit electrical charges of opposite sign. Some chemists restrict the term to compounds with the charges on non-adjacent atoms.